



Thiago Pinheiro da Silva

**Enhanced fluid rheology characterization for
Managed Pressure Drilling**

Dissertação de Mestrado

Dissertation presente to the Programa de Pós-graduação em Engenharia Mecânica of the Departamento de Engenharia Mecânica, PUC-Rio as partial fulfillment of the requirements for the degree of Mestre em Engenharia Mecânica.

Advisor: Profa. Mônica Feijó Naccache

Rio de Janeiro
March 2016



Thiago Pinheiro da Silva

**Enhanced fluid rheology
characterization for Managed
Pressure Drilling**

Dissertation presented to the Programa de Pós-Graduação em Engenharia Mecânica of the Departamento de Engenharia Mecânica do Centro Técnico Científico da PUC-Rio, as partial fulfillment of the requirements for the degree of Mestre.

Profa. Mônica Feijó Naccache

Advisor

Departamento de Engenharia Mecânica – PUC-Rio

Dr. Sidney Stuckenbruck

Olympus Software Científico e Engenharia Ltda. - OLYMPUS

Dr. Antonio Carlos Vieira Martins Lage

Petróleo Brasileiro

Márcio da Silveira Carvalho

Coordinador of the Centro Técnico Científico da PUC-Rio

Rio de Janeiro, March 17th, 2016

All rights reserved

Thiago Pinheiro da Silva

He graduated in Mechanical Engineering from the Federal University of Itajubá in 2003. He has over 13 years of professional experience in the oil industry with emphasis on Underbalanced Drilling (UBD), Coiled Tubing Drilling (CTD) and Managed Pressure Drilling (MPD) working in more than 20 countries. He is currently a consultant for new technologies and a project manager for Blade Energy Partners Ltd. He's a Member of the Society of Petroleum Engineers (SPE) and a guest instructor at the Federal University of Itajubá within the Human Resources program of the National Petroleum Agency (ANP).

Bibliographic data

Silva, Thiago Pinheiro da

Enhanced fluid rheology characterization for managed pressure drilling / Thiago Pinheiro da Silva ; advisor: Mônica Feijó Naccache. – 2016.

(em Inglês)

114 f. ; 30 cm

Dissertação (mestrado)–Pontifícia Universidade Católica do Rio de Janeiro, Departamento de Engenharia Mecânica, 2016.

Inclui bibliografia

1. Engenharia Mecânica – Teses. 2. MPD. 3. Perfuração com gerenciamento de pressão. 4. Reologia. 5. Caracterização de Fluido. I. Naccache, Mônica Feijó. II. Pontifícia Universidade Católica do Rio de Janeiro. Departamento de Engenharia Mecânica. III. Título. (em português)

CDD: 621

To my family, Ana Gabriela, Maria Cecilia and Helena, thank you for believing in me and supporting me at all times and in all circumstances, making my dream a reality. I am grateful for the support, care and love. I love you.

Acknowledgments

Above all, I'd like to thank God. Because of my faith, it allows me to believe that everything is possible.

I'd also like to thank Blade Energy Partners for providing the opportunity, technical support and financial support for me to participate in this program.

The Rheological Characterization Laboratory at PUC-Rio and friends there have given me some (several) hours of conversations, ideas and experiences regarding the characterization of fluids. In particular, I'd like to thank the student of chemical engineering, Carolina Dias Grossi, for technical support, which was of fundamental importance, showing patience and remaining calm even when everything seemed to go wrong.

To Victor Meléndez Rock-Fluid Interaction Laboratory (LIRF PUC-Rio) for the availability and aid in the characterization of fluids.

To CENPES and Petrobras also for providing the necessary equipment in this work.

To my friends, Antonio Lage and Emmanuel Franco Nogueira for their recommendation.

To my teacher and supervisor, Monica Feijo Naccache for believing in the proposal and the project and her masterful guidance so that the objectives were achieved.

To PUC-Rio, for the knowledge acquired during these two years.

To Rio de Janeiro, for welcoming me and my family.

To my parents and sister, who cheered me on every step of the way and always gave me positive encouragement.

Finally, I would like to especially thank my wife and friend Ana Gabriela, for making my dream our dream, to be next to me in the best and worst moments of my life, and endure with love and patience all the time and effort devoted to obtaining this title.

After completing this study it is clear to me that I would not have gone so far without the help of you and many others. As the popular African saying goes, "If you want to go quickly, go alone. If you want to go far, go together."

My sincere thanks to all of you.

Abstract

Silva, Thiago Pinheiro da; Naccache, Mônica Feijó (Advisor). **Enhanced fluid rheology characterization for Managed Pressure Drilling**. Rio de Janeiro, 2016. 114p. MSc. Dissertation – Departamento de Engenharia Mecânica, Pontifícia Universidade Católica do Rio de Janeiro.

Enhanced fluid rheology characterization for Managed Pressure Drilling. Hydraulics play an important role in many oil field operations including drilling, completion, fracturing, acidizing, workover and production. In Managed Pressure Drilling (MPD) applications, where pressure losses become critical to accurately estimate and control the well within the operational window, it is necessary to use the correct rheology for a precise mathematical modelling of fluid behavior. The standard API methods for drilling fluid hydraulics employ Herschel-Bulkley (H-B), Power Law (PL) or Bingham plastic as rheological models. This work summarizes the results of an extensive study on issues and relevant aspects related to the equipment and methods used to characterize the drilling fluids for MPD applications, as well as the operational implications that diverge from conventional practices. A comparison of fluid rheology characterization is made using high precision rheometers versus conventional FANN35 methods. Subsequently, a comparison of rheology model selection proposed by API 13B and by Non Linear Regression (NLR) is presented. Further investigation of shear rate ranges is presented in a MPD “typical” annular geometry. Results obtained via Computational Fluid Dynamics (CFD), and with the formulas suggested in API RP 13D are compared. To conclude, the effects of measurements, data treatment (Curve Fit), and environment (laboratory observations versus field experiences) in the accuracy of fluid rheology characterization and annulus pressure loss estimation are presented and discussed.

Keywords

MPD; Managed Pressure Drilling; Rheology; Fluid Characterization.

Resumo

Silva, Thiago Pinheiro da; Naccache, Mônica Feijó. **Caracterização Reológica de Fluidos para Perfuração com Gerenciamento de Pressão**. Rio de Janeiro, 2016. 114p. Dissertação de Mestrado – Departamento de Engenharia Mecânica, Pontifícia Universidade Católica do Rio de Janeiro.

Caracterização Reológica de Fluidos para Perfuração com Gerenciamento de Pressão. Forças Hidráulicas desempenham uma função importante em muitas operações de campo de petróleo, incluindo perfuração, completação, fraturamento, acidificação, workover e produção. Em aplicações de Perfuração com Gerenciamento de Pressão (Managed Pressure Drilling - MPD), onde as estimativas de perdas de pressão são críticas para controlar o poço dentro da janela de operacional, é necessário utilizar a reologia correta para a modelagem matemática precisa do comportamento do fluido. Os métodos API (American Petroleum Institute) empregam para os cálculos de hidráulica os modelos reológicos de Herschel-Bulkley (H-B), Power Law (PL) ou plástico de Bingham. Este trabalho resume os resultados de um estudo aprofundado sobre as questões e os aspectos relevantes relacionados com o equipamento e os métodos utilizados para caracterizar os fluidos de perfuração para aplicações MPD, bem como as implicações operacionais que divergem das práticas convencionais. Uma comparação da caracterização reológica de fluidos é feita usando reômetros de alta precisão contra métodos convencionais tais como o viscosímetro FANN35. Subsequentemente, é apresentada uma comparação da seleção do modelo reológico proposto por API 13B em contrapartida com o método de Regressão Não Linear (NLR). Investigações detalhadas das faixas de taxas de cisalhamento são apresentadas para geometrias de um poço anular MPD "típico", calculadas através de Dinâmica de Fluidos Computacional (CFD) e comparadas com as fórmulas sugeridas na API RP 13D. Para concluir, é apresentada uma discussão sobre os efeitos das medições, do tratamento de dados (Curve Fit) e do meio ambiente (observações de laboratório em comparação com experiências de campo) na precisão da obtenção da reologia do fluido e as consequências na estimativa das perdas de carga no anular.

Palavras-chave

MPD; Perfuração com Gerenciamento de Pressão; Reologia; Caracterização de Fluido.

Contents

1 Introduction	19
1.1. Managed Pressure Drilling Concept	20
1.1.1. Pressure Gradients	21
1.2. Controlling BHP	24
1.3. Literature Review	24
2 Aspects and Issues of Managed Pressure Drilling Connections	27
2.1. Hydraulic Simulations determines Applied Surface Back Pressure	28
2.1.1. MPD Industry Software	29
2.2. Rheology Measurements: Equipment	31
2.2.1. FANN - Model 35 Viscometer [19]	31
2.2.2. Rheometer Geometry Considerations	32
2.2.3. Shear Rate Operating Range – FANN 35 speeds	34
3 The Thought	35
3.1. The Motivation	35
3.2. Thesis Objectives	35
3.3. Scope of Work & Methodology	36
4 Industry Practices, Equipment and Standards	39
4.1. Drilling Fluid Characterization according Recommended Practice for Field Testing Water-based Drilling Fluids - ANSI/API RP 13B-1	39
4.2. API Recommended Practice 13D — Rheology and hydraulics of oilwell drilling fluids	40
4.2.1. API RP 13 D - Clause 4 -Fundamentals and fluid models	40
4.2.2. API RP 13 D - Clause 5 - Determination of Drilling Fluid Rheological Parameters	42
4.2.2.1. Herschel-Bulkley Rheological Model	42
4.2.2.1.1. Solution Methods for H-B Fluid Parameters	43
4.2.2.2. Other rheological models used in API 13 D	44
4.2.3. API RP 13 D - Clause 7 - Pressure-loss modeling	44
4.2.3.1. Shear Rate at the Wall	45
4.2.3.2. Flow regime: Reynolds number (generalized)	47
4.2.3.3. Critical Reynolds number (laminar to transitional regimes)	47
4.2.3.4. Friction factor	48
4.2.3.5. Laminar-flow pressure loss	48
4.2.3.5.1. Laminar-flow pressure loss (special case)	48
4.3. Standard Oilfield Viscometer Correction Factors	49
5 Fluid Characterization	50
5.1. Fluids Selection and Preparation	50
5.1.1. Fluid Selection Criteria	50

5.1.1.1. Viscosity Range and Concentration Criteria	50
5.1.2. Xanthan Gum preparation	51
5.2. Measurements of Rheological Properties	54
5.2.1. Equipment and Laboratories	54
5.2.2. Tests and Methodology	55
5.2.3. Rheology Measurements Results	56
5.2.3.1. Steady Flow Time Tests	56
5.2.3.2. Flow Curve Tests	57
5.2.3.3. Evaluation of FANN 35 Performance	60
5.2.3.4. Representativeness of Chosen Fluid Samples	62
5.3. Drilling Fluid Model Characterization	63
5.3.1. Curve Fitting Influence	63
5.3.2. Solving the Rheological Parameters with Nonlinear Regression	63
5.3.2.1. Xanthan Gum 0.8%	65
5.3.2.1.1. "Test #1 - PP50/P2(Cross Hatch) - Anton Paar - Physica MCR 301"	65
5.3.2.1.2. "Test #2 - PP50/P2(Cross Hatch) - Anton Paar - Physica MCR 301"	66
5.3.2.1.3. "Fann 35 - PUC - F1 B1 R1"	67
5.3.2.2. Low Lime WBM	68
5.3.2.2.1. Test #1 - PP50/P2(Cross Hatch) - Anton Paar - Physica MCR 301	68
5.3.2.2.2. Test #2 - PP50/P2 (Cross Hatch) - Anton Paar - Physica MCR 301	69
5.3.2.2.3. Test #1 - "Fann 35 - PUC - F1 B1 R1"	70
5.3.2.2.4. Test #2 - "Fann 35 - PUC - F1 B1 R1"	71
5.3.3. Solving the Rheological Parameters: API RP 13 D - Clause 5	71
5.3.4. Curve Fitting & Model Selection	73
5.3.4.1. Accuracy of the process	77
6 Mapping Shear Rate	80
6.1. Fluid Properties Selection	80
6.2. Geometry Selection	80
6.3. Flow Rate Selection	81
6.4. Shear Rate and Shear Stress Calculations as per API 13 D	82
7 Validating the Shear Rate Map: CFD Numerical Verification	86
7.1. About ANSYS Fluent	86
7.2. Computational Fluid Dynamics Setup	87
7.2.1. Solver and Solution Methods	87
7.2.1.1. Pressure Based Solver	87
7.2.1.2. General Scalar Transport Equation Setup – Solution Methods	88
7.2.1.2.1. Discretization (Interpolation Method)	90
7.2.1.2.2. Interpolation Method - Gradients	90

7.2.1.2.3. Interpolation Methods for Face Pressure	91
7.3. Critical Shear Rate Selection for Non-Newtonian Fluids	91
7.4. Geometry and Meshing Considerations	94
7.5. Physics and Boundaries	95
7.6. Convergence Criteria & Monitoring	96
7.7. CFD ANSYS Fluent: Shear Rates Mapping Cases	99
7.7.1. Influence of Hydraulics and Environment: Results	101
8 Pressure Losses Estimations	103
8.1. Case (a): "8.5 Section"	103
8.2. Case (b): "12.25 Section"	104
9 Recommendations and Conclusions	107
10 Bibliographic References	109
APPENDIX A API 13 D Method - Results	112
APPENDIX B CFD by ANSYS Fluent - Results	113

List of Figures

Figure 1 - The blowout at Spindletop	19
Figure 2 - Conventional drilling fluid gradients & casing setting points.	22
Figure 3 - MPD fluid gradients and drilling window.	23
Figure 4 - Pump Step-Down Schedule	27
Figure 5 – Automatic Connection - Ramp Schedule for 12-¼” Section	28
Figure 6 - Automatic Connection - Ramp Schedule for 8-½” Section	28
Figure 7 – Drillbench: Rheology Input User Interface Screen	30
Figure 8 - SafeVision: Rheology Input User Interface Screen	30
Figure 9 – MC2: Rheology Input User Interface Screen	31
Figure 10 – FANN Model 35 Viscometer	32
Figure 11 - Schematic diagram of basic tool geometries for the rotational rheometer: concentric cylinder	33
Figure 12 - Schematic diagram showing alternative cylindrical tool design in cut-away view: Double Gap	33
Figure 13 - Brazil MPD Operations Rheogram: IADC Historical Field Data	51
Figure 14 – Preparation of Xanthan Gum in the Mechanical Shaker at 300 rpm	53
Figure 15 – Xanthan Gum being stirred	53
Figure 16 – Xanthan Gum bottle samples	54
Figure 17 - Anton Paar - Physica MCR 301	55
Figure 18 - Steady State Flow Behavior Test: Equilibrium time and Flow Curve Optimization	56
Figure 19 - Flow Curve: Xanthan Gum 0.1% - Shear Stress vs. Shear Rate	58
Figure 20 - Flow Curve: Xanthan Gum 0.1% - Viscosity vs Shear Rate	58
Figure 21 - Flow Curve: Xanthan Gum 0.8% - Viscosity vs. Shear Rate	59
Figure 22 - Flow Curve: Xanthan Gum 0.8% - Shear Stress vs Shear Rate	59
Figure 23 - Flow Curve: Low Lime WBM - Viscosity vs. Shear Rate	60
Figure 24 - Flow Curve: Low Lime WBM - Shear Stress vs Shear Rate	60
Figure 25 - Cross Hatch Geometry	61
Figure 26 - Kaleidah Graph NLR – Xanthan Gum 0.8% - “Test #1 - PP50/P2(Cross Hatch) - Anton Paar - Physica MCR 301”	65
Figure 27 - Kaleidah Graph NLR – Xanthan Gum 0.8% - “Test #2 - PP50/P2(Cross Hatch) - Anton Paar - Physica MCR 301”	66
Figure 28 - Kaleidah Graph NLR – Xanthan Gum 0.8% - “Fann 35 - PUC - F1 B1 R1”	67
Figure 29 - Kaleidah Graph NLR – Low Lime WBM - “Test #1 - PP50/P2(Cross Hatch) - Anton Paar - Physica MCR 301”	68
Figure 30 - Kaleidah Graph NLR – Low Lime WBM - “Test #2 - PP50/P2(Cross Hatch) - Anton Paar - Physica MCR 301”	69

Figure 31 - Kaleidah Graph NLR – Low Lime WBM - “Fann 35 - PUC - F1 B1 R1” – Test#1	70
Figure 32 - Kaleidah Graph NLR – Low Lime WBM - “Fann 35 - PUC - F1 B1 R1” – Test#2	71
Figure 33 - Curve Fitting for Low Lime Water Based Mud	73
Figure 34 - Curve Fitting for Xanthan Gum 0.8%	74
Figure 35 – Shear Rate Interval of Interest and Model Selection	75
Figure 36 - Xhantam Gum 0.8% - Power Law Curve Fit Comparison	76
Figure 37 – Curve Fit vs Actual Fluid Properties	78
Figure 38 – Fluid Properties versus Curve Fit Accuracy	79
Figure 39 - Case (a): “8.5 Section”	81
Figure 40 - Case (b): “12.25 Section”	81
Figure 41 – Map of Shear Rate at Wall, according API 13 D – 8.5 and 12.25 Section	84
Figure 42 – FANN 35 Rheogram and “Shear Rate vs Shear Stress API 13 D Results”	85
Figure 43 - Typical Casing Program and Annulus	85
Figure 44 - Control Volume Example	87
Figure 45 - Transport Equations	88
Figure 46 - Fluent Solution Methods	89
Figure 47 - Fluent Solution Controls	89
Figure 48 - Discretization - Interpolation Methods	90
Figure 49 - Gradients - Interpolation Methods	90
Figure 50 - ANSYS Fluent - Fluid Properties Input Screen (H-B Model)	93
Figure 51 - Critical Shear Rate Selection and Behavior	93
Figure 52 – 2D Mesh Transversal View	94
Figure 53 - Velocity Profile of Newtonian Fluid at 1000 gpm in the 12.25 Section	95
Figure 54 - Velocity Profile of Non-Newtonian Fluid at 1000 gpm in the 12.25 Section	95
Figure 55 – Representation of the Annulus Flow: 3D Mesh – Perspective View	96
Figure 56 - Annulus Flow Development - Case (a) - 400 gpm	97
Figure 57 - Annulus Flow Development - Case (b) - 1000 gpm	97
Figure 58 - Velocity Distribution at Observation Point (12.25 Section - GX0.8% - Physica NLR)	98
Figure 59 -Strain Rate distribution at Observation Point	98
Figure 60 – Wall Shear Stress at Observation Point	99
Figure 61 - Influence of Hydraulic Modeling: Analytical vs Numerical	99
Figure 62 – Influence of Environment: Field versus Laboratory	100
Figure 63 - Numerical Solution for Shear Rate vs. Flow Rate in 8.5” Section and API13D Comparison	101
Figure 64 - Numerical Solution for Shear Rate vs. Flow Rate in 12.25” Section and API13D Comparison.	102

Figure 65 - Pressure Loss Estimation: 8.5" Section (case (a))	104
Figure 66 - Pressure Loss Estimation: 12.25" Section (case (b))	105

List of Tables

Table 1 - Xanthan Gum 0.1% Recipe	52
Table 2 - Xanthan Gum 0.8% Recipe	52
Table 3 - Xanthan Gum 0.1% - Fann 35 - CENPES - F1 B1 R1 (3 readings average)	62
Table 4 - Xanthan Gum 0.1% - Fann 35 - PUC - F1 B1 R1 (2 readings average)	62
Table 5 - Rheological Parameters: PL Model - NLR Method - Xanthan Gum 0.8% Test#1	65
Table 6 - Rheological Parameters: H-B Model - NLR Method - Xanthan Gum 0.8% Test#1	65
Table 7 - Rheological Parameters: PL Model - NLR Method - Xanthan Gum 0.8% Test#2	66
Table 8 - Rheological Parameters: H-B Model - NLR Method - Xanthan Gum 0.8% Test#2	66
Table 9 - Rheological Parameters: PL Model - NLR Method - Xanthan Gum 0.8% - Fann 35 PUC	67
Table 10 - Rheological Parameters: H-B Model - NLR Method - Xanthan Gum 0.8% - Fann 35 PUC	67
Table 11 - Rheological Parameters: PL Model - NLR Method – Low Lime WBM - Test#1	68
Table 12 - - Rheological Parameters: H-B Model - NLR Method – Low Lime WBM - Test#1	68
Table 13 - Rheological Parameters: PL Model - NLR Method – Low Lime WBM - Test#2	69
Table 14 - Rheological Parameters: H-B Model - NLR Method – Low Lime WBM - Test#2	69
Table 15 - Rheological Parameters: PL Model - NLR Method – Low Lime WBM - “Fann 35 - PUC - F1 B1 R1” – Test#1	70
Table 16 - Rheological Parameters: H-B Model - NLR Method – Low Lime WBM - “Fann 35 - PUC - F1 B1 R1” – Test#1	70
Table 17 - - Rheological Parameters: PL Model - NLR Method – Low Lime WBM - “Fann 35 - PUC - F1 B1 R1” – Test#2	71
Table 18 - Rheological Parameters: H-B Model - NLR Method – Low Lime WBM - “Fann 35 - PUC - F1 B1 R1” – Test#2	71
Table 19 - Rheological Parameters: PL Model - API RP 13 D Method- Xanthan Gum 0.8% - Fann 35 PUC	72
Table 20 - Rheological Parameters: H-B Model - API RP 13 D Method- Xanthan Gum 0.8% - Fann 35 PUC	72
Table 21 – API 13 D Curve Fit Method - Comparison	72
Table 22 – Curve Fitting and Coefficient of Determination Results	77
Table 23 - Annulus Fluid Velocity for 8.5 Section – Case (a)	82

Table 24 – Annulus Fluid Velocity for 12.25 Section – Case (b)	82
Table 25 – Shear Stress and Shear Rate as per API 13 D Method - Herschel-Bulkley Model - 8.5 Section.	83
Table 26 - Shear Stress and Shear Rate as per API 13 D Method - Herschel-Bulkley Model – 12.25 Section	83
Table 27 - API 13 D Method - Herschel-Bulkley Model - 8.5 Section - GX0.8_FANN35	112
Table 28 - API 13 D Method - Herschel-Bulkley Model - 12.25 Section - GX0.8_FANN35	112
Table 29 - Fluent Ansys - Herschel-Bulkley Model - 8.5 Section - GX0.8_FANN35_γ.critical 5e-05_1e-10	113
Table 30 - Fluent Ansys - Herschel-Bulkley Model - 8.5 Section - GX0.8_DG#2-NLR_γ.critical 5e-05_1e-10	113
Table 31 - Fluent Ansys - Herschel-Bulkley Model - 12.25 Section - GX0.8_FANN35_γ.critical 5e-05_1e-10	114
Table 32 - Fluent Ansys - Herschel-Bulkley Model - 12.25 Section - GX0.8_DG#2-NLR_γ.critical 5e-05_1e-10	114

Terms, Definitions, symbols and abbreviations

Symbol	Definition	Standard Units	Conversion Multiplier	SI Units
A	Surface area	in ²	6.4516E+02	mm ²
B _a	Well geometry correction factor	dimensionless	-	dimensionless
B _x	Viscometer geometry correction factor	dimensionless	-	dimensionless
d	Diameter	in.	2.54E+01	mm
d _h	Hole diameter or casing inside diameter	in.	2.54E+01	mm
d _{hyd}	Hydraulic diameter	in.	2.54E+01	mm
d _i	Pipe internal diameter	in.	2.54E+01	mm
d _p	Pipe outside diameter	in.	2.54E+01	mm
ECD	Equivalent Circulating Density	lb _m /gal	1.198264E+02	kg/m ³
EMW	Equivalent Mud Weight	lb _m /gal	1.198264E+02	kg/m ³
f	Fanning friction factor	dimensionless	-	dimensionless
F	Force	lb _f	4.448222E+00	N
f _{lam}	Friction factor (laminar)	dimensionless	-	dimensionless
f _{trans}	Friction factor (transitional)	dimensionless	-	dimensionless
f _{turb}	Friction factor (turbulent)	dimensionless	-	dimensionless
g	Acceleration of gravity	32.152 ft/s ²	3.048E-01	m/s ²
G	Geometry shear-rate correction (Herschel-Bulkley fluids)	dimensionless	-	dimensionless
G _p	Geometry shear-rate correction (power-law fluids)	dimensionless	-	dimensionless
K, k	Consistency factor (Herschel-Bulkley fluids)	lb _f •s _n /100 ft ²	4.78803E-01	Pa•s _n
k _p	Consistency factor (power-law fluids)	lb _f •s _n /100 ft ²	4.78803E-01	Pa•s _n
L	Length of drillstring or annular segment	ft	3.048E-01	M
N, n	Flow behavior index (Herschel-Bulkley fluids)	dimensionless	-	dimensionless
N	Viscometer rotary speed	r/min	-	r/min
n _p	Flow behavior index (power-law fluids)	dimensionless	-	dimensionless
N _{Re}	Reynolds number	dimensionless	-	dimensionless
N _{ReG}	Generalized Reynolds number	dimensionless	-	dimensionless
N _{Rep}	Particle Reynolds number	dimensionless	-	dimensionless
P	Pressure	lb _f /in ²	6.894757E+00	kPa
P _a	Annular pressure loss	lb _f /in ²	6.894757E+00	kPa
PV	Plastic Viscosity	cP	1.0E-03	Pa•s
Q	Flow rate	gal/min	6.309.20E-02	dm ³ /s
Q _c	Critical flow rate	gal/min	6.309.20E-02	dm ³ /s
R	Ratio yield stress / yield point (τ _y / YP)	dimensionless	-	dimensionless
Θ ₁₀₀ , R ₁₀₀	Viscometer reading at 100 r/min	° deflection	-	° deflection
Θ ₂₀₀ , R ₂₀₀	Viscometer reading at 200 r/min	° deflection	-	° deflection
Θ ₃ , R ₃	Viscometer reading at 3 r/min	° deflection	-	° deflection

Θ_{300} , R_{300}	Viscometer reading at 300 r/min	° deflection	-	° deflection
Θ_6 , R_6	Viscometer reading at 6 r/min	° deflection	-	° deflection
Θ_{600} , R_{600}	Viscometer reading at 600 r/min	° deflection	-	° deflection
RF	Rheology Factor	-	-	-
T	Temperature	°F	(°F-32)/1.8	°C
V	Velocity	ft/min	5.08E-03	m/s
V_a	Fluid velocity in annulus	ft/min	5.08E-03	m/s
V_c	Critical velocity	ft/min	5.08E-03	m/s
V_{cb}	Critical velocity (Bingham plastic fluids)	ft/min	5.08E-03	m/s
V_{cp}	Critical velocity (power-law fluids)	ft/min	5.08E-03	m/s
V_p	Fluid velocity inside pipe	ft/min	5.08E-03	m/s
x	Viscometer ratio (sleeve radius / bob radius)	dimensionless	-	dimensionless
YP	Yield point	lbf/100 ft ²	4.788026E-01	Pa
A	Geometry factor	dimensionless	-	dimensionless
γ , $\dot{\gamma}$	Shear rate	s ⁻¹	-	s ⁻¹
γ_w	Shear rate at the wall	s ⁻¹	-	s ⁻¹
μ	Viscosity	cP	1.0E-03	Pa•s
ρ	Fluid density	lb _m /gal	1.198264E+02	kg/m ³
τ , τ	Shear stress	lbf/100 ft ²	4.788026E-01	Pa
τ_b	Shear stress at viscometer bob	° deflection	-	° deflection
τ_i	Iterative shear stress in curve-fit method	lbf/100 ft ²	4.788026E-01	Pa
τ_w	Shear stress at the wall	lbf/100 ft ²	4.788026E-01	Pa
τ_y , τ_y	Yield stress	lbf/100 ft ²	4.788026E-01	Pa

"Ipsa scientia potestas est"

1 Introduction

Controlling the pressure in a wellbore while drilling for oil or gas is an operation that draws its roots from Colonel Drake's Spindletop well drilled in the late 1800's. Arguably thought of as the moment which gave rise to the modern Blow Out Preventer (BOP) and drilling fluid industries, the geyser of oil at Spindletop graphically demonstrated that geological pressure must be respected in order to access what lies beneath.

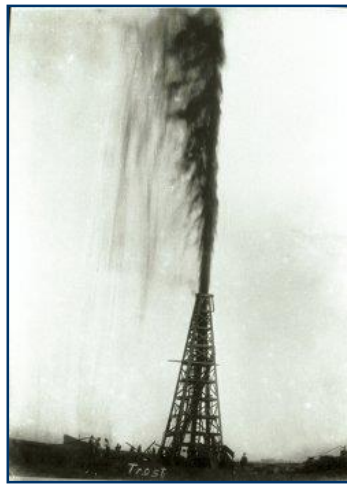


Figure 1 - The blowout at Spindletop

Historically, the most apparent way to control subterranean pressure was to take advantage of hydrostatics. Altering the density of the drilling fluid, or mud, allowed the driller to keep those hydrocarbons at bay while drilling and reach the desired target 'safely'. Drilling in this manner continued for decades, until three key characteristics began to emerge:

- ✓ Reservoir pressures do not remain at 'virgin' conditions and eventually decline below the hydrostatic pressure of even the lightest drilling fluids,
- ✓ Exerting excessive hydrostatic pressure on a formation could (in some cases) cause terminal loss of drilling mud, and
- ✓ Although hydrostatically over-pressuring the reservoir kept hydrocarbons in place, the exerted pressure on the porous rock had (in some cases) limited the reservoir's productive potential through damaging the near wellbore.

These characteristics, amongst a host of others, prompted the drilling industry to explore new avenues of annular pressure control. Technological advances in surface equipment resulted in a host of new terms and acronyms thrust upon drillers and engineers to describe these new techniques:

- ✓ Mud Cap Drilling
- ✓ Dual-gradient Drilling
- ✓ Air Drilling
- ✓ Managed Pressure Drilling (MPD)
- ✓ Underbalanced Drilling (UBD)

The common theme linking these different drilling techniques is the attempt to actively or proactively control the annular wellbore pressure profile. In contrast, conventional drilling practices react to changing wellbore conditions by altering the mud weight according to observations of differences in mud volumes (kicks or losses). All of the terms mentioned in the bulleted list above have come to signify specific annular pressure control techniques, and thus none can be used as an umbrella term to adequately describe them all.

1.1. Managed Pressure Drilling Concept

In conventional drilling operations, the mud weight is selected such that its static gradient is higher than the exposed formation pressure. The system is open, returning the fluid to atmospheric tanks. When circulating, the pressure imposed on the formation increases due to frictional pressure of fluid moving in the wellbore. The Bottom Hole Pressure (BHP) is controlled by the following equation:

Equation 1 – Conventional Drilling BHP variables

$$BHP = P_{Gravity} + P_{Friction}$$

Where:

$P_{Gravity}$ = hydrostatic pressure due to mud weight

$P_{Friction}$ = friction pressure due to circulation

While conventional drilling uses only fluid density to manage pressure, MPD uses a combination of surface pressure, fluid density, friction, and energy terms to balance the exposed formation pressure [1]. The addition of specialized MPD equipment like the Rotating Control Device (RCD) and MPD choke enable the

application of surface pressure to achieve the desired annular pressure profile. Other variables are now introduced into the pressure equation:

Equation 2 – MPD Drilling BHP variables

$$BHP = P_{Gravity} + P_{Friction} + P_{Surface} + P_{Energy} + P_{Acceleration}$$

Where: BHP = bottom hole pressure

$P_{Gravity}$ = hydrostatic pressure due to mud weight

$P_{Friction}$ = friction pressure due to circulation

$P_{Surface}$ = applied surface pressure

P_{Energy} = pressure changes as a result of the energy of another device (ie; sea floor pump)

$P_{Acceleration}$ = friction pressure due to acceleration of fluids ¹

The point is that conventional drilling only uses gravity and friction, while MPD uses the other components of the equation to manage the pressure.

1.1.1. Pressure Gradients

Pressure gradient curves are commonly used to map out the subterranean pressure profiles. Pore pressure may be thought of as the pressure limit which traps subterranean fluids, while fracture pressure delimits an upper bound in pressure, above which the rock would fracture as a result of the injection of fluids. Pore and Fracture pressures can vary with depth and are typically non-linear. The pressure exerted by a single phase fluid in a wellbore follows a linear gradient, or slope. A column of static, unmoving fluid follows a pressure gradient dependent upon its density. Pumping the same fluid will alter the slope of the fluid gradient due to the additional friction in the system. At any given depth, the pressure exerted by pumping fluid will be higher than that of a static fluid. These fluid gradients are commonly referred to as static and dynamic fluid gradients. The term Equivalent Circulating Density (ECD) is used to describe the equivalent static density of a fluid if it were to follow the dynamic fluid gradient curve. ECD is comprised of the static mud weight and friction pressure term, and is usually expressed in pound per gallon (ppg).

¹ Pressure change due to acceleration, $P_{Acceleration}$ is also considered in high energy applications. The pressure effects due to acceleration are negligible in most MPD applications.

Figure 2 and Figure 3 illustrate the differences between conventional and managed pressure drilling pictorially. Figure 2 depicts a traditional pore-fracture gradient window for a hypothetical well. Static and dynamic fluid gradient curves are superimposed. Simplistically, the next casing point is highlighted at the bottom of the figure where the dynamic circulating density line approaches the fracture gradient.

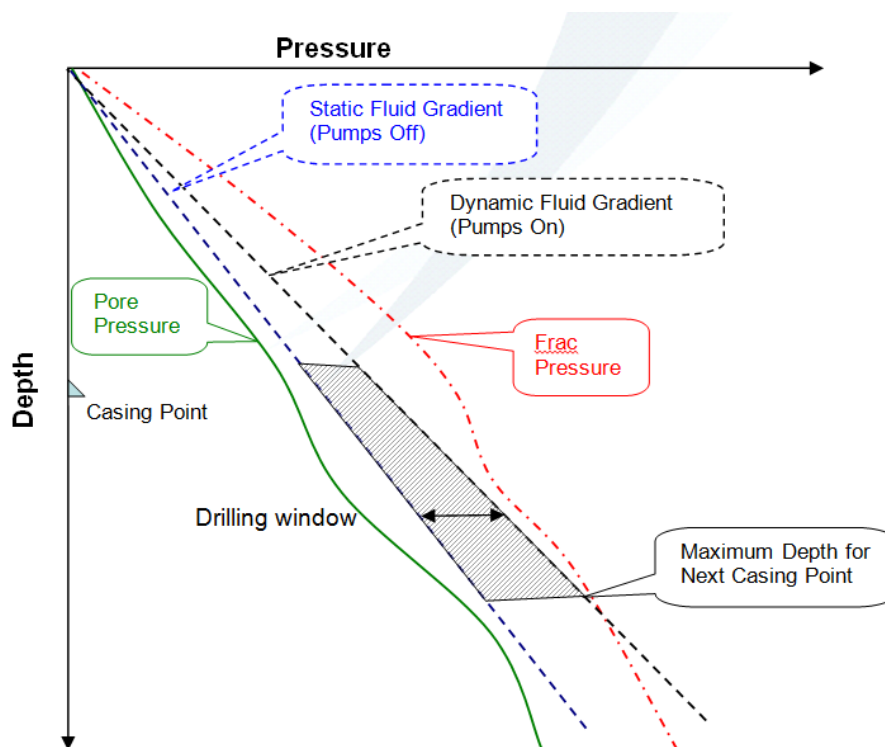


Figure 2 - Conventional drilling fluid gradients & casing setting points.

The margin between the static and dynamic gradients defines the drilling window, shown shaded. Figure 3 shows the same hypothetical well, demonstrating an MPD option with a static mud weight gradient (blue) less than pore pressure. Note that although the dynamic gradient (black) results in an overbalanced state while, the system is statically underbalanced at some points in the wellbore. Application of surface back pressure however, results in a shift of the static gradient (orange) above pore pressure. In this example, an anchor point pressure at the bit is chosen, whereby the pressure is matched with pumps on and pumps off at this point. Higher in the wellbore, this curve crosses frac pressure, however the result is inconsequential as this point is behind casing.

The one dramatic result demonstrated in this figure is the ability to drill deeper with the same mud system, thus extending the casing depth or reaching the planned target.

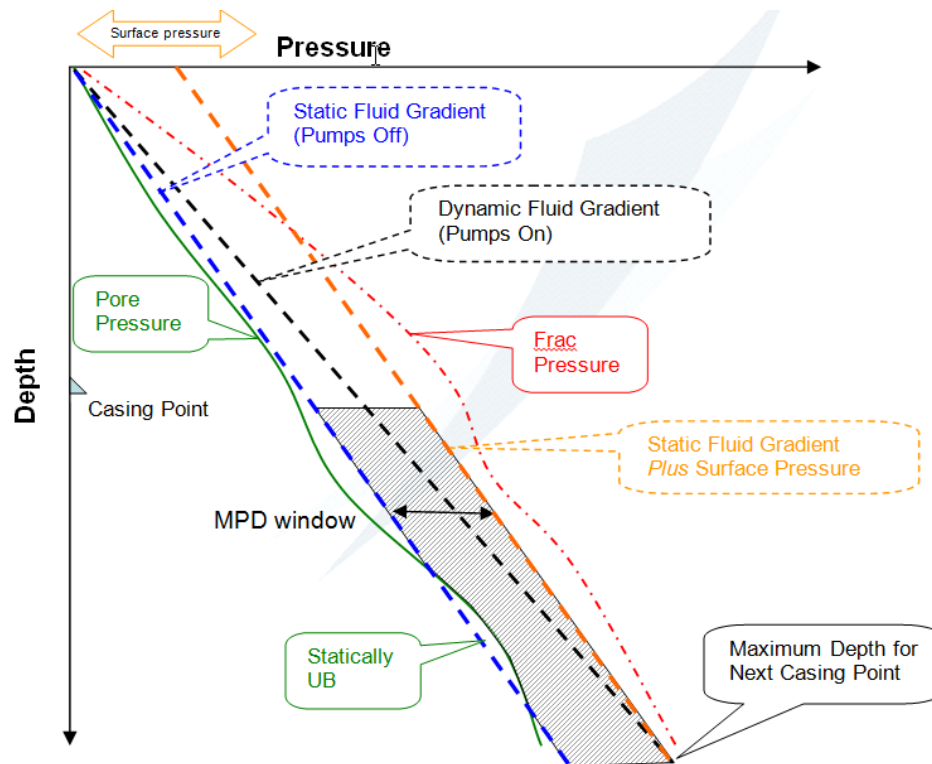


Figure 3 - MPD fluid gradients and drilling window.

Applied back pressure MPD wells may be distinguished by the chosen fluid density, whereby the resultant annular pressure system may be **statically underbalanced**, or **statically overbalanced**. As alluded to previously, the 'static' term in this case refers to the state of the rig's mud pumps, whereby static means 'pumps off' and dynamic means 'with rig pumps on', both with no applied back pressure (ABP). The chosen weight of the fluid, therefore will dictate the complexity in further planning of an MPD well relative to inherent risk. A statically overbalanced well is considered less risky as the well is controlled with the rig's pumps off simply by the weight of the drilling fluid. In a statically underbalanced system, the well may ONLY be controlled with the application of further surface back pressure when the rig's pumps are off. The risk of an unplanned influx from the wellbore must then be accounted for appropriately.

Therefore, the international Association of Drilling Contractors (IADC) [2] defines managed pressure drilling (MPD) as follows: "MPD is an adaptive drilling process used to precisely control the annular pressure profile throughout the wellbore". IADC further states that

The objectives are to ascertain the downhole pressure environment limits and to manage the annular hydraulic pressure profile accordingly. It is the intention of MPD to avoid continuous influx of formation fluids to the surface. Any influx incidental to the operation will be safely contained using an appropriate process.

1.2. Controlling BHP

The purpose of managed pressure drilling is to create a pressure profile in the annulus within the operating window guided by pore and fracture pressures. Most often, pressure control in the annulus is achieved by employing the following techniques: adjusting fluid density, frictional pressure losses and the surface backpressure by using a combination inclusive of a rotating control device (RCD), choke, pump, and the design of well bore and drill string configuration.

An important goal of all drilling is to manage the bottom hole pressure.

In **conventional overbalanced drilling**, the *ABP* is by definition zero (or atmospheric), and only density and friction loss are available as control parameters. Changing density means changing the mud weight, which takes time. Moreover, for the full impact of density change to be felt in terms of BHP, the new density fluid has to circulate all the way to surface. This means that in practice, BHP control through change in density is slow. Frictional pressure loss can be changed more easily, by changing the flow rate. The main limitation of this approach is the minor impact of frictional pressure loss on BHP in large-clearance annuli. In tighter clearances (or if the clearance is deliberately reduced by using, for example, large OD drill collars), frictional pressure loss can have a significant impact on BHP control. It should be remembered that there is a lower limit of rate governed by hole cleaning requirements, and an upper limit dictated by the downhole motors and equipment used.

In **classical MPD**, where a rotating control device is used to allow applied back pressure, greater control is now available. Density and friction are still available as control parameters, just as in conventional drilling. Moreover, since *ABP* is now a control parameter, far greater flexibility is available in the design of the operation. This is a common MPD variation.

1.3. Literature Review

The importance of hydraulic calculations and rheology models used to characterize the flow behavior of drilling fluids are widely known as first illustrated by Bourgoyne et al [3] and later investigated by Pilehvari [4].

The simplicity of fluid rheology calculations provided by the Bingham Plastic [5] and Power Law [6] models contributed to the widespread use of those models in the oil and gas industry, although Herschel Bulkley [7] has become the model of choice to predict pressure losses when drilling fluids are circulated in a well [8].

Several studies have been carried out considering the Herschel-Bulkley flow in wellbores. Fairly complex model covering laminar, transitional and turbulent flows and eccentricity effects in hydraulics were presented by Reed and Pilehvari (1993) [9].

The approach has also been followed also by Merlo et al. (1995) [10], Bailey and Peden (2000) [11], and Maglione et al. (2000) [12] to cover all flow regimes for flow of Herschel–Bulkley fluids and of generalized non-Newtonian fluids in concentric annuli for different types of applications. The main contributions of these studies have been of high relevance for the evolution of the calculations performed.

Merlo et al. (1995) [10] proposed a prediction of the exact pressure distribution along the well and the circulating temperature distribution in the fluid based on viscometer readings for the Newton, Bingham, Power law and Herschel-Bulkley models.

Peden (2000) [11] proposed a new rheological parameter which couples laminar flow and turbulent flow functions whereas pressure loss functions for flow of non-Newtonian fluids in pipes and concentric annuli are independent of the rheological model of choice. His work highlights the importance of a rigorous method for providing confidence bounds on any fitted nonlinear functions. It is considered beneficial for any calculation requiring fitted nonlinear functions.

On other side, it has been demonstrated by Maglione et al. (2000) [12] that rheological triad from the viscometer data obtained in the laboratory using a Fann VG 35 viscometer does not always coincide with the rheological triad from the in-situ drilling test.

Moreover, Okafor & Evens, (1992) [13] illustrated that no single rheological model is able to accurately represent the flow behavior of most pseudoplastic and yield-pseudoplastic fluids over the full spectrum of shear rates and proved that the chosen rheology model can be found to approximate the behavior of an actual fluid (within certain ranges) with an accuracy commensurate with the reproducibility of measured field data.

The understanding and efficient control of drilling-fluid behavior requires a fundamentally sound method of flow-properties analysis which is practical to use in the field, especially on Managed Pressure Drilling (MPD) applications. It appears that the practical application of sound rheological concepts had been the lack of

suitable viscometric methods for the routinely measurement of fundamental flow properties outside the laboratory and the concern raised by Savins & Ropers (1954) [14] remains unresolved whenever considering the newer models that drilling industry has adopted.

Nguyen and Boger (1987) [15] confirmed that the methods normally employed for shear rate calculations from concentric cylinder viscometer data generally are not applicable for fluids with a yield stress and proposed a correct calculation of the shear rate for time-independent yield stress fluids. In particular when cylindrical systems with large radius ratios the yield stress induces two possible flow regimes in the annulus.

Another perspective of the issue can be attributed to the fact that several controversial measurement and curve-fitting techniques remains a great challenge to determine the rheological parameters for a given fluid. Klotz and Brigham (1998) [16] presents an accurate method for determining the three coefficients of the Herschel-Bulkley equation from six-speed Fann viscometer data in attempt to fulfill the determination of these coefficients from the data points.

Zamora and Power (2002) [8] discussed techniques to determine key rheological parameters using the measurement method as well as complexities involved in rheological modeling. It is important to mention that iterative techniques available to solve daunting Herschel-Bulkley assume true Herschel-Bulkley behavior before processing or relies on the raw data and technically assumes no particular rheological model. The same drawback was observed on the API method [17] is the wide shear-rate span between data points (especially in the range of 5 to 170 s⁻¹, or 3 to 100 rpm).

Aided by computational fluid dynamics (CFD), recent study performed by Erge et al. (2015) [18] evaluated the behavior of the flow of Newtonian and non-Newtonian fluids in annuli demonstrating that CFD as the accurate pressure loss estimations. However, the determination of fluid properties and selection of rheology also remains vital for the convergence of the numerical results when compared to the experimental results.

After all, it is trusted that the requirements to measure the rheology properties are not well understood or explored. It is proposed that while MPD is a concern, equipment and techniques should be reassessed. Followed by the characterization and adoption of a rheology model to best describe the physics and the fluid dynamics.

2 Aspects and Issues of Managed Pressure Drilling Connections

Traditionally, Managed Pressure Drilling Connections, the back pressure values must follow a pump rate versus pressure schedule to maintain the annular pressure constant down the hole. As the example presented in Figure 4 it can be observed that the bottom hole pressure is kept constant (represented by the ECD – red curve) while the pumps are lowered in a preparation for a connection.

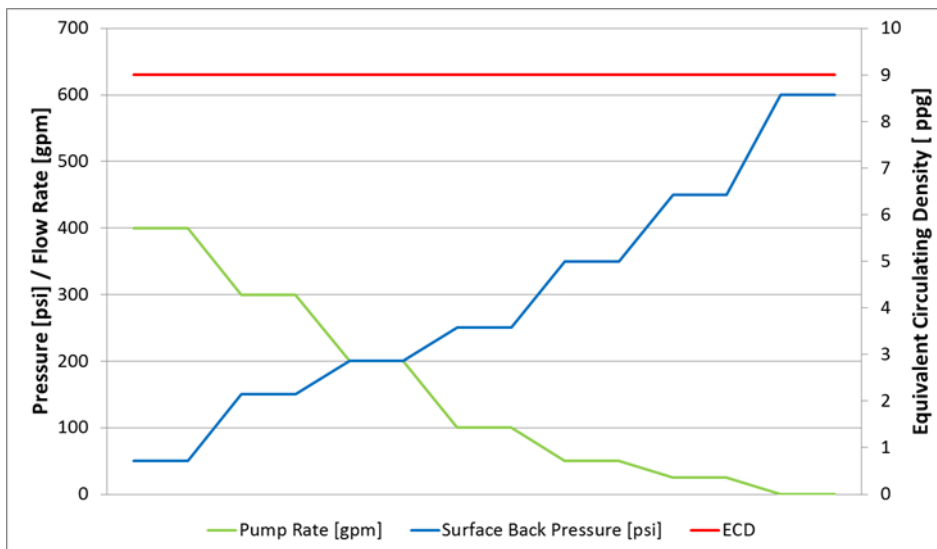


Figure 4 - Pump Step-Down Schedule

The most recent MPD system adjusts the applied surface back pressure automatically based on the desired calculated bottom hole pressure by predicting the friction annular losses through a hydraulics model. As the model uses the real time data of pump flow rate, at any time the pump rate is changed, an automatic adjustment in the surface back pressure will be produced to maintain a constant bottom hole pressure by compensating the friction losses by surface back pressure. Opposed to manual MPD connections, in automatic MPD systems the pump rate versus pressure schedule plots are presented in a smoother way, as the steps changes are automatically compensate and calculated by the hydraulic simulators installed on the MPD's Control Units (Figure 5 and Figure 6).

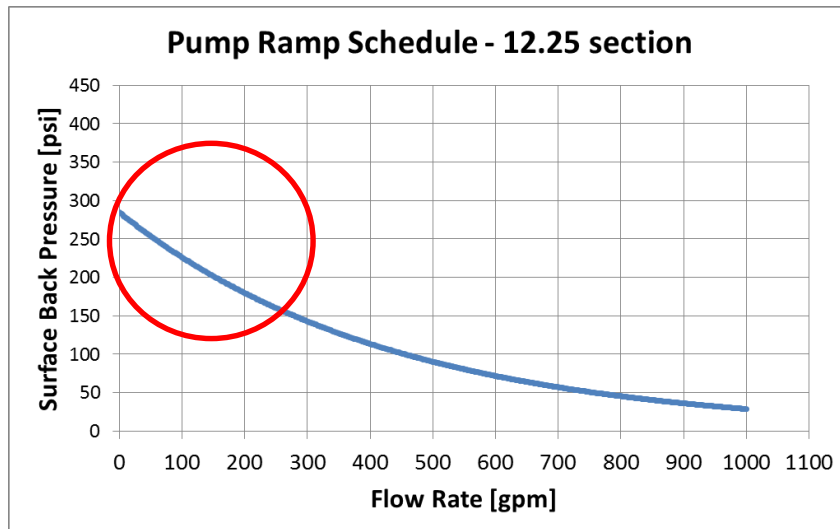


Figure 5 – Automatic Connection - Ramp Schedule for 12-¼" Section

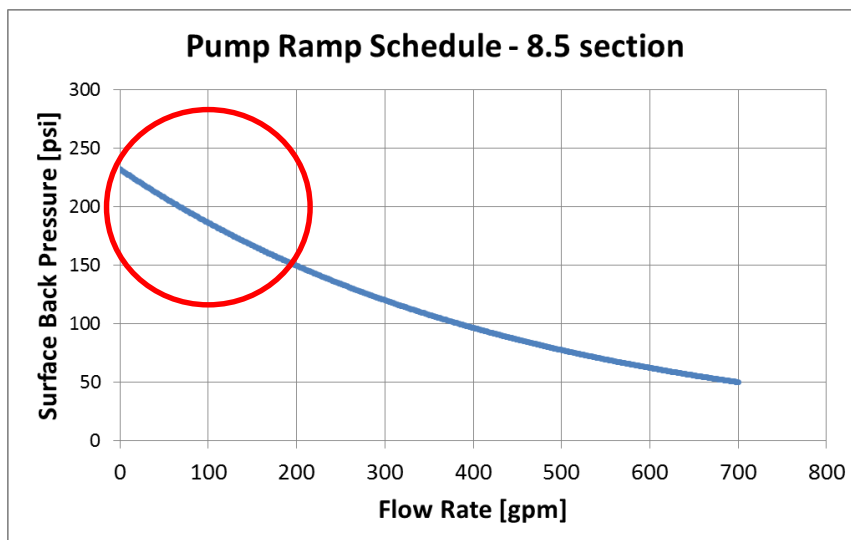


Figure 6 - Automatic Connection - Ramp Schedule for 8-½" Section

2.1. Hydraulic Simulations determines Applied Surface Back Pressure

As the drilling flow rates, during connections, vary from maximum design point to null and vice versa. Still, it must be considered that the biggest difference in pressure drop in the annulus will occur at low rates (10-20% of its maximum) and the surface back pressure enforced to compensate it at that interval.

One may express that an alternate method to control bottom hole pressure could be the use of downhole pressure sensors, such as measurement while drilling (MWD) devices, to directly measure the pressure loss in the annulus. In this case, hydraulic models that calculate the friction losses at given rate could be

replaced. Although, at lower rates falls outside the operating range of the existing technology for MWD tools which turning them inoperable and not an option.

The issue gets importance as the only method to accurately predict the requirements for surface back pressure as the connection progresses relies on hydraulic model. All the information needed to correctly calculate the friction losses, such as amount of data points to characterize a drilling fluid rheology, the range of shear rate observed in the flow, the rheology model selection, curve fit and rheology parameters and ultimately the equipment and calculation method itself among others becomes critical for an accurate and safe connection procedure.

2.1.1. MPD Industry Software

The common software used in “Managed Pressure Drilling (MPD) Design and Operations” are the Drillbench Dynamic Drilling Simulation Software by Schlumberger, Microflux Control System MC2 by Weatherford and SafeVision by Safe Kick.

It is well-known that the existing systems mentioned above poses limitations to MPD design such as:

1. only a single rheology model can be selected from an existing database, usually available Bingham, Power Law (PL), Herschel-Bulkley (H-B) and Newtonian;
2. the number of rheology readings, shear rate vs. shear stress, commonly known in the industry as FANN readings [degrees] by rotor speed are limited from 6 to 8 [rpm] reading maximum.
3. the readings for rotor speed [rpm] (or shear rate [1/s]) are defined as fixed values where the lowest available input is defined as 3 [rpm] (or 5.11 [1/s]) and the maximum as 600 [rpm] (or 1021.38 [1/s]) in accordance to the API standards and common practices .

The user interface input screen for Drillbench, SafeVision and MC2 can be found below on Figure 7, Figure 8 and Figure 9 respectively.

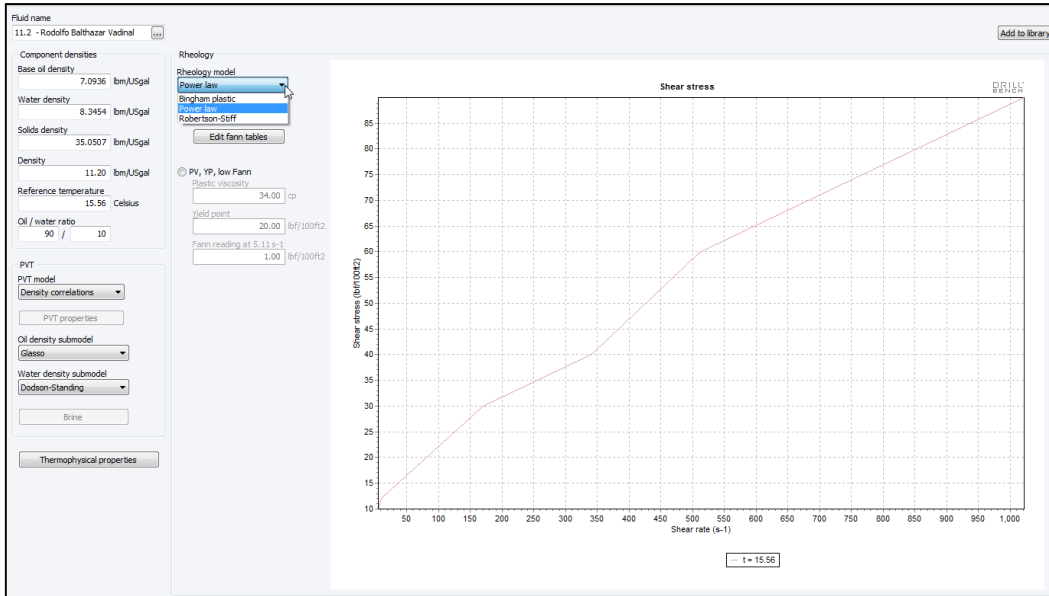


Figure 7 – Drillbench: Rheology Input User Interface Screen

PUC-Rio - Certificação Digital Nº 1412759/CA

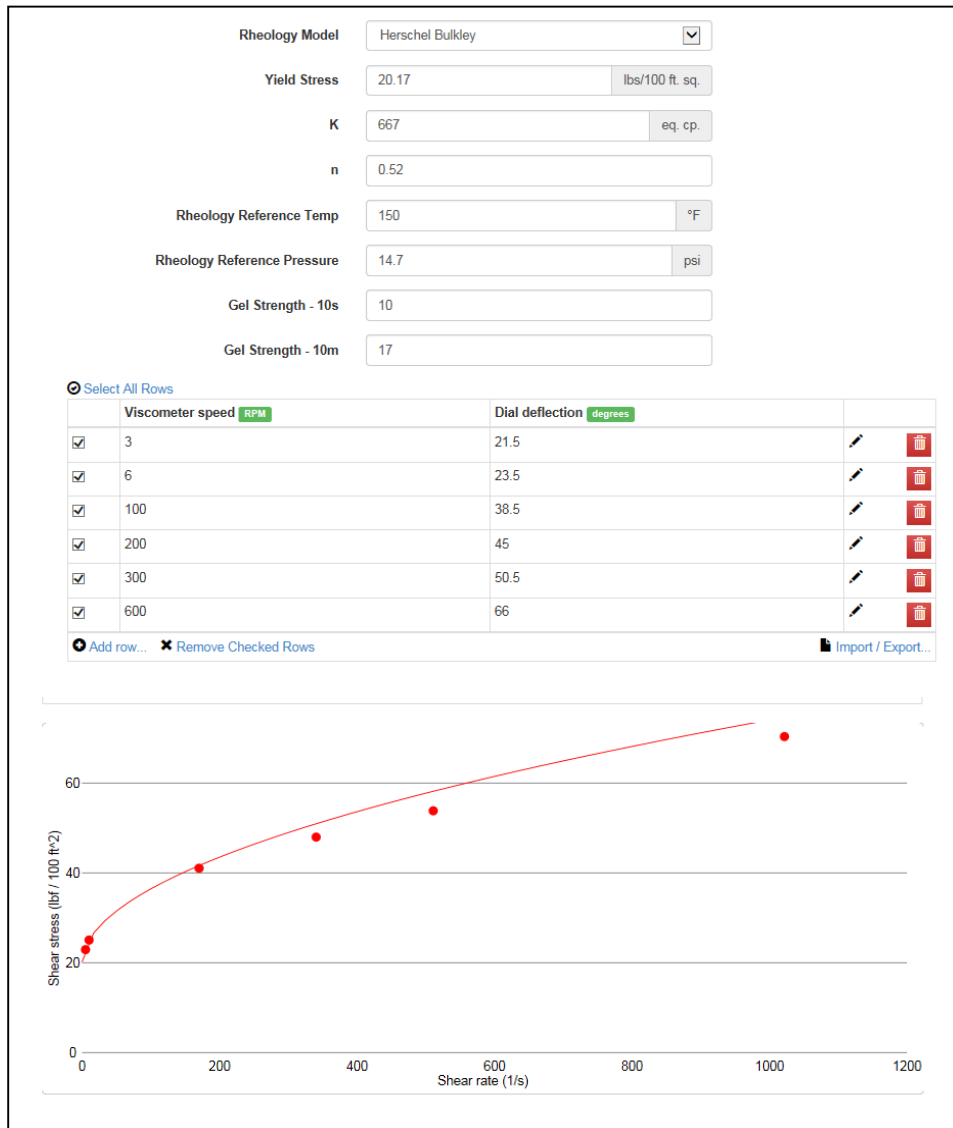


Figure 8 - SafeVision: Rheology Input User Interface Screen

Rheology Model	Newtonian	Mud Type	Water	1
600 rpm, °Fann	42.00	API Fluid Loss, cc/30min	99.00	2
300 rpm, °Fann	31.00	Mud Temperature, °C	26.67	
200 rpm, °Fann	24.00	Retort Oil, 0-1	0.00	
100 rpm, °Fann	15.00	Retort Water, 0-1	1.00	
6 rpm, °Fann	7.00	Conductivity, W/(m-°C)	0.60	
3 rpm, °Fann	5.00	Specific Heat, J/(kg-°C)	4186.80	
Gels 10", °Fann	3.00	HTHP Fluid Loss, cc/30min	1.00	
Gels 30", °Fann	7.00	pH	7.00	
Gels 10', °Fann	15.00	Cake API, mm	1.59	
Gels 30', °Fann	20.00	LG Solids, 0-1	0.03	
Ref. Temperature, °C	32.22	HG Solids, 0-1	0.03	
Ref. Pressure, kPa	103.42	Chlorides, kg/m3	0.00	
		Mud Weight In, kg/m3	0.00	
Density of the fluid entering the wellbore				
Value for Mud Weight In must be between 718.96 and 2995.66 (kg/m3)				
   				

Figure 9 – MC2: Rheology Input User Interface Screen

2.2. Rheology Measurements: Equipment

2.2.1. FANN - Model 35 Viscometer [19]

The Model 35 Viscometer is the best known and most commonly used as the Standard of the Industry for drilling fluid viscosity.

As true Couette coaxial cylinder rotational viscometer, the test fluid is contained in the annular space or shear gap between the cylinders. Rotation of the outer cylinder at known velocities accomplished through precision gearing. The viscous drag exerted by the fluid creates a torque on the inner cylinder or bob. This torque is transmitted to a precision spring where its deflection is measured and then related to the test conditions and instrument constants.



Figure 10 – FANN Model 35 Viscometer

Direct Indicating Viscometers combine accuracy with simplicity of design and are recommended for evaluating materials that are Bingham plastics. In particular, the Model 35 Viscometer is equipped with factory installed R1 Rotor Sleeve, B1 Bob, F1 Torsion Spring, and a stainless steel sample cup for testing according to American Petroleum Institute Specification RP 13B-1 [20]

Shear stress is read directly from a calibrated scale. Plastic viscosity and yield point of a fluid can be determined easily by making two simple subtractions from the observed data when the instrument is used with the R1-B1 combination and the standard F1 torsion spring.

2.2.2. Rheometer Geometry Considerations

Obviously material functions (the viscosity η , the yield stress τ_0 , storage modules and loss G' , G'' , among others) do not depend on the geometry chosen to measure them. Therefore, rheological tests with two different geometries are expected to deliver the same result. However, this may not be observed in practice, since often one or more of available geometries may not be appropriate for characteristics of the sample question [21]. In this case, assessment of each case and selection of geometry and test type that will provide the most reliable data is required.

In the concentric cylinder (also called Couette or Coaxial geometry), either the inner, outer, or both cylinders may rotate, depending on instrument design. The test fluid is maintained in the annulus between the cylinder surfaces. The double-gap configuration is useful for low viscosity fluids, as it increases the total area,

and therefore the viscous drag, on the rotating inner cylinder, and generally increases the accuracy of the measurement.

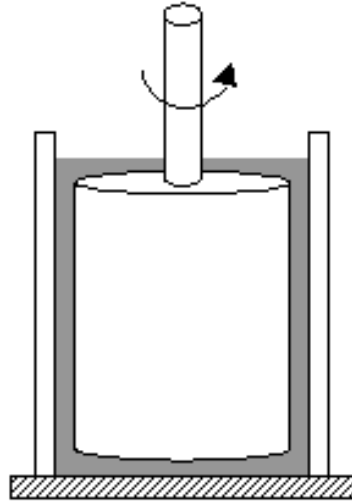


Figure 11 -
Schematic diagram of
basic tool geometries for
the rotational rheometer:
concentric cylinder

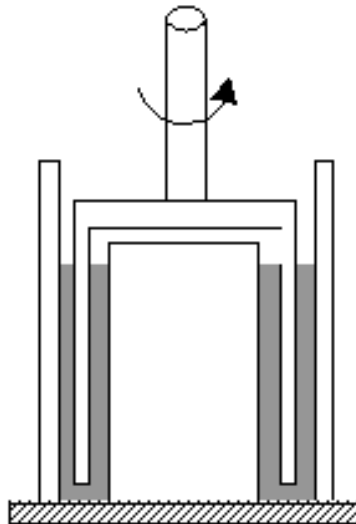


Figure 12 -
Schematic diagram
showing alternative
cylindrical tool design in
cut-away view: Double Gap

The rheometer FANN 35 consists of a single geometry the Couette. Hence, it is objective of this study to evaluate if encompass its applicability for the broad range of drilling fluid samples encountered on Managed Pressure Drilling operations. Further issues are presented to be investigated.

2.2.3. Shear Rate Operating Range – FANN 35 speeds

In the past and the present, conventional drilling applications are concerned to equivalent circulating densities (ECD) at full drilling rates. The ECD generated at the transition from pumps off to pumps on at full drilling rates had not represented a problem, thus never investigated. One reason for that is the conventional drilling maintains a fluid density (mud weight) higher than the pore pressure all times, removing the risk of a kick due to the lack of hydrostatic. As briefly commented on Chapter “1.1. Managed Pressure Drilling Concept”, the MPD allows the utilization of statically underbalance fluid density meaning the hydrostatically only exerted by the drilling fluid will not suffice to balance the pore pressure and an additional pressure at the surface – Applied Surface Back Pressure – plus the friction losses will constitute the terms to balance the well statically.

Under this perspective, Managed Pressure Drilling mandates the full spectrum of ECD's to be investigated for the drilling fluid and well geometry, from a static condition (pumps off) to full drilling rates (ECD drilling), possibly covering and extrapolating the limits offered by a FANN 35 operating range (3rpm as minimum and 600 rpm as maximum).

Pointed out all, becomes clear that the rheological properties obtained from the FANN 35 based on 6 points readings only - six speeds of 600, 300, 200, 100, 6, and 3 rpm – does not suffice completely the MPD requirements by its nature.

As a final point, FANN 35 for several years was the default equipment for oilfield applications as variation in drilling rates had not impacted the operations but implementation of new technologies should evaluate if the measurements reproduced by existing practices and equipment suffice the technique, especially when low flow rates and flow rates variations are critical part of the system.

3

The Thought

“Would you be able to design a wing and not know the air properties?”

3.1.

The Motivation

Successfully drilling challenging wells requires an in-depth understanding of the hydraulics during all phases of the operation. The drilling process is highly dynamic and complicated to model; thus, much of the dynamics have traditionally been neglected. However, with diminishing operational margins, the impact of dynamic effects is growing. Coupled with increasing well construction costs, modeling the dynamics becomes essential and strategically important [22].

3.2.

Thesis Objectives

With the adoption of Managed Pressure Drilling (MPD), the drilling industry is exploring new avenues of annular pressure control. Current drilling practices has reacted to changing wellbore conditions by altering the mud weight according to observed differences in mud volumes (influxes or losses), and via the application of MPD to actively or proactively control the annular pressure profile. To be able to accomplish this goal, this technique may include control of back pressure, fluid density, fluid rheology, annular fluid level, circulating friction and hole geometry, or a combination thereof.

This study ensures that the current methods, standards and equipment are able to satisfy the design of MPD operations in terms of Fluid Rheology Characterization and Pressure Loss estimations.

The following ideas will constitute the goals of the present work:

Identify the shear rates usually seen on 12-1/4" Section and 8-1/2" Section drilling geometries executed by the MPD system at the entire flow rate range;

Assessment of shear rate points measurements as per API RP 13B in the range relevant for its applications (3rpm - 600 rpm);

Evaluation of FANN35 capabilities to characterize the rheology properties of a drilling fluid designed for MPD Applications;

Evaluate Curve Fit Methods proposed by API RP 13D versus Non Linear Regression (NLR), the influence of 6 points vs. "wide range full flow curve" quantifying the variance and its impact on pressure loss estimation;

Leverage the utilization of Computational Fluid Dynamics (CFD) analysis in comparison of API RP 13D Formulas to predict Annular Pressure Losses (APL).

3.3. Scope of Work & Methodology

The issues and aspects of the equipment and methods used to characterize the drilling fluids for MPD Applications as well as the operational aspects that diverge from conventional practices aimed to be investigated.

Three fluid samples will be selected that would suggest a representation of the drilling fluid properties of MPD applications based on field data available from several operations performed by the industry. For each sample, the methodology to be used is to be unfolded as follows.

The sampling will be prepared and the data required to describe a Steady Flow Time (Shear Rate Constant) and Flow Curve (Shear Rate x Shear Stress) will be performed. The Flow Time will be used to identify the time requisite to the sample reach the steady state flow and a reliable measurement acquired. The Flow Curve will map the viscosity across a range of shear rates from which a viscosity value at a shear rate relevant to the process usage conditions can be read.

The measurements of Shear Rate [1/s], Shear Stress [Pa], Viscosity [Pa·s] and Torque [μ Nm] at controlled temperature of 25 [Celsius] will be taken at High Precision Rheometers (HPR) - Anton-Paar Physica MCR301, Anton-Paar Physica MCR 501 and Thermo Scientific Haake Mars II – depending upon availability.

The Flow Curve obtained from HPR will consist of 50 shear rate points ranging between 0.1 to 1000 [1/s]. Then and there, the same sample will be measured at FANN35 following the API Recommended Practice 13B (API RP 13B). A graphical comparison of the readings between the HPR and FANN35 will be used to evaluate the performance of FANN 35 having the HPR as base line for

all the 3 samples in question. All tests will be performed twice to guarantee the reliability and repeatability of the results.

After, the data points will be curve fitted to select the Rheology Model that best represent the fluid sample – in this work, limited to Herschel-Bulkley (HB) and Power Law (PL). As the API Recommended Practice 13D (API RP 13D) suggests a “field” approximation for curve fitting, it also becomes part of the scope of the work to evaluate and compare both cases, the one proposed by API RP 13D against a mathematical NLR, and the discrepancy among them. A brief argument about the implications of curve fitting and single rheology model selection for MPD applications is discussed.

The graphical comparison will be provided followed by the estimation Coefficient of Determination (R^2) to determine the Fluid Rheology Characterization in a laboratory environment using HPR versus conventional FANN35 methods as well as Curve Fitting Techniques – API 13D and NLR. Fluid Rheological Parameters - such as flow index (n) and consistency index (k) - that describes each Rheology Model - PL and HB - will be estimated.

Subsequently, the study will continue to develop by further investigating the Shear Rates presented in two typical annular geometries generally seen MPD application. They will be calculated with the aid of Computational Fluid Dynamics (CFD) by the utilization of the ANSYS Fluent software and compared against the direct formulas suggested in API RP 13D. This step will be done only for the most representative fluid sample; however it will consider the Rheological Parameters obtained from Curve Fitting from NLR and from API RP 13D. As a result of mapping the shear rate range, it will allow to infer the measurement range obtained when API RP 13B is followed (limited 6 points) satisfy or not the MPD requirements of viscosity values and how a wider flow curve would be beneficial.

The geometries for the sake of calculations and model simplicity are defined as 12-1/4” Open Hole Diameter by a drill pipe of 5.5” referred as “12-1/4” Section” and 8-1/2” Open Hole Section by a drill pipe of 5.5” referred as “8-1/2” Section”.

The selection of flow rates will be an approximation of the field conditions usually seen that assures proper hole cleaning and other requirements during drilling operations. The flow rates in the 8-1/2” Section case will vary from 10 [gpm] (which represents a flow velocity and 0.029645 [m/s]) to 400 [gpm] (equivalent to 1.185817 [m/s]). The flow rates in the 12-1/4” Section case will vary from 10 [gpm] (or 0.01039 [m/s]) to 1000 gpm (or 1.03921 [m/s]).

Finally, conclusions will present the Pressure Loss comparison for the 3 conditions on both geometries (12-1/4” and 8-1/2”) below:

1. Rheological Properties measured by FANN35 following the API RP 13B guidelines, curve fitted and HB rheological parameter described by API RP 13D Method and Pressure Loss calculated by API RP 13D direct formula Method.
2. Rheological Properties measured by FANN35 following the API RP 13B guidelines, curve fitted and HB rheological parameter described by API RP 13D Method and Pressure Loss calculated by Fluent ANSYS CFD.
3. Rheological Properties measured by HPR, curve fitted and HB rheological parameter described by NLR Method and Pressure Loss calculated by Fluent ANSYS CFD.

While the comparison between condition 1 and 2 will allow determining the accuracy of API RP 13D Direct Formula Calculation, the comparison between condition 2 and 3 will permit to conclude if Curve Fitting and Equipment should be revisited for MPD Applications.

4 Industry Practices, Equipment and Standards

4.1. Drilling Fluid Characterization according Recommended Practice for Field Testing Water-based Drilling Fluids - ANSI/API RP 13B-1

The scope of API RP 13B is to provide standard procedures for determining the characteristics of water based drilling fluids, among them the viscosity. The latest version - 5th Edition - was issued in March 2009. The errata released in August 2014, although without changes to the Section 6 - Viscosity and Gel Strength. Relevant to note that the API standard is also refereed as ISO 10414-1:2008, Petroleum and natural gas industries—Field testing of drilling fluids— Part 1: Water-based fluids.

Revisiting the API RP 13B, it is found the measurements of viscosity must be done through a direct-indicating viscometer and it shall meet fixed specifications in terms of geometry. It delimits fixed shear rate values to characterize the drilling fluid [1], being the most common 3 – 6 – 100 – 200 – 300 – 600 rpm (5.11 – 10.21 170.23 – 340.46 – 510.69 – 1021.38s⁻¹ respectively)

These 2 aspects restrict the available equipment in the market that can be used for fluid rheology characterization.

The recommended practice also suggests waiting for viscometer dial reading to reach a steady value as the time required is dependent on the drilling-fluid characteristic. Although, it does not recommend the minimum time requirements nor suggests acquiring the information from laboratory.

Overall, the recommended practice does not allow flexibility or adaptability for rheology and applications that may be needed for different device geometries and other shear rate values not available on direct viscometer devices. Moreover, the indication of time to reach the steady reading are often neglected for conventional drilling, but become critical aspect for MPD.

4.2. API Recommended Practice 13D — Rheology and hydraulics of oilwell drilling fluids

The objective of API Recommended Practice 13D (API RP 13D) is to provide a basic understanding of and guidance about drilling fluid rheology and hydraulics, and their application to drilling operations. The latest revision was issued in May 2010 as its sixth edition. The purpose for updating the existing RP, last published in May 2003, is to make the work more applicable to the complex wells. These included: High-Temperature/High-Pressure (HTHP), Extended-Reach Drilling (ERD), and High-Angle Wells (HAW) [17]. Although the revision included complex wells on the 2010 version, MPD Applications was left aside and not addressed.

The API RP 13 D likewise highlight that drilling fluid rheology is important in the following determinations: calculating frictional pressure losses in pipes and annuli, determining equivalent circulating density of the drilling fluid under downhole conditions and determining flow regimes in the annulus, among others.

The discussion of rheology on that document is limited to single-phase liquid flow and some commonly used concepts pertinent to rheology and flow are presented. Mathematical models relating shear stress to shear rate and formulas for estimating pressure losses, equivalent circulating densities and hole cleaning are included.

The following 3 Clauses of API 13 D are relevant to this study: 4 - Fundamentals and fluid models, 5 - Determination of drilling fluid rheological parameters and 7 - Pressure-loss modeling.

4.2.1. API RP 13 D - Clause 4 -Fundamentals and fluid models

Flow Regime Principles are presented along with the turbulent and laminar flow explanation. Importance of viscous forces and inertial forces in the flow are explained and the concept of Reynolds Number in a pipe is introduced and defined.

The Reynolds Number in a Pipe is defined in equation (1):

$$N_{Re} = \frac{dV\rho}{\mu} \quad (1)$$

where:

d is the diameter of the flow channel

V is the average flow velocity

ρ is the fluid density

μ is the fluid viscosity

The concept of Hydraulic Diameter is presented. Later, viscosity (μ), shear stress (τ) and shear rate ($\dot{\gamma}$) are presented for Newtonian fluids along with mathematical relationship of shear stress and shear rate, viscosity.

Still on this Clause, the classification of fluid rheological behavior is publicized: fluids whose viscosity remains constant with changing shear rate are known as Newtonian fluids and Non-Newtonian fluids are those fluids whose viscosity varies with changing shear rate.

In terms of Rheological Models, the API RP 13 D states Rheological models are intended to provide assistance in characterizing fluid flow. No single, commonly-used model completely describes rheological characteristics of drilling fluids over their entire shear rate range. Knowledge of rheological models combined with practical experience is necessary to fully understand fluid behavior. A plot of shear stress versus shear rate (rheogram) is often used to graphically depict a rheological model.

Extracted from the API 13 D, the most common Rheological models are presented. The mathematical treatment of Herschel-Bulkley, Bingham plastic and Power Law fluids is described in Clause 5.

Bingham Plastic Model—This model describes fluids in which the shear stress/shear rate ratio is linear once a specific shear stress has been exceeded. Two parameters, plastic viscosity and yield point, are used to describe this model. Because these parameters are determined from shear rates of 511 s^{-1} (300 rpm) and 1022 s^{-1} (600 rpm) this model characterizes fluids in the higher shear-rate range. A rheogram of the Bingham plastic model on rectilinear coordinates is a straight line that intersects the zero shear-rate axis at a shear stress greater than zero (yield point).

Power Law—The Power Law is used to describe the flow of shear thinning or pseudoplastic drilling fluids. This model describes fluids in which the rheogram is a straight line when plotted on a log-log graph. Such a line has no intercept, so a true Power Law fluid does not exhibit a yield stress. The two required Power Law constants, n and K , from this model are typically determined from data taken at shear rates of 511 s^{-1} (300 rpm) and 1022 s^{-1} (600 rpm). However, the generalized

Power Law applies if several shear-rate pairs are defined along the shear-rate range of interest. This approach has been used in the recent versions of API 13D.

Herschel-Bulkley Model—Also called the “modified” Power Law and yield-pseudoplastic model, the Herschel-Bulkley model is used to describe the flow of pseudoplastic drilling fluids which require a yield stress to initiate flow. A rheogram of shear stress minus yield stress versus shear rate is a straight line on log-log coordinates. This model is widely used because it (a) describes the flow behavior of most drilling fluids, (b) includes a yield stress value important for several hydraulics issues, and (c) includes the Bingham plastic model and Power Law as special cases.

4.2.2.

API RP 13 D - Clause 5 - Determination of Drilling Fluid Rheological Parameters

Measurements of rheological parameters are distinct by the standard to be either by Orifice viscometer (Marsh funnel) and/or concentric-cylinder viscometer divided in Low-temperature, non-pressurized instruments and High-temperature, pressurized instruments.

It is suggested in this section, the rheological model recommended for field and office use as the Herschel-Bulkley (H-B) rheological model. Originally developed in 1926, the model consistently provides good simulation of measured rheological data for both water-based and non-aqueous drilling fluids. According to the API RP 13 D, it has become the drilling industry’s de facto rheological model for advanced engineering calculations.

4.2.2.1.

Herschel-Bulkley Rheological Model

The H-B model requires three parameters as per Herschel-Bulkley rheological model equation defined in equation (2):

$$\begin{array}{ll} \tau = \tau_y + k\dot{\gamma}^n & \tau_y < \tau \\ \dot{\gamma} = 0 & \tau_y > \tau \end{array} \quad (2)$$

Where:

τ – Shear stress, (force/area)

τ_y – Yield point, (force/area)

k – Consistency index, (force/area times time)

$\dot{\gamma}$ – Shear rate, s^{-1}

n – Flow behavior index (dimensionless)

It should be noted that the H-B governing equation reduces to more commonly-known rheological models under certain conditions. When the yield stress τ_y equals the yield point (YP) and the flow index (n) is defined as 1, the H-B equation reduces to the Bingham plastic model. When $\tau_y = 0$ (e.g. a drilling fluid with no yield stress), the H-B model reduces to the Power Law. Consequently, the H-B model can be considered the unifying model that fits Bingham plastic fluids, Power Law fluids, and everything else in between.

4.2.2.1.1. Solution Methods for H-B Fluid Parameters

Solving for drilling fluid H-B parameters using the measurement method [17], [8] involves the following steps:

The true yield stress τ_y can be approximated using measurements from field viscometers. API 13 D suggests approximates the fluid yield stress, commonly known as the low-shear-rate yield point, by the following equation. The τ_y value should be between zero and the yield stress (also known as “Bingham yield point”):

The low-shear-rate yield point is defined in equation (3):

$$\tau_y = 2\theta_3 - \theta_6 \quad (3)$$

The fluid flow index n is defined in equation (4):

$$n = 3.32 \log_{10} \left(\frac{\theta_{600} - \tau_y}{\theta_{300} - \tau_y} \right) \quad (4)$$

The fluid consistency index K is defined in equation (5):

$$k = \frac{(\theta_{300} - \tau_y)}{511^n} \quad (5)$$

4.2.2.2.

Other rheological models used in API 13 D

API 13 D also suggests parameters from the Bingham plastic and Power Law rheological models. As the interest of scope of this study, only the Power Law is cited below.

The model uses two sets of viscometer dial readings to calculate flow index n and consistency index K for pipe flow and annular flow. As concerned, the Power Law Annular Flow is presented. The values obtained using the calculation methods given below will produce values of n and K that are usually significantly different from those calculated using the Herschel-Bulkley rheological model.

The fluid flow index n (Power Law - Annular) as per API 13 D is defined in equation (6):

$$n_a = 0.657 \log_{10} \left(\frac{\theta_{100}}{\theta_3} \right) \quad (6)$$

The fluid consistency index K (Power Law Annular) as per API 13 D is defined in equation (7):

$$k_a = \frac{(\theta_{100})}{170.3^{n_a}} \quad (7)$$

4.2.3.

API RP 13 D - Clause 7 - Pressure-loss modeling

The Clause 7 explores the methods and equations to calculate frictional pressure losses and hydrostatic pressures through the different elements of the circulating system of a drilling well. It is believed the information is suitable for hydraulics analyses, planning, and optimization.

Although it does mentioned that useful for modeling special well-construction operations such as well control, cementing, tripping, and casing runs, it will be later verified in this study it's applicability on MPD Operations.

The subsequent formulas and concepts are replicate to illustrate the method implemented on this study:

- Fluid velocity: Average (bulk) velocities (V_a) in the annulus are inversely proportional to the cross-sectional area of the respective fluid conduit. The Fluid Velocity in the Annulus is defined in equation (8):

$$V_a = \frac{24.51 Q}{d_h^2 - d_p^2} \quad (8)$$

where:

V - Fluid velocity in annulus	[ft/min]
Q -Flow rate	[gal/min]
d_h -Hole diameter or casing inside diameter	[in.]
d_p - Pipe outside diameter	[in.]

- Hydraulic diameter: based on the ratio of the cross-sectional area to the wetted perimeter of the annular section, the annular hydraulic diameter to relate fluid behavior in an annulus is presented in equation (9):

$$d_{hyd} = d_h - d_p \quad (9)$$

4.2.3.1. Shear Rate at the Wall

According to the API 13 D, the Newtonian (or “nominal”) shear rate ($\dot{\gamma}$) first must be converted to shear rate at the wall ($\dot{\gamma}_w$) in order to calculate pressure loss. By using correction factors that adjust for the geometry of the flow conduit and oilfield viscometers used to measure rheological properties – such as FANN35 - , the appropriate corrections are combined into a single factor, labeled as “G”. This technique was proposed by Zamora et all in 1974 [23]:

- **Well geometry shear-rate correction:** Shear-rate correction for well geometry B_a is also dependent on the rheological parameter n . It is convenient to use a geometry factor α so that flow in pipes and annuli can be considered in a single expression. For simplicity without significant loss of accuracy, the annulus can be treated as an equivalent slot ($\alpha =1$). The Well geometry shear-rate correction is defined in equation (10):

$$B_a = \left[\frac{(3 - \alpha)n + 1}{(4 - \alpha)n} \right] \left[1 + \frac{\alpha}{2} \right] \quad (10)$$

where

$\alpha = 0$ is the geometry factor in the pipe

$\alpha = 1$ is the geometry factor in the annulus

- **Field viscometer shear-rate correction:** Unfortunately, closed analytical solutions do not exist for Herschel-Bulkley fluids, and complex numerical methods are inaccurate at very low shear rates. Practically speaking, it can be assumed that the viscometer correction $B_x \approx 1$. Otherwise, if Power Law Fluids, the following formula can be used if desired to preserve the exact solution. The Field viscometer shear-rate correction is defined in equation (11):

$$B_x = \left[\frac{x^{2/\eta_p}}{\eta_p x^2} \right] \left[\frac{x^2 - 1}{x^{2/\eta_p - 1}} \right] \approx 1 \quad (11)$$

where

$x = 1.0678$ in the standard bob/sleeve combination R1B1 [dimensionless]

B_x Viscometer geometry correction factor [dimensionless]

- **Combined geometry shear-rate correction factor:** Shear rate at the wall (γ_w) required to determine the shear stress at the wall is calculated by multiplying nominal shear rate by the geometry factor **G**. The Combined geometry shear-rate correction factor is defined in equation (12).

$$\gamma_w = \frac{1.6GV}{d_{hyd}} \quad (12)$$

where

G Geometry shear-rate correction (Herschel-Bulkley fluids)
[dimensionless]

V Velocity [ft/min]

d_{hyd} Hydraulic diameter [in.]

- **Shear stress at the wall (flow equation):** Frictional pressure loss is directly proportional to the shear stress at the wall τ_w defined by the fluid-model dependent flow equation. Flow equations for Bingham-plastic and Herschel-Bulkley fluids are complex and require iterative

solutions; however, they can be approximated by an expression of the same recognizable form as the respective constitutive equations. The Shear stress at the wall in viscometer units is defined in equation (13) and the shear stress at the wall in engineering units is defined in equation (14):

$$\tau_f = \left(\frac{4-\alpha}{3-\alpha} \right)^n \tau_y + k \gamma_w^n \quad (13)$$

$$\tau_w = 1.066 \tau_f \quad (14)$$

4.2.3.2.

Flow regime: Reynolds number (generalized)

Generalized Reynolds number N_{ReG} applies to both pipes and annuli [17], [24]. The most convenient form of the equation involves the shear stress at the wall.

The Generalized Reynolds Number is defined in equation (15).

$$N_{ReG} = \frac{\rho V^2}{19.36 \tau_w} \quad (15)$$

where

ρ	Fluid density	lbm/gal
V	Velocity	ft/min
τ_w	Shear stress at the wall	lbf/100 ft ²

4.2.3.3.

Critical Reynolds number (laminar to transitional regimes)

The critical Reynolds number N_{CRe} is defined by API 13 D as the value of N_{ReG} where the regime changes from laminar to transitional flow.

The Critical Reynolds number is defined in equation (16):

$$N_{CRe} = 3470 - 1370n \quad (16)$$

4.2.3.4. Friction factor

Pressure loss in pipes and annuli is proportional to the fanning friction factor f , which is a function of generalized Reynolds number, flow regime, and fluid rheological properties. Laminar-flow friction factors f_{lam} for pipes and concentric annuli are combined into a single relationship when using the generalized Reynolds number N_{ReG} .

The Laminar-flow friction factor is defined in equation (17):

$$f_{lam} = \frac{16}{N_{ReG}} \quad (17)$$

4.2.3.5. Laminar-flow pressure loss

Frictional pressure losses in the drillstring and annulus are equal to the sum of the losses in the individual segments. The fanning equation is used to calculate incremental pressure losses; however, the various parameters should be defined for each segment in the drillstring and annulus.

The Laminar-flow pressure loss is defined in equation (18):

$$P_a = \sum \frac{1.076 \rho_a V_a^2 f L}{10^5 d_{hyd}} \quad (18)$$

4.2.3.5.1. Laminar-flow pressure loss (special case)

Substitution of the laminar-flow friction factor f_{lam} into the general equations yields simplified relationships for laminar-flow pressure loss that also can be derived by force-balance analysis [17], [3]. The individual parameters should be defined for each well segment.

The special case for Laminar-flow pressure loss is defined in equation (19):

$$P_a = \sum \frac{\tau_w L}{300 d_{hyd}} \quad (19)$$

4.3. Standard Oilfield Viscometer Correction Factors

In the mathematics of fluid rheology as measured using a standard oilfield viscometer, there are instrument conversion factors that need to be applied in the calculations. [19]

a) *Shear stress (lbf/100 ft²) is determined by multiplying the dial reading (° deflection) by 1.066. This correction is sometimes ignored in doing simple calculations.*

Relevant to highlight that is found in this study that the correction factor must only be applied when the combination of spring-bob-rotor F1 - B1 - R1 is used on FANN 35 devices. According to the FANN 35 Operations Manual [19], Indexes F1 - B1 - R1 will composed the following constants:

k1 - Torsion Spring Constant [Dynes/cm/degree deflection]: 386

k2 - Shear Stress constant for the effective bob surface [cm³]: 0.01323

k3 - Shear Rate Constant [1/s /rpm]: 1.7023

Therefore, the 1.066 factor to obtain the shear stress from the deflection is resultant from the k1 - Torsion Spring Constant times the k2 - Shear stress constant for the effective bob surface times the conversion value from Pascals to (lbf/100 ft²) (noted 2.08854342). Field personnel must pay attention if other combination of spring-bob-rotor is used, as the deflection to shear-stress factor must be revised.

On this study, as accuracy is aimed, the value (with 6 decimals) of 1.066573 is used.

b) *Shear rate (s⁻¹) is determined by multiplying the rotor speed (r/min) by 1.7023.*

5 Fluid Characterization

5.1. Fluids Selection and Preparation

5.1.1. Fluid Selection Criteria

Water-based fluids (WBFs) are used to drill approximately 80% of all wells. The base fluid may be fresh water, seawater, brine, saturated brine, or formate brine. The type of fluid selected depends on anticipated well conditions or on the specific interval of the well being drilled [25]. Xanthan gum is often used in most types of water-based fluids and as it provides excellent carrying and suspending characteristics.

It also represents a versatile rheology control in a wide range of brines, drilling and fracturing fluids. Xanthan gum is considered non-hazardous and suitable for use in environmentally sensitive locations and applications. Another important characteristic of Xanthan Gum is readily disperses and can be mixed into water under low shear conditions without the formation of lumps and “fisheyes” often seen with non-dispersible polymers.

Due to those reasons, Xanthan Gum was chosen as a representative fluid to evaluate the performance of field viscometer FANN 35 in comparison with high precision viscometers.

5.1.1.1. Viscosity Range and Concentration Criteria

In terms of the concentration, a brief historical analysis was performed to better identify the range of viscosity most common in MPD Applications and then validate the selection of two Xanthan Gum concentrations - 0.1% and 0.8% - in an effort to ensure representativeness for the experiment. Mud rheology field data recorded from FANN 35 readings from several field operations in Brazil that used

water based drilling fluids was retrieved from the available IADC Daily Drilling Reports.

The rheograms are shown in Figure 13 and plotted against the planned Xanthan Gum Concentration of 0.1% and 0.8%. In addition, an actual sample of Low Lime Water Based Fluid (labeled as LLMEG) recently used in a MPD Operation carried out in Brazil during the 2013/2014 was used as baseline to ensure that the historical data matched with the range of viscosities observed in the field.

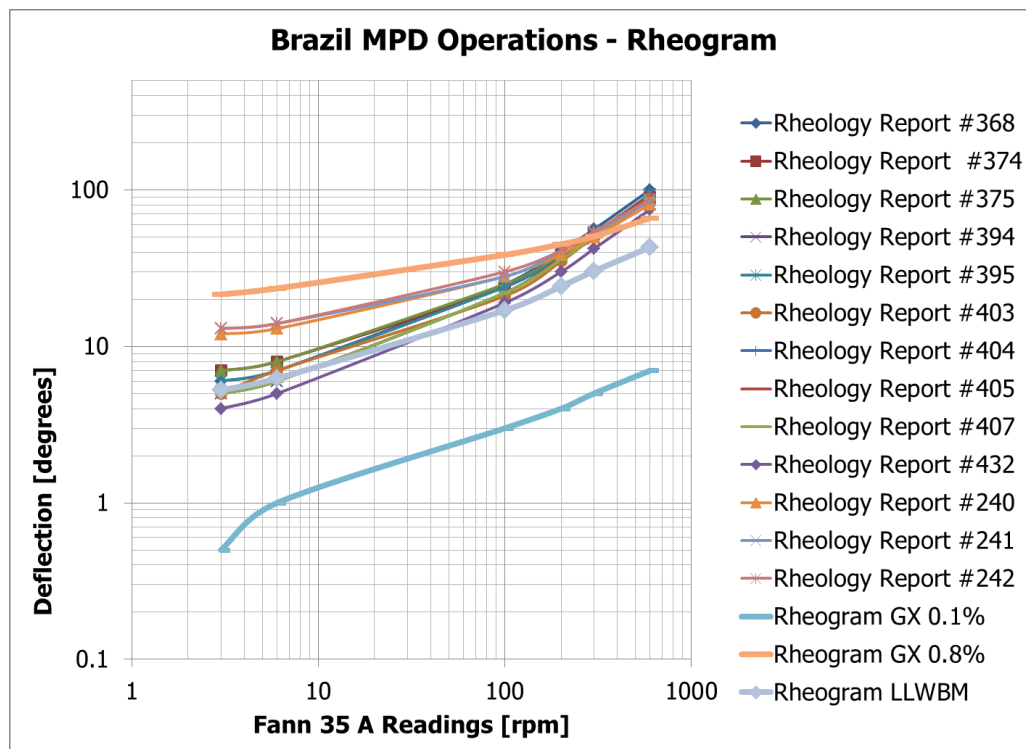


Figure 13 - Brazil MPD Operations Rheogram: IADC Historical Field Data

5.1.2. Xanthan Gum preparation

The following recipe and list of materials were used to prepare the Xanthan Gum at concentrations of 0.1% and 0.8% according to Table 1 and Table 2

Materials

- Bucket
- 3 beaker glass
- Spatula
- Analytical Balance
- Mechanical mixer
- Impeller type anchor

Reagents

- Xanthan Gum
- Water Deionized
- Sodium Benzoate
- Potassium sorbate

Table 1 - Xanthan Gum 0.1% Recipe

	%	mass (g)
Xanthan Gum	0.10%	3
Water Deionized		2997
Solution	-	3000
Potassium sorbate	0.50%	15.00
Sodium Benzoate	0.50%	15.00

Table 2 - Xanthan Gum 0.8% Recipe

	%	mass (g)
Xanthan Gum	0.80%	24
Water Deionized		2976
Solution	-	3000
Potassium sorbate	0.50%	15.00
Sodium Benzoate	0.50%	15.00

Procedure

1. Weigh reagents according to concentration (see table) to be used;
2. Place the bucket of water on the mechanical shaker (Fisaton, model 723) with the anchor blade, using the rotation of 300 rpm;
3. Carefully add the heavy xanthan gum, lest disperse too (hint: play between the blade and the wall of the bucket);

4. Stir this rotation for 15 minutes;
5. Add the heavy bactericidal and stir for 1 hour;
6. Let stand 24 hours before testing.



Figure 14 – Preparation of Xanthan Gum in the Mechanical Shaker at 300 rpm



Figure 15 – Xanthan Gum being stirred

After the samples were prepared, they were divided in bottles and labeled (Figure 16) in preparation to be shipped and used in the different laboratories and devices.

Important to note that it was observed an expiration date of 7 days in the Xanthan Gum, even with the addition of stabilizers and preservatives..



Figure 16 – Xanthan Gum bottle samples

5.2. Measurements of Rheological Properties

5.2.1. Equipment and Laboratories

The Equipment and Laboratories utilized to measure the rheological properties of the 3 selected fluids were done in three different locations:

- at Petrobras Research Center “CENPES”
 - “Fann 35 - CENPES - F1 B1 R1”: Viscometer FANN 35 using the combination of bob-rotor-spring “F1 B1 R1” strictly according to the guidelines of API RP 13B and API RP 13D.
- at Pontifical Catholic University of Rio de Janeiro - Fluid-Rock Interaction Laboratory (LIRF) Technology Group and Petroleum Engineering Department of Civil Engineering (GTEP)
 - “Fann 35 - PUC - F1 B1 R1”: Viscometer FANN 35 using the combination of bob-rotor-spring “F1 B1 R1” strictly according to the guidelines of API RP 13 B and API 13 API D.
- at Rheological Characterization Laboratory - Rheology Group (GReo) at Pontifical Catholic University of Rio de Janeiro.
 - Anton Paar - Physica MCR 501 as geometry selected the Double Gap DG#26.7
 - Anton Paar - Physica MCR 301 as geometry selected the Cross Hatch PP50/P2



Figure 17 - Anton Paar - Physica MCR 301

5.2.2. Tests and Methodology

Flow Curve (Shear Rate x Shear Stress): In order to determine the general flow behavior of a sample the viscosity is measured as a function of the shear rate in a rotational rheometer. For the presentation of the data either the viscosity or the shear stress is plotted against the shear rate for steady state regime. The thus obtained graph is called flow curve. It shows the flow behavior for low shear rates (slow motions) as well as high shear rates (fast motion).

The flow curves obtained from FANN35 Viscometers were performed following the API 13 B and API 13 D Recommended Practices. The sample's temperature was kept at 25 Celsius through the entire experiment.

The flow curves range performed at Physica's Rheometers (MC 301 and 501) were set from 0.1 to 1000 s^{-1} and data 50 points. Although the API RP lowest shear rate is 5.11 s^{-1} , it is relevant to MPD flow rate transitions and connections the observation of flows at low shear rates, hence the decision to evaluate as the minimum value of 0.1 s^{-1} , observed equipment limitations. Temperature was also controlled at 25 Celsius.

Torque and equipment's range of operations and limitations were verified on all cases.

Steady Flow Time (Shear Rate Constant): The viscosity has to be obtained at different shear rates, and it's critical to define the time to reach equilibrium at any given shear rate. It is known that the time to reach the steady state increases as the shear rate decreases. Therefore, a 'Single Point Test' was run at lowest shear rate to determine 'delay before measure' for steady rate sweep and the time

to reach the equilibrium is used as 'delay before measurement'. As higher shear rates will require less time to reach equilibrium that will ensure all data acquired was collected under steady state conditions in addition to shorten experiment time.

5.2.3. Rheology Measurements Results

5.2.3.1. Steady Flow Time Tests

Steady Flow Time Tests were conducted for all samples using Physica's Rheometers (MC 501 and 301) since it allows for programmable test parameters and for the duration to reach more than 2000 seconds in few cases.

Four different shear rate tests were performed using Xanthan Gum 0.1%. The rates were 0.1, 2.5, 5 and 10 s^{-1} ; and each sample stabilized in approximately 10 seconds. Two tests, both at 1.0 s^{-1} , were performed using Xanthan Gum 0.8%, and again stabilized at 10 seconds. Finally, two 1.0 s^{-1} , shear rate tests were performed on Low Lime samples and it required almost 100 seconds before the stabilization was reached.

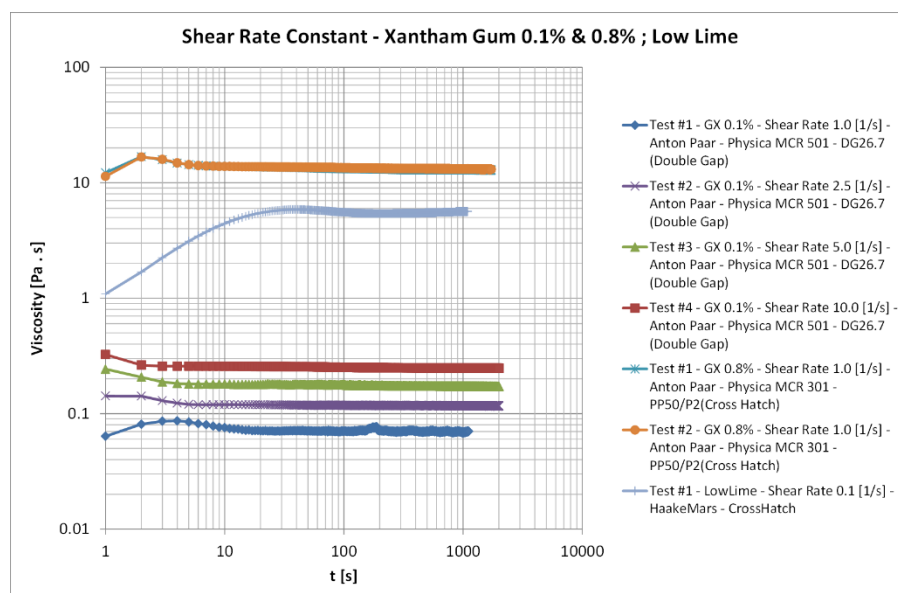


Figure 18 - Steady State Flow Behavior Test: Equilibrium time and Flow Curve Optimization

Prior to determining the viscosity at different shear rates, it was important to define the time to reach equilibrium for a given shear rate. The steady flow time determines the delay that must be applied prior a reading is taking during the rheogram. Optimizing the delay will lead to a faster flow curve experiment and will ensure that the measurement points are obtained at a steady state condition.

The stabilization time found on this test was then used on the subsequent flow curves for each respective fluid sample.

As a remark, API RP 13B advises to “wait for the viscometer dial reading to reach a steady value (the time required is dependent on the drilling fluid characteristics)”. However, based on the results gained from the Steady State Flow Behavior Test, equilibrium time must be closely observed. There is a risk of jeopardizing the entire fluid characterization test when completed under field conditions.

5.2.3.2. Flow Curve Tests

Figure 19 to Figure 24 represent combined results from flow curves obtained from FANN35 and Physica’s Rheometers (MC 501 and 301). The flow curves range performed at Physica’s Rheometers were set from 0.1 to 1000 s⁻¹ and 50 data points. Even though API recommended lowest shear rate is 5.11 s⁻¹, for MPD applications lower shear rates might be observed, hence the decision to evaluate as the minimum value of 0.1 s⁻¹, observed equipment limitations.

Rheogram results for all three samples (Xanthan Gum 0.1%, Xanthan Gum 0.8% and Low Lime Water Based Mud (LL WBM) were compared with the graphical results being presented in Figure 19 through Figure 24.

Xanthan Gum 0.1%

- 3 readings Fann 35 - CENPES - F1 B1 R1.
- 2 readings Fann 35 - PUC - F1 B1 R1.
- 3 readings Anton Paar - Physica MCR 501 - DG26.7 (Double Gap).

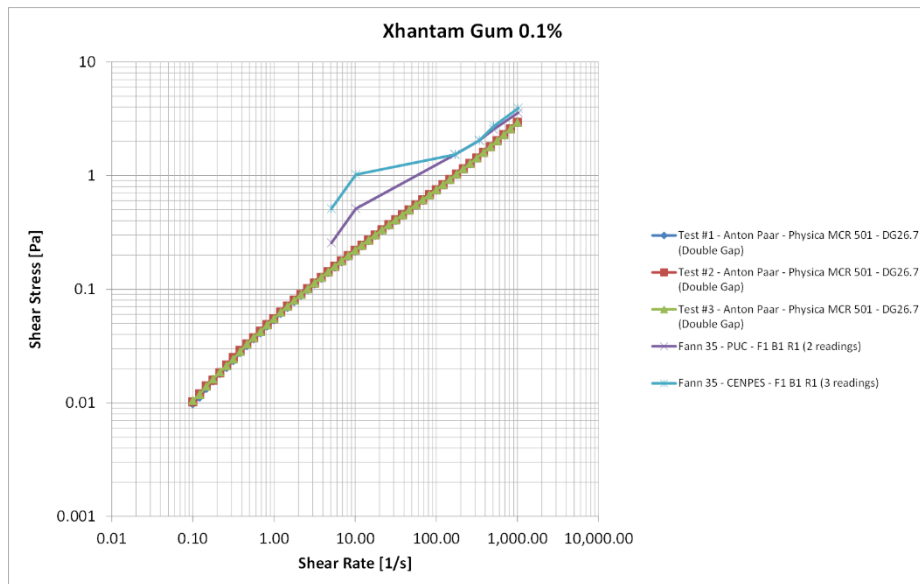


Figure 19 - Flow Curve: Xanthan Gum 0.1% - Shear Stress vs. Shear Rate

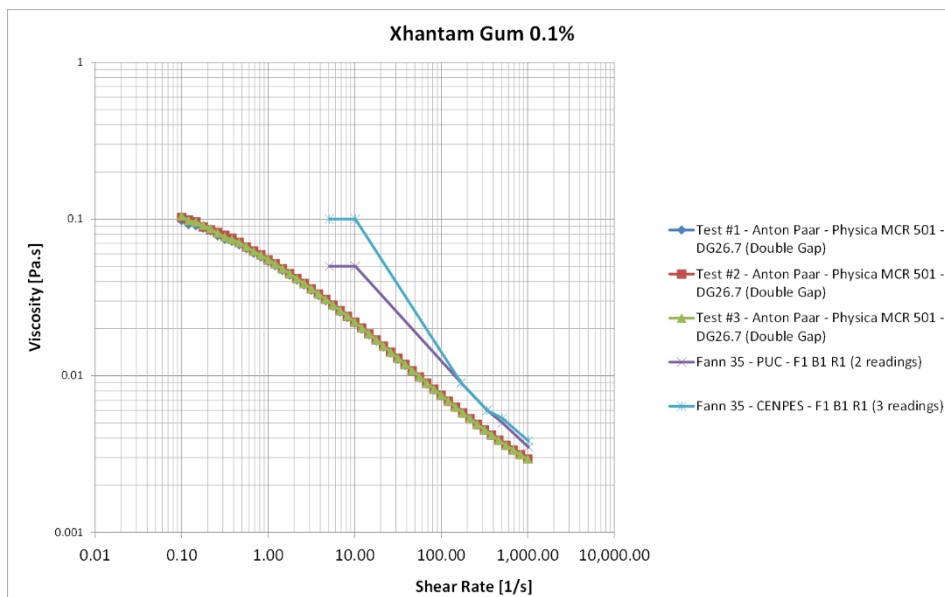


Figure 20 - Flow Curve: Xanthan Gum 0.1% - Viscosity vs Shear Rate

Xanthan Gum 0.8%

- 2 readings Fann 35 - PUC - F1 B1 R1.
- 3 readings Anton Paar - Physica MCR 301 - Cross Hatch PP50/P2.

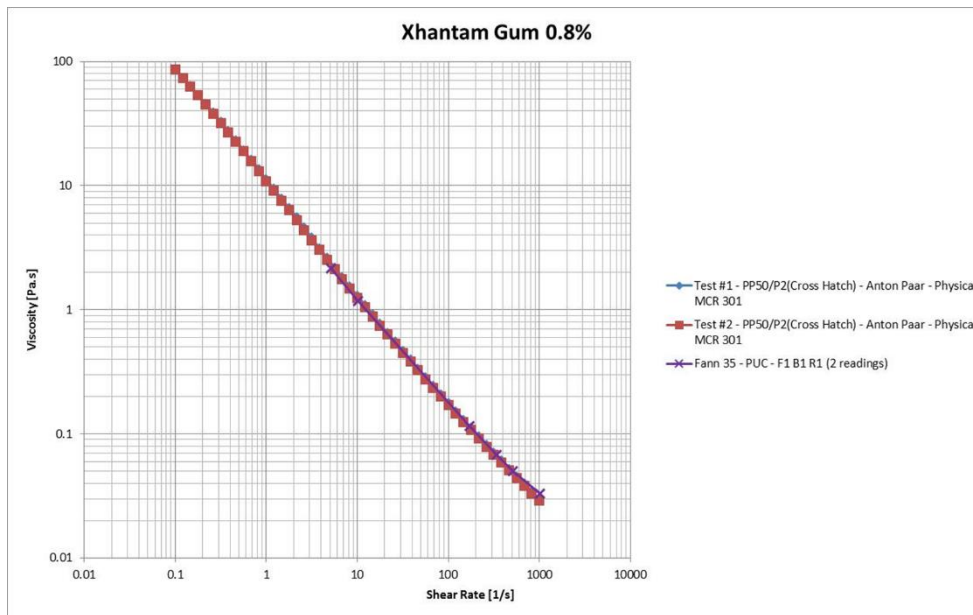


Figure 21 - Flow Curve: Xanthan Gum 0.8% - Viscosity vs. Shear Rate

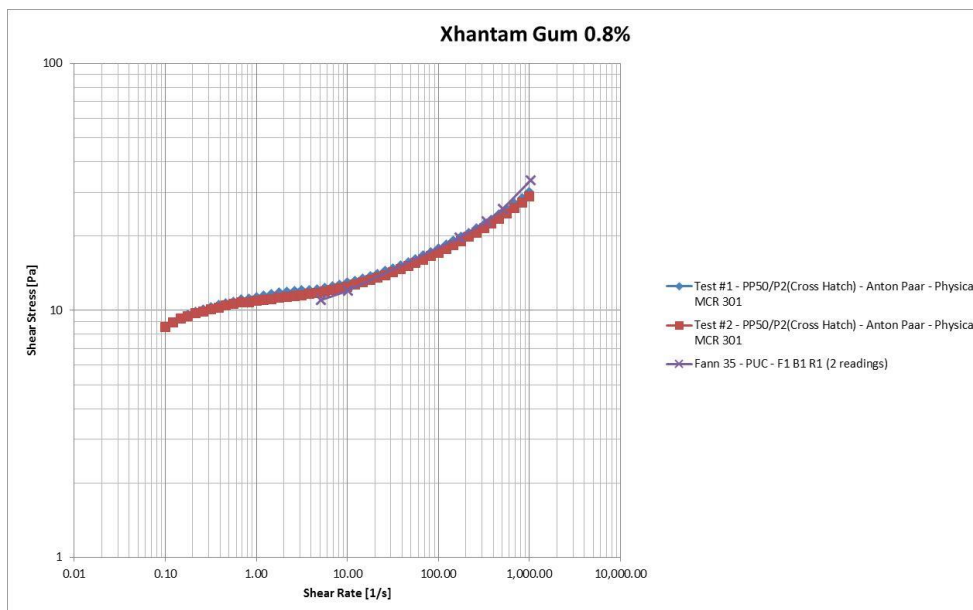


Figure 22 - Flow Curve: Xanthan Gum 0.8% - Shear Stress vs Shear Rate

Low Lime Water Based Mud

- 2 readings Fann 35 - PUC - F1 B1 R1.
- 3 readings Anton Paar - Physica MCR 301 - Cross Hatch PP50/P2.

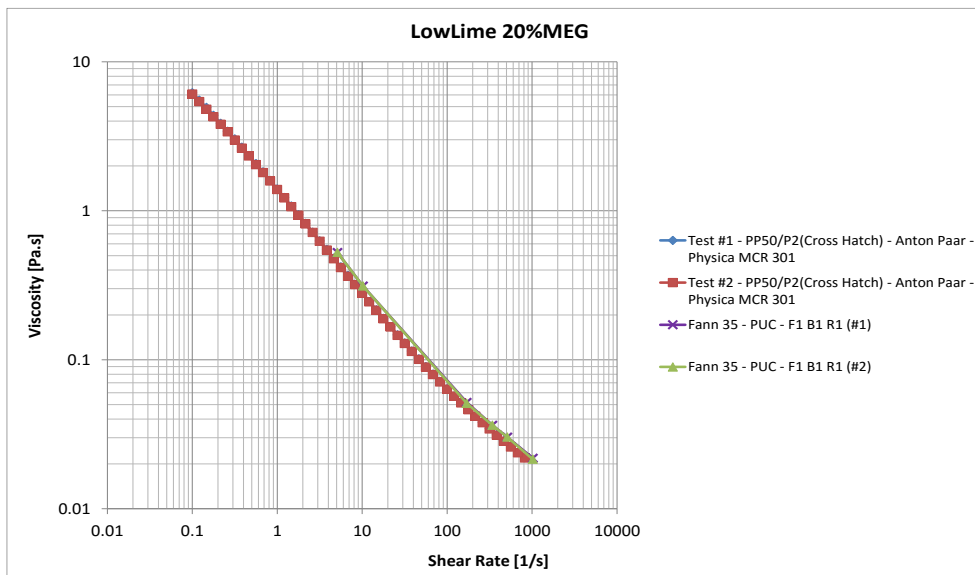


Figure 23 - Flow Curve: Low Lime WBM - Viscosity vs. Shear Rate

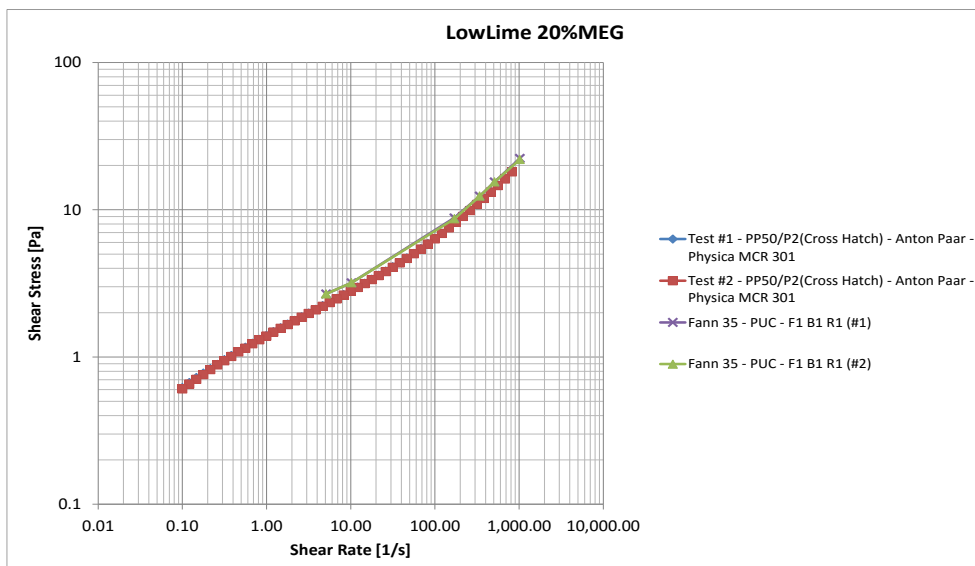


Figure 24 - Flow Curve: Low Lime WBM - Shear Stress vs Shear Rate

5.2.3.3. Evaluation of FANN 35 Performance

In the respect of the statement from API RP 13 B, “wait for the viscometer dial reading to reach a steady value (the time required is dependent on the drilling fluid characteristics)” it becomes clear that based on the results of Steady State Flow Behavior Test, the equilibrium time must be always observed, with the risk of jeopardize the entire fluid characterization when this is done under field conditions.

While the rheograms results for all 3 samples were compared, it is fair to say results obtained using the FANN 35 and the Physica for Xanthan Gum 0.8% and Low Lime WBM are similar. The results achieved by FANN 35 were satisfactory when within its range capabilities.

For the very low rheology fluids, in this testing, Xanthan Gum 0.1%, results from the FANN 35 do not correspond with Physica's results as the second presents superior performance for dealing with low viscosity fluids.

A possible cause for the reading discrepancies between FANN 35 and the Physica rheometer when evaluating the 0.1% concentration could be attributed to the physical geometry of the rotational rheometer. As the selection of the geometry - Couette, plate-cone and plate-plate - are dependent on three factors: the type of fluid, the viscosity range and strain rate [26].

Whereas the cross hatched geometry (Figure 25) comprises of grooves etched into the inner surfaces of the plates thus preventing the sliding of material observed when a smooth surface is used.

While, the plate-plate cross hatch PP50/2 type was selected for Physica's test, the Couette was the standard configuration for the FANN35.



Figure 25 - Cross Hatch Geometry

Another possible reason for the disparity in results when testing the Xanthan Gum 0.1% could be the low shear rate itself. 3 rpm (5.11 s^{-1}) and 6 rpm (10.21 s^{-1}) are very much at the low-end capability of the FANN 35 specified operating range as indicated on Table 3 and Table 4.

Table 3 - Xanthan Gum 0.1% - Fann 35 - CENPES - F1 B1 R1 (3 readings average)

Xanthan Gum 0.1 %	
Fann 35 - CENPES - F1 B1 R1	
Rotation [rpm]	Deflection [degrees]
600	7.67
300	5.33
200	4.00
100	3.00
6	2.00
3	1.00

Table 4 - Xanthan Gum 0.1% - Fann 35 - PUC - F1 B1 R1 (2 readings average)

Xanthan Gum 0.1 %	
Fann 35 - PUC - F1 B1 R1	
Rotation [rpm]	Deflection [degrees]
600	7.00
300	5.00
200	4.00
100	3.00
6	1.00
3	0.50

5.2.3.4. Representativeness of Chosen Fluid Samples

For this study purposes, it was important to verify that the three chosen fluid samples – 0.1% Xanthan Gum , 0.8% Xanthan Gum and Low Lime WBM - were a representative sample of ‘real’ WBM drilling fluid used in MPD operations.

To achieve this, data recorded using the FANN 35 rheometer from actual wells in Brazil was plot against the three muds tests as characterized in Figure 13 - Brazil MPD Operations Rheogram: IADC Historical Field Data compares the test muds with the actual field muds used.

Due to the lack of representativeness of 0.1% Xanthan Gum as a possible MPD drilling fluid, the 0.1% Xanthan gum was then removed from all further testing.

The FANN 35 rheometer applicability must be further investigated for testing very low rheology fluids. Also, the identification of lower limits of very low rheology fluids used for drilling MPD by obtaining additional historical data from similar operations.

Moreover, it is suggested for future works the study of applicability of FANN 35 performances in higher viscosities ranges than the ones found in Xanthan Gum 0.1%, such as 0.3% or 0.5%, in attempt to identify where it can be used with confidence and results accurately enough to real rheological properties.

5.3. Drilling Fluid Model Characterization

5.3.1. Curve Fitting Influence

The definitions of curve fitting², interpolation and extrapolation becomes serious as a point of matter as one of the objectives is to evaluate the boundary limits - 3 rpm and 600 rpm - in terms of shear rates when characterizing drilling fluids in the field. The implications of those limits are later discussed in this chapter.

5.3.2. Solving the Rheological Parameters with Nonlinear Regression

Although the API RP 13 D Clause 5 also point out solving the parameters using numerical techniques, a Nonlinear Regression (NLR) software package – Kaleida Graph – was utilized to calculate them for PL and H-B models.

In statistics, NLR is a form of regression analysis in which observational data are modeled by a function, which is a nonlinear combination of the model parameters and depends on one or more independent variables. The data are fitted by a method of successive approximations.

The curve fitting software Kaleida Graph supports both linear and nonlinear curve fitting. Nonlinear curve fitting was accomplished through general curve fit. The equations for PL Model (n and K) and H-B Model (n, K and To) were set and the

² Curve fitting [30] is known as the process of constructing a curve, or mathematical function that has the best fit to a series of data points, possibly subject to constraints. Curve fitting can involve either interpolation, where an exact fit to the data is required, or smoothing, in which a "smooth" function is constructed that approximately fits the data. A related topic is regression analysis, which focuses more on questions of statistical inference such as how much uncertainty is present in a curve that is fit to data observed with random errors. Fitted curves can be used as an aid for data visualization, to infer values of a function where no data are available, and to summarize the relationships among two or more variables. Extrapolation refers to the use of a fitted curve beyond the range of the observed data, and is subject to a degree of uncertainty since it may reflect the method used to construct the curve as much as it reflects the observed data.

variables retrieved for all readings listed on 5.2.3.2. Flow Curve Tests of Xanthan Gum 0.8% and the Low Lime WBM:

- Xanthan Gum 0.8%
 - “Test #1 - PP50/P2(Cross Hatch) - Anton Paar - Physica MCR 301”
 - “Test #2 - PP50/P2(Cross Hatch) - Anton Paar - Physica MCR 301”
 - “Fann 35 - PUC - F1 B1 R1” (3 equal readings)
- Low Lime WBM
 - Test #1 - PP50/P2(Cross Hatch) - Anton Paar - Physica MCR 301
 - Test #2 - PP50/P2 (Cross Hatch) - Anton Paar - Physica MCR 301
 - Test #1 - “Fann 35 - PUC - F1 B1 R1”
 - Test #2 - “Fann 35 - PUC - F1 B1 R1”

In addition, the coefficient of determination, denoted R^2 , was calculated for all cases. The coefficient of determination was used to indicate how well the data fitted the model. To note, an R^2 of 1 indicates that the regression line perfectly fits the data, while an R^2 of 0 indicates that the line does not fit the data at all. It provides a measure of how well observed outcomes are replicated by the model, as the proportion of total variation of outcomes explained by the model.

5.3.2.1. Xanthan Gum 0.8%

5.3.2.1.1. “Test #1 - PP50/P2(Cross Hatch) - Anton Paar - Physica MCR 301”

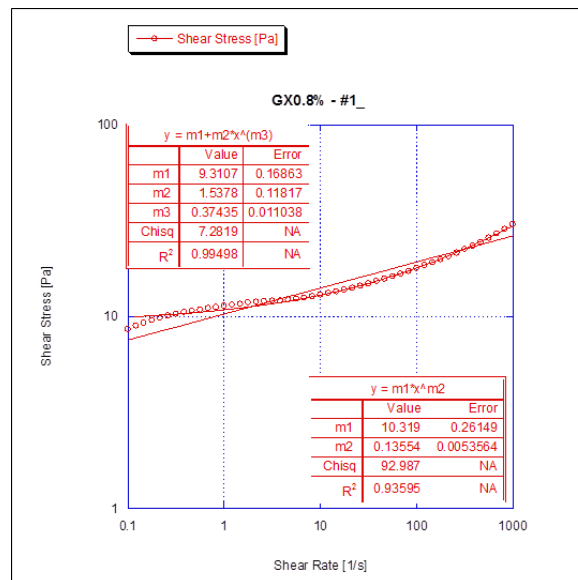


Figure 26 - Kaleidagraph NLR – Xanthan Gum 0.8% - “Test #1 - PP50/P2(Cross Hatch) - Anton Paar - Physica MCR 301”

Table 5 - Rheological Parameters: PL Model - NLR Method - Xanthan Gum 0.8% Test#1

Curve Fit: Power-Law (Test #1)	
K	10.319000
n	0.135540
R ²	0.935950

Table 6 - Rheological Parameters: H-B Model - NLR Method - Xanthan Gum 0.8% Test#1

Curve Fit: Herschel-Bulkley (Test #1)	
τ_0	9.310700
K	1.537800
n	0.374350
R ²	0.994980

5.3.2.1.2.

“Test #2 - PP50/P2(Cross Hatch) - Anton Paar - Physica MCR 301”

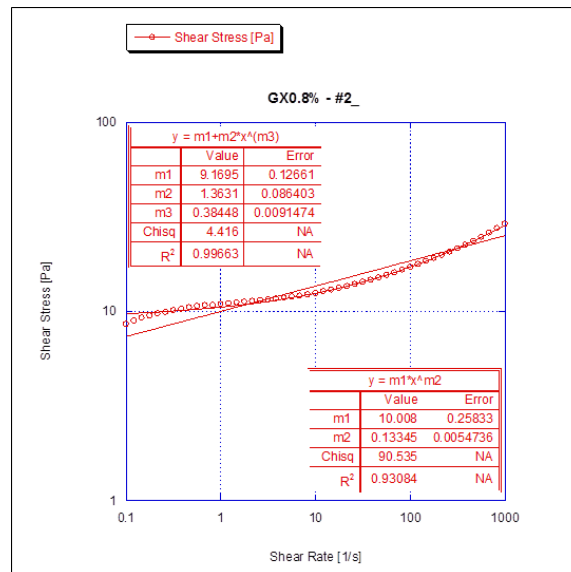


Figure 27 - Kaleidagraph NLR – Xanthan Gum 0.8% - “Test #2 - PP50/P2(Cross Hatch) - Anton Paar - Physica MCR 301”

Table 7 - Rheological Parameters: PL Model - NLR Method - Xanthan Gum 0.8% Test#2

Curve Fit: Power-Law (Test #2)	
K	10.008000
n	0.133450
R ²	0.930840

Table 8 - Rheological Parameters: H-B Model - NLR Method - Xanthan Gum 0.8% Test#2

Curve Fit: Herschel-Bulkley (Test #2)	
τ_0	9.169500
K	1.363100
n	0.384480
R ²	0.996630

5.3.2.1.3.
 “Fann 35 - PUC - F1 B1 R1”

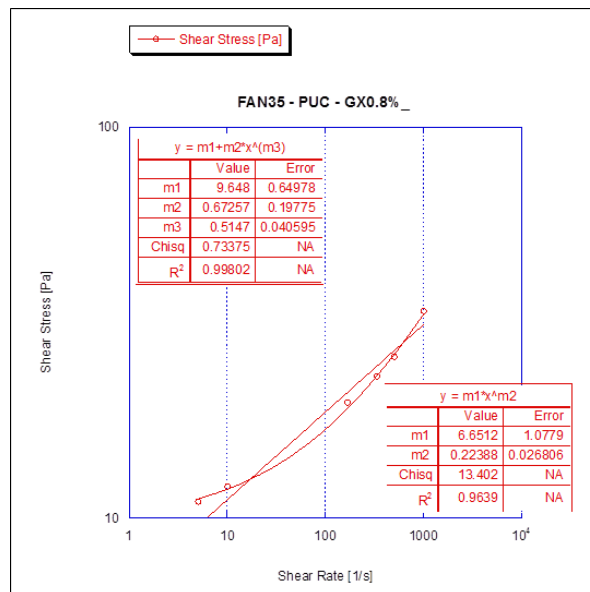


Figure 28 - Kaleidagraph NLR – Xanthan Gum 0.8%
 - “Fann 35 - PUC - F1 B1 R1”

Table 9 - Rheological Parameters: PL Model - NLR Method - Xanthan Gum 0.8% - Fann 35 PUC

Curve Fit: Power-Law (Fann 35 - PUC)	
K	6.651200
n	0.223880
R ²	0.963900

Table 10 - Rheological Parameters: H-B Model - NLR Method - Xanthan Gum 0.8% - Fann 35 PUC

Curve Fit: Herschel-Bulkley (Fann 35 - PUC)	
τ_0	9.648000
K	0.672570
n	0.514700
R ²	0.998012

5.3.2.2. Low Lime WBM

5.3.2.2.1. Test #1 - PP50/P2(Cross Hatch) - Anton Paar - Physica MCR 301

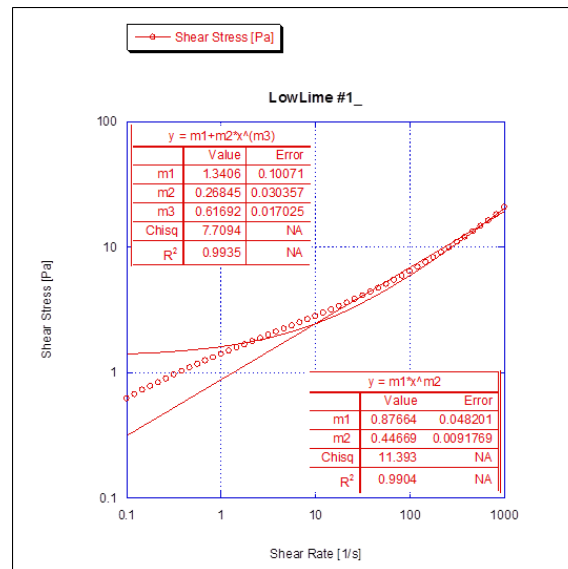


Figure 29 - Kaleidagraph NLR – Low Lime WBM - “Test #1 - PP50/P2(Cross Hatch) - Anton Paar - Physica MCR 301”

Table 11 - Rheological Parameters: PL Model - NLR Method – Low Lime WBM - Test#1

Curve Fit: Power-Law (Test #1)	
K	0.876640
n	0.446690
R ²	0.9904

Table 12 - - Rheological Parameters: H-B Model - NLR Method - – Low Lime WBM - Test#1

Curve Fit: Herschel-Bulkley (Test #1)	
τ_0	1.340600
K	0.268450
n	0.616920
R ²	0.9935

5.3.2.2.2.

Test #2 - PP50/P2 (Cross Hatch) - Anton Paar - Physica MCR 301

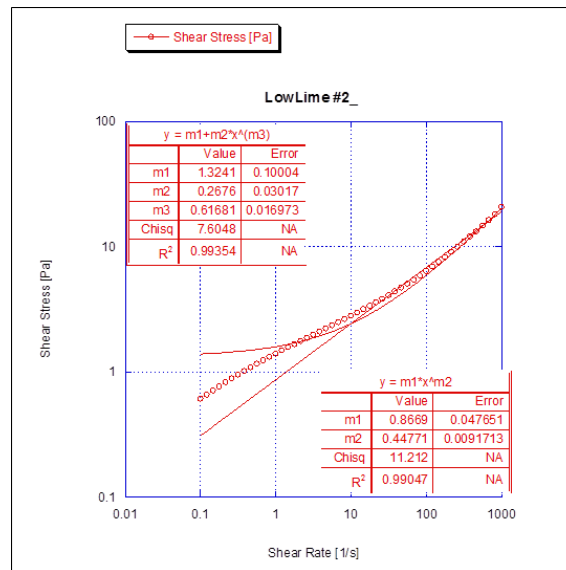


Figure 30 - Kaleidagraph NLR – Low Lime WBM -
 “Test #2 - PP50/P2(Cross Hatch) - Anton Paar -
 Physica MCR 301”

Table 13 - Rheological Parameters: PL Model - NLR Method – Low Lime WBM - Test#2

Curve Fit: Power-Law (Test #1)	
K	0.866900
n	0.447710
R ²	0.99047

Table 14 - Rheological Parameters: H-B Model - NLR Method – Low Lime WBM - Test#2

Curve Fit: Herschel-Bulkley (Test #1)	
τ_0	1.324100
K	0.267600
n	0.626810
R ²	0.99354

5.3.2.2.3.
Test #1 - “Fann 35 - PUC - F1 B1 R1”

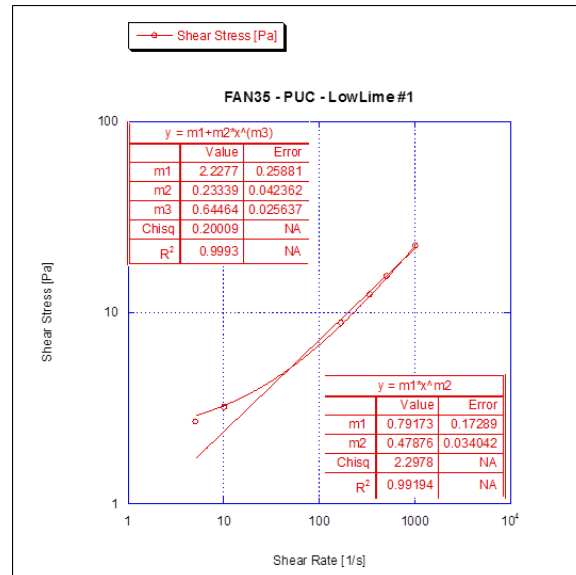


Figure 31 - Kaleidagraph NLR – Low Lime WBM - “Fann 35 - PUC - F1 B1 R1” – Test#1

Table 15 - Rheological Parameters: PL Model - NLR Method – Low Lime WBM - “Fann 35 - PUC - F1 B1 R1” – Test#1

Curve Fit: Power-Law (Fann 35 - PUC #1)	
K	0.791730
n	0.478760
R ²	0.991940

Table 16 - Rheological Parameters: H-B Model - NLR Method – Low Lime WBM - “Fann 35 - PUC - F1 B1 R1” – Test#1

Curve Fit: Herschel-Bulkley (Fann 35 - PUC #1)	
τ_0	2.227700
K	0.233390
n	0.644640
R ²	0.999300

5.3.2.2.4. Test #2 - “Fann 35 - PUC - F1 B1 R1”

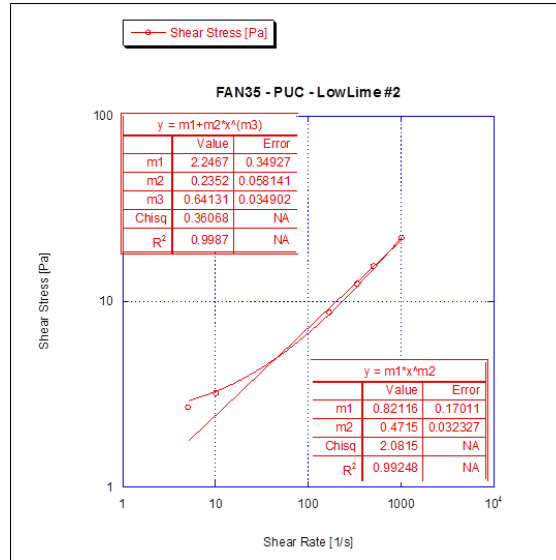


Figure 32 - Kaleidagraph NLR – Low Lime WBM - “Fann 35 - PUC - F1 B1 R1” – Test#2

Table 17 - - Rheological Parameters: PL Model - NLR Method – Low Lime WBM - “Fann 35 - PUC - F1 B1 R1” – Test#2

Curve Fit: Power-Law (Fann 35 - PUC #2)	
K	0.82116
n	0.4715
R ²	0.99248

Table 18 - Rheological Parameters: H-B Model - NLR Method – Low Lime WBM - “Fann 35 - PUC - F1 B1 R1” – Test#2

Curve Fit: Herschel-Bulkley (Fann 35 - PUC #2)	
τ_0	2.2467
K	0.2352
n	0.64131
R ²	0.99870

5.3.3. Solving the Rheological Parameters: API RP 13 D - Clause 5

Following the guidelines and formulas presented on section 4.2.2.

API RP 13 D - Clause 5 - Determination of Drilling Fluid Rheological Parameters, the Rheological Parameters were only calculated for Xanthan Gum

0.8% according the PL (Annular Flow) and H-B models, based on the readings performed at the FANN 35 PUC. The coefficient of determination also determined as per this methodology and results presented on Table 19 and Table 20.

Table 19 - Rheological Parameters: PL Model - API RP 13 D Method- Xanthan Gum 0.8% - Fann 35 PUC

Curve Fit: Power-Law (Fann 35 - PUC) - API 13D Method (Annular Flow)	
K	8.369519069
n	0.166235631
R²	0.951181

Table 20 - Rheological Parameters: H-B Model - API RP 13 D Method- Xanthan Gum 0.8% - Fann 35 PUC

Curve Fit: Herschel-Bulkley (Fann 35 - PUC) - API 13D Method	
τ_y	9.958221
K	0.413146183
n	0.58462298
R²	0.996197

The Curve Fitting values, could then be compared against the real values obtained from the rheogram and a direct comparison made, as illustrate on Table 21 along with the coefficient of determination for each set of values.

Table 21 – API 13 D Curve Fit Method - Comparison

Rotation	Shear Rate	FANN 35 Actual Values	Power Law Shear Stress (Curve Fit)		Herschel-Bulkley Shear Stress (Curve Fit)	
			[Pa]	%	[Pa]	%
[rpm]	[1/s]	[Pa]	[Pa]	%	[Pa]	%
600	1021.38	33.705	26.481	21.43%	33.691	0.04%
300	510.69	25.789	23.599	8.49%	25.784	0.02%
200	340.46	22.981	22.061	4.00%	22.444	2.34%
100	170.23	19.661	19.660	0.01%	18.284	7.00%
6	10.21	12.001	12.316	-2.62%	11.566	3.63%
3	5.11	10.980	10.975	0.04%	11.030	-0.46%
		R ²	0.951180634		R ²	0.996197333

Due to time and resource limitations, the Low Lime WBM rheogram results obtained from FANN35 were not used and the parameters not determined as per API RP 13D guidelines. For this reason only the 0.8% Xanthan Gum samples were used to demonstrate the importance of equipment, curve fitting technique, model selection and calculation method of friction loss pressure.

5.3.4. Curve Fitting & Model Selection

In drilling, because of thin clearances used, the estimation of dynamic pressure in the annulus is very sensitive to the choice of the mud model (smaller the annulus clearance - more difficult prediction). Application of model has important implications for calculating mud hydraulics in drilling process to neither select a model that overestimates nor underestimates pressure loss in annulus [27].

Assuming a high degree of fit between the measured and predicted dial readings, the calculated values of the rheological models - H-B or PL - parameters can be applied with confidence in hydraulics and hole-cleaning equations to calculate pressure losses and Equivalent Circulating Density (ECD).

To graphically demonstrate the issue, the curve fitting curves were plotted for the shear rate interval of 0.1 to 1000 s^{-1} (Figure 33 and Figure 34). The data obtained by the utilization of curve fitting technique may lead to errors not affordable on the MPD process. In the particular case, it worsens for shear rates lower than 10 s^{-1} . Still, it is expected that the range of shear rates observed in an annulus during a MPD connection is below the 10 s^{-1} , which can further complicate the problem.

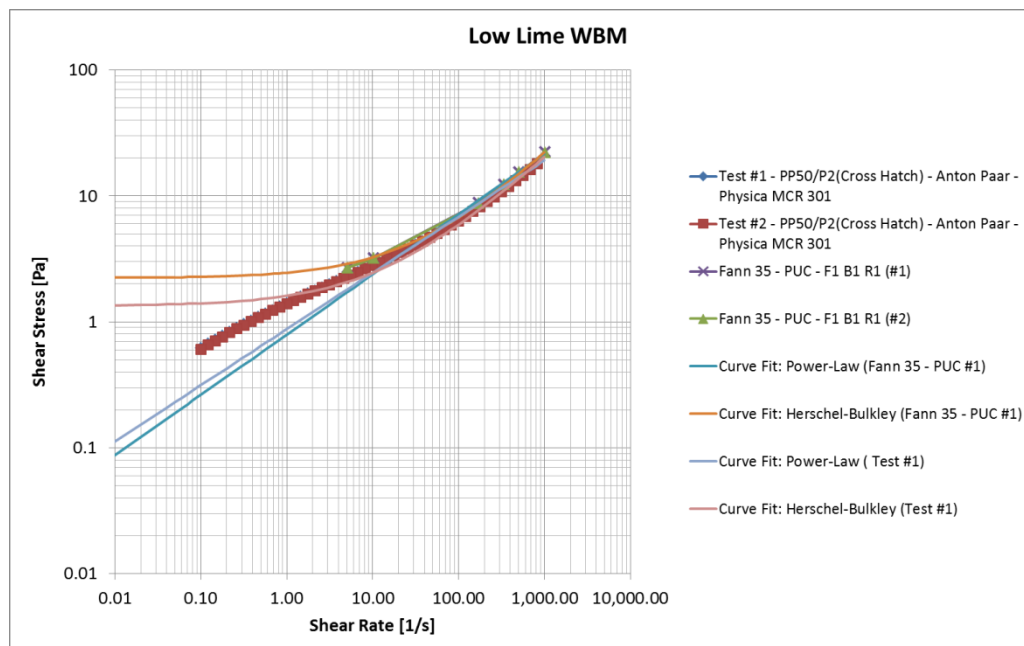


Figure 33 - Curve Fitting for Low Lime Water Based Mud

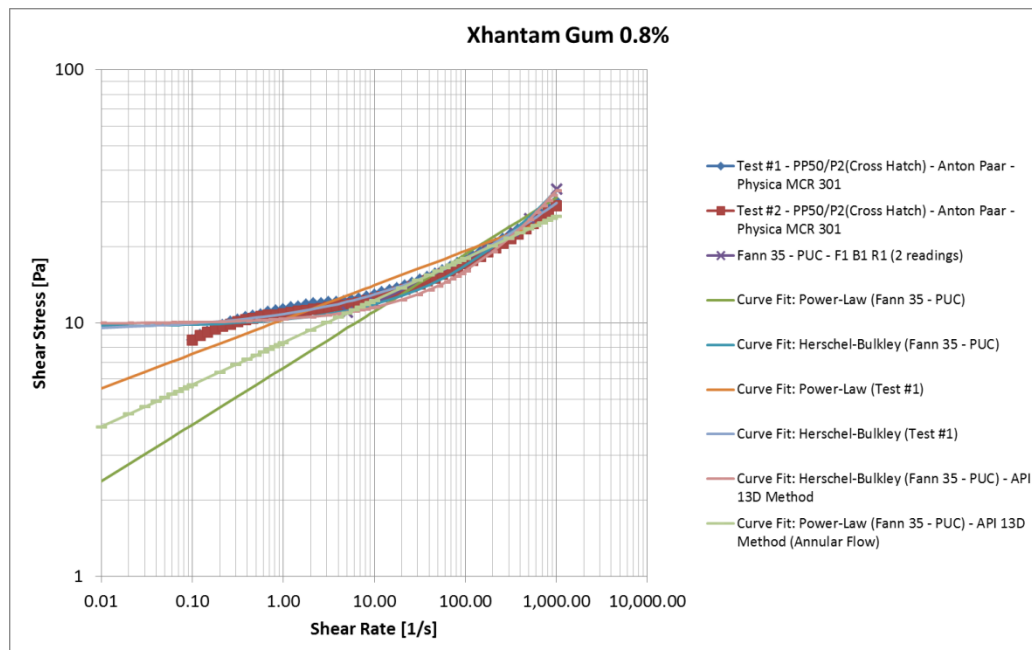


Figure 34 - Curve Fitting for Xanthan Gum 0.8%

Although it may appear a straight forward process, further complications might be added due to the amount of data points available (shear stress vs. shear rate), which may mislead to false interpretation of the true rheological model to be adopted to better describe the fluid in question. The consequences are the wrong prediction of pressure losses, as explained earlier, which are of the extreme importance for MPD applications, reason why it is important to raise awareness to the amount of readings required when characterizing a drilling fluid and identification of the range of shear rates that the flow in the annulus will experience during the drilling operations.

It can be observed based on Table 21 – API 13 D Curve Fit Method - Comparison that, although the coefficient of determination is one tool to assist in Model Rheology selection, it still may induce to errors if the interval of interest is not observed. For instance, on the example below illustrated by Figure 35, one may select the Power Law Model curve fitted by the API 13 D Method as satisfactory for the interval of shear rate between 10 and 100 s^{-1} , but it's known that the fluid in question is a H-B as the Curve Fitting performed by NLR indicates. In this case, an erroneous selection of Power Law Model for application below shear rate of 5 s^{-1} can lead to severe consequences in terms of pressure loss predictions.

Utilization of PL rheology model may not capture the entire interval of interest for the shear rates present in annular flow during MPD applications. In addition,

API RP 13D Curve Fitting for Power Law Model does not capture the flow behavior and may lead to wrong interpretation.

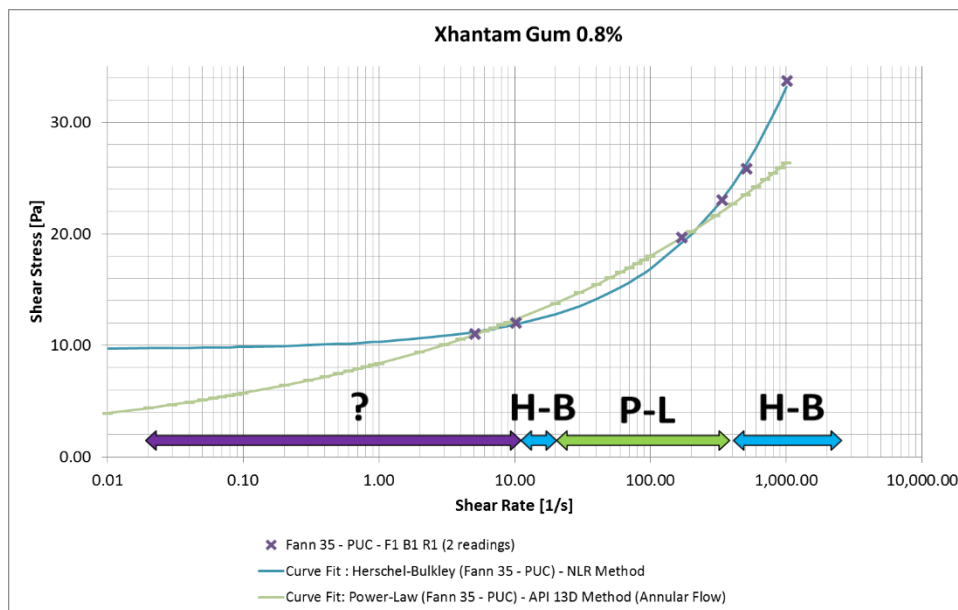


Figure 35 – Shear Rate Interval of Interest and Model Selection

Ideally, the range of shear rates where the flow will be evaluated should be known in advance in order to ensure that the model selected will be appropriate for the operational conditions. However, in most cases, it tends to happen the other way around, whereby the fluid rheology is required in order to estimate the shear rates in a given geometry and to subsequently determine the interval of shear rate.

A typical approach is to select the best estimate for the fluid rheology model, perform the calculations for shear rates, and verify if the selected model corresponds to the best description of the fluid properties within the desired interval. In cases where it is known that flow will be studied from “no flow” condition to its maximum flow rate (such in MPD connections) the range of shear rates becomes from zero to its maximum calculated. In addition, it is relevant that the fluid model must be representative for the entire range of values for shear rates versus shear stresses.

Nevertheless, as for the Curve Fit results from the API 13 D method, a brief investigation leads to conclude that the curve fit matches with 3 and 100 rpm readings (5.11 and 170.23 s^{-1}) as the rheological parameters are calculated based on those 2 readings. Conversely, applications between 6 and 100 rpm (10.21 and 170.23 s^{-1}) are susceptible to minor failures. Beyond that interval, the consequences can be poorest as illustrated on Figure 36. If shear rates are observed within the above range, it may be pertinent to the industry to evaluate the

necessity of additional viscosity readings in between the 3 and 100 rpm readings. Later on this study, this affirmation is verified.

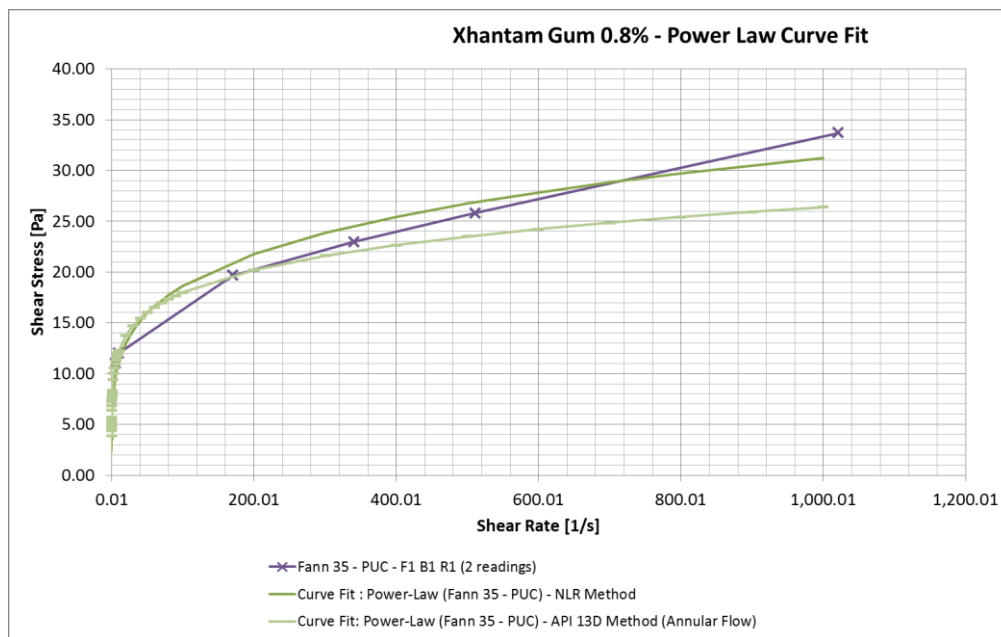


Figure 36 - Xhantam Gum 0.8% - Power Law Curve Fit Comparison

The remaining question would be how to best select a rheology model. The answer could be both graphically by looking at the interval of shear rates that the process is implemented and, as suggested, via the coefficient of determination.

All the results from the Xantham Gum 0.8 are presented on the Table 22. Direct comparison of coefficient of determination allows selecting between the two models evaluated - PL (red tab) and H-B (green tab) - by comparing the coefficient of determination regardless the instrument used (FANN 35 or Physica) to perform the rheogram or the curve fitting method implemented (NLR or API 13 D). On all cases, the H-B model has been identified as a most appropriate rheology model for the samples.

The second conclusion is, once the model is chosen, the rheograms done by the Physica rheometers (50 points readings) lead to coefficient of determination lower than the FANN35 (6 points readings) through NLR Curve Fitting, and it should be carefully evaluated. As coefficient of determination being a statistical measure of how well the regression line approximates the real data points, it is expected that larger amount of data points returns a higher variation over the total variation. In this manner, to be able to further decide the best curve fitting may not be possible in comparing values obtained from 6 points versus 50 points and for different range intervals, as the Physica's data points extended the readings to down low 0.1 s^{-1} . In this specific case, it should be done by graphical observation.

The graphical observation indicates that 50 points still have a better performance in representing the fluid model on its range as earlier exemplified.

Table 22 – Curve Fitting and Coefficient of Determination Results

	Non Linear Regression			API 13D
	GX 0.8% Curve Fit: Power-Law			
	Test #1 (DG1)	Test #2 (DG2)	Fann 35 - PUC	Fann 35 - PUC - API 13D
K	10.319000	10.008000	6.651200	8.369519
n	0.135540	0.133450	0.223880	0.166236
R ²	0.935950	0.930840	0.963900	0.951181
			← →	
	GX 0.8% Curve Fit: Herschel-Bulkley			
	Test #1 (DG1)	Test #2 (DG2)	Fann 35 - PUC	Fann 35 - PUC - API 13D
τ_0	9.310700	9.169500	9.648000	9.958221
K	1.537800	1.363100	0.672570	0.413146
n	0.374350	0.384480	0.514700	0.584623
R ²	0.994980	0.996630	0.998012	0.996197
			← →	
	50 points – 0.1 : 1000 [1/s]		6 points – 5 : 1022 [1/s]	

The third affirmation is direct comparison of curve fitting by NLR versus API 13D, given the exception of the direct comparison of the number of points. In the case of 6 data points following the API 13 B guidelines, certainly the NLR method offers a superior result than API 13 D for the FANN 35 reading. Then the NLR method must be the preferable method for determining curve fitting parameters.

5.3.4.1. Accuracy of the process

The importance of the entire process to obtain a mathematical representation of rheology properties of a fluid relies on taking into account several factors, and the accurate selection of: equipment, geometry, range of specification, means of measurements, amount of data available, curve fitting method and statistical tools to better infer on the final result selection.

In reality, it must be bear in mind that curve fit is only an approximation for the real fluid properties. As earlier discussed, it is highly dependent of the process implemented:

- the equipment used for the rheogram,
- the amount of data points collected and the range and
- method to fit the points and retrieve a mathematical model that represents the set of data.

Exemplified on Figure 37, further illustrate the relationship of all the three aspects listed above. The information is then absent when less precise equipment is used to measure the same data and the amount of readings lower with narrow interval. In this case, it is observed that the FANN35 readings for shear rates lower than 10 s^{-1} missed the accuracy.

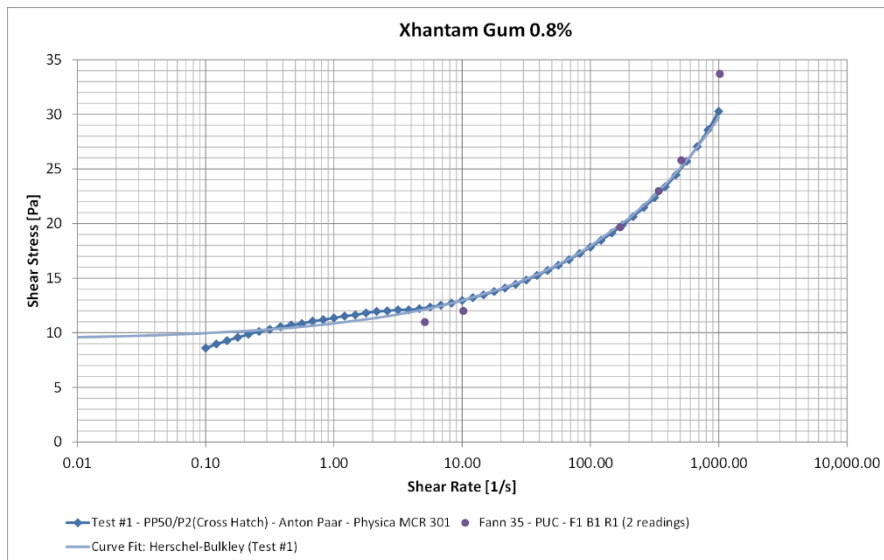


Figure 37 – Curve Fit vs Actual Fluid Properties

Subsequently, the discrepancy in results between the field³ and the laboratory environment⁴ was analyzed. Such comparison allowed understand in a better way how the measurement process and curve fitting technique can influence the results for pressure loss estimation in a given annulus. It is important to remark that, the equipment used may not be able to capture the fluid rheology properly. In addition, the mathematical manipulation of data might not be representative of real properties on its entire domain.

The Figure 38 concludes and exemplifies the Xanthan Gum 0.8% fluid sample with the six data points acquired by FANN35 Oilfield Viscometer and curve fitted for an H-B Model following the API 13D Method. It also embraces the 50 points acquired through the Physica Rheometer in the laboratory and curve fitted using NLR method.

³ Defined as the fluid properties measured at FANN35 and Curve Fitted by API RP 13D Method.

⁴ Defined as the fluid properties measured at Physica and Curve Fitted by Non Linear Regression.

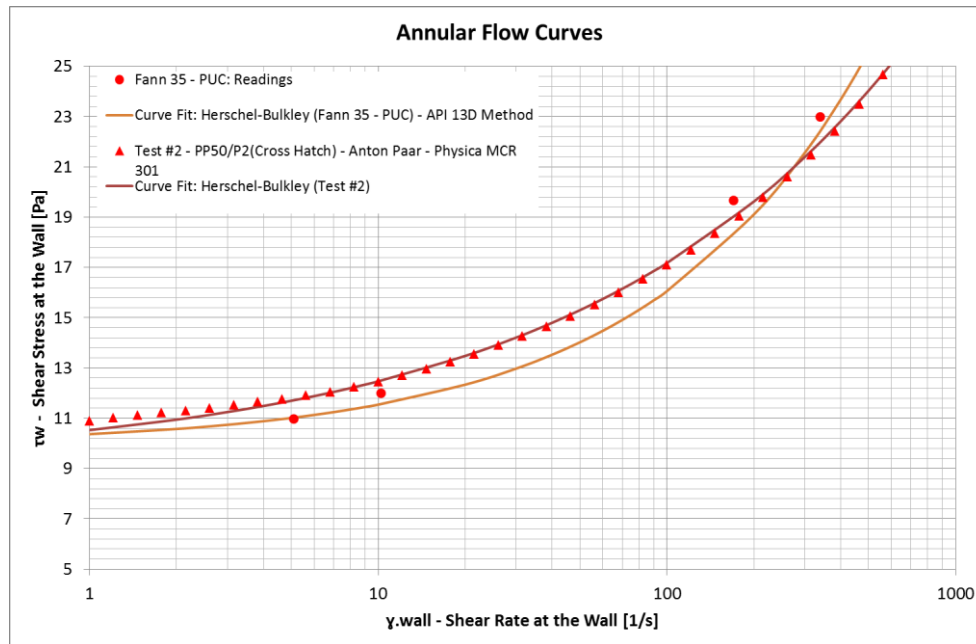


Figure 38 – Fluid Properties versus Curve Fit Accuracy

To enhance the prediction of rheology model selection it is suggested to include additional measurements between the 3 and 100 rpm FANN 35 readings when this equipment is used, thus increasing the amount of points and delivering a more accurate mathematical model.

Ultimately, MPD design would benefit from a model rheology that could represent the fluid rheology property to a near zero shear rate and be continuous numeric solved on entire domain as the H-B curve fitting calculated for the case above does not properly fit for the very low end of the curve.

6 Mapping Shear Rate

6.1. Fluid Properties Selection

For the subsequent analysis of the shear mapping following the API13 D guidelines, the results obtained for the Xanthan Gum 0.8% were used. The following two sets of fluid properties results were selected as most representative results between different environment conditions:

1. Rheogram performed on the Anton Paar - Physica MCR 301 with PP50/P2 Cross Hatch geometry. Rheological Parameters and curve fit calculated as H-B Model using NLR Method (Table 8).
2. Rheogram performed on the Fann 35 – PUC as per API RP 13 B. Rheological Parameters calculated as H-B Model using the API RP 13 D Method (Table 20).

While set (1) intended to represent the controlled laboratory condition, the set (2) is the standard oilfield practice suggested by API under field conditions.

6.2. Geometry Selection

Two typical hole sections and a drill pipe were stipulated based on the most commonly drilled hole sizes using MPD with the objective of illustrate a annular geometry and allows to verify the range of shear rates.

Hence, two different geometries have been assumed to illustrate the goals of this study:

- Case (a): “8.5 Section” set as Open Hole Diameter of 8.5 inches (215.9 mm) and Drill Pipe of 5.5 inches (139.7 mm).
- Case (b): “12.25 Section” set as Open Hole Diameter of 12.25 inches (215.9 mm) and Drill Pipe of 5.5 inches (139.7 mm).



Figure 39 - Case (a): "8.5 Section"



Figure 40 - Case (b): "12.25 Section"

While in case (a) it is believed that the major impact of inaccuracies from equipment and estimations leads to higher differences in pressure loss calculations due to the smaller clearance when compared with case (b), case (b) is expected to encompass the lower end range of shear rate values due to the lower flow velocities (larger annulus) when compared with (a).

6.3. Flow Rate Selection

As for the flow rate range selection, typical maximum drilling flow rates on the cases (a) and (b) above are in the range of 400 gpm (0.0252 m³/s) and 1,000 gpm (0.063 m³/s). Care was taken to ensure that the flow observed under these conditions were still on the laminar region.

Although the stipulated maximum flow rates above may slightly differ from operation to operation, the objective was to map the shear rate during a transition process, in other words, from its maximum estimation to zero.

The average (bulk) velocities (V_a), for both geometries – (a) and (b) - given the flow rate range are found Table 23 and Table 24 calculated by the application of the equation (8).

Table 23 - Annulus Fluid Velocity for 8.5 Section – Case (a)

Q - Flow Rate [gpm]	Va - Annulus Fluid Velocity [m/s]
10	0.029645
20	0.059291
30	0.088936
40	0.118582
50	0.148227
60	0.177873
70	0.207518
80	0.237163
90	0.266809
100	0.296454
200	0.592909
300	0.889363
400	1.185817

Table 24 – Annulus Fluid Velocity for 12.25 Section – Case (b)

Q - Flow Rate [gpm]	Va - Annulus Fluid Velocity [m/s]
10	0.010392
20	0.020784
30	0.031176
40	0.041569
50	0.051961
60	0.062353
70	0.072745
80	0.083137
90	0.093529
100	0.103921
200	0.207843
300	0.311764
400	0.415686
500	0.519607
700	0.727450
1000	1.039214

6.4. Shear Rate and Shear Stress Calculations as per API 13 D

As discussed on section 0, API RP 13 D suggests a set of formulae and procedures to estimate the shear stress at wall. The utilization of the formulae presented on API 13D and reproduced in this study by equations (10), (11) and (12), allowed to calculate the Shear Rate in the Annulus (measured at the wall).

The corresponding value of shear stress for both geometries (case “a” and case “b” previously mentioned) using the fluid properties as per field conditions⁵, and using the equations (13) and (14) were also estimated.

Values obtained are presented in the results Table 25 and Table 26.

Table 25 – Shear Stress and Shear Rate as per API 13 D Method - Herschel-Bulkley Model - 8.5 Section.

Q - Flow Rate [gpm]	$\dot{\gamma}_{wall}$ - (API 13 D - 7.4.7) Shear Rate at the Wall [1/s]	τ_f - Shear Stress at the Wall [lbf / 100 ft ²]	τ_f - Shear Stress at the Wall [Pa]
10	2.4528	27.8047	13.3130
20	4.9057	28.5328	13.6616
30	7.3585	29.1173	13.9415
40	9.8114	29.6247	14.1844
50	12.2642	30.0813	14.4030
60	14.7171	30.5013	14.6041
70	17.1699	30.8930	14.7917
80	19.6228	31.2621	14.9684
90	22.0756	31.6124	15.1361
100	24.5285	31.9469	15.2963
200	49.0569	34.7447	16.6359
300	73.5854	36.9909	17.7114
400	98.1139	38.9403	18.6447

Table 26 - Shear Stress and Shear Rate as per API 13 D Method - Herschel-Bulkley Model – 12.25 Section

Q - Flow Rate [gpm]	$\dot{\gamma}_{wall}$ - (API 13 D - 7.4.7) Shear Rate at the Wall [1/s]	τ_f - Shear Stress at the Wall [lbf / 100 ft ²]	τ_f - Shear Stress at the Wall [Pa]
10	0.3822	26.8389	12.8505
20	0.7643	27.0845	12.9681
30	1.1465	27.2816	13.0625
40	1.5286	27.4527	13.1444
50	1.9108	27.6067	13.2182
60	2.2929	27.7484	13.2860
70	2.6751	27.8805	13.3492
80	3.0572	28.0049	13.4088
90	3.4394	28.1231	13.4654
100	3.8215	28.2359	13.5194
200	7.6430	29.1794	13.9712
300	11.4645	29.9370	14.3339
400	15.2860	30.5944	14.6487
500	19.1076	31.1862	14.9321
600	22.9291	31.7305	15.1926
700	26.7506	32.2381	15.4357
800	30.5721	32.7164	15.6647
900	34.3936	33.1704	15.8821
1000	38.2151	33.6039	16.0896

In possession of the results, it was possible to make the verification regarding the range of values suggested by API 13 B (6 points). Maximum shear rates observed for maximum flows, 400 gpm on case (a) and 1000 gpm on case (b) are lower than 100 s⁻¹. In these cases, only 2 actual readings from FANN 35 are then used to infer about the rheology model calculations: 3 rpm (5.11 s⁻¹) and 6 rpm

⁵ Defined as the fluid properties measured at FANN35 and Curve Fitted by API RP 13D Method.

(10.21 s^{-1}). The 12.25 section is further hampered as the flow rates lower than 200 gpm leads to utilize the extrapolation values of the curve fit attributed. Plots of flow rate versus shear rate at the wall, calculated as per API 13 D, aid to illustrate the issue (Figure 41). The complete set of results are found on the APPENDIX A API 13 D Method – Results.

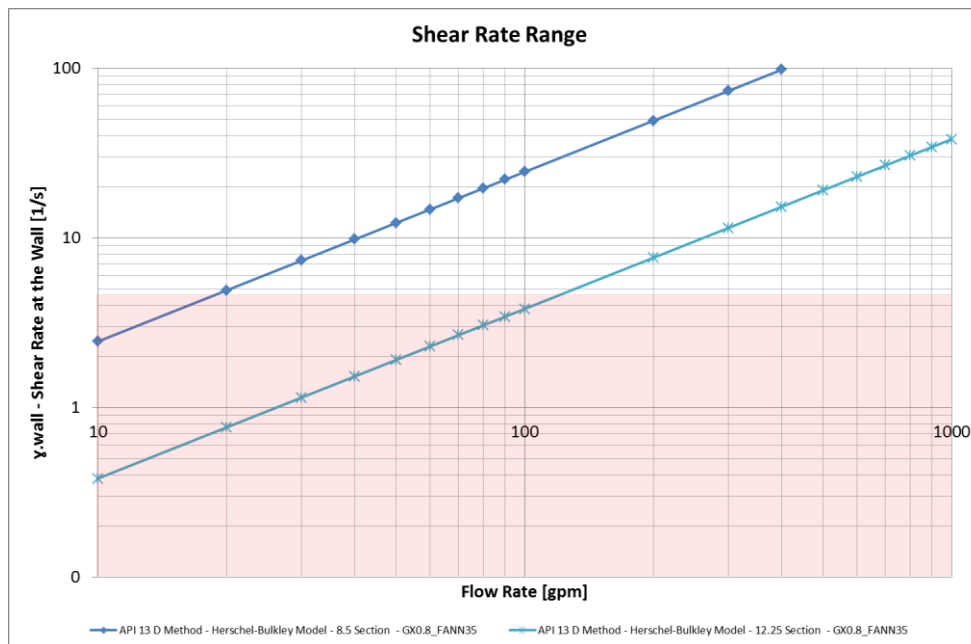


Figure 41 – Map of Shear Rate at Wall, according API 13 D – 8.5 and 12.25 Section

The highlighted red zone encompasses the calculated shear rates falling outside the measured interval of 3 rpm (5.11 s^{-1}).

Another observation obtained from the application of formulas suggested by API 13 D is that they indicate not be respectful of the pair shear rate vs. shear stress (or viscosity of the fluid) as indicated on the Figure 42.

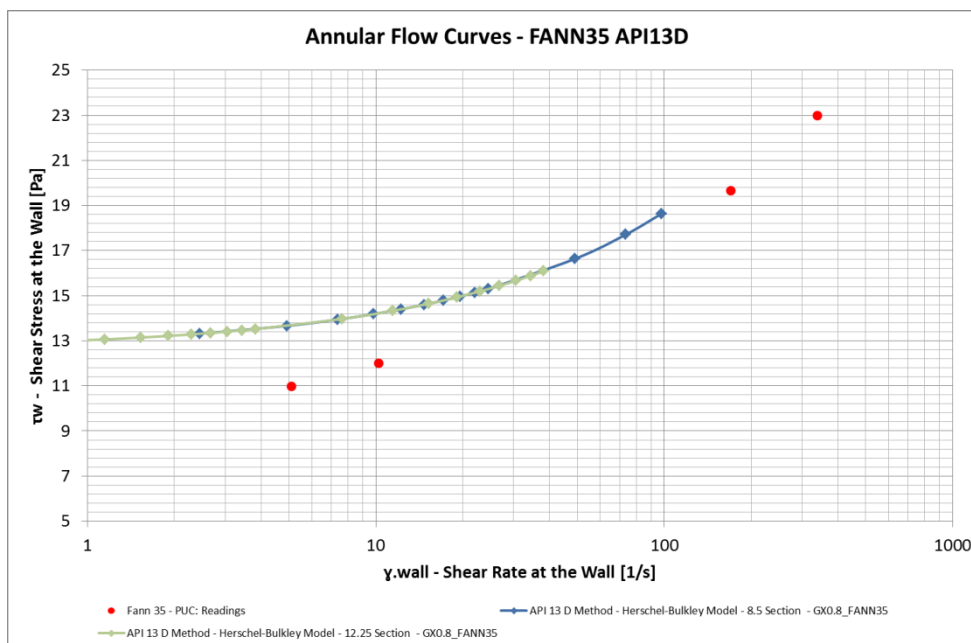


Figure 42 – FANN 35 Rheogram and “Shear Rate vs Shear Stress API 13 D Results”

The calculated shear rate will not reproduce a correspondent shear stress obeying the fluid rheology measurements.

As a final remark to note, lower fluid velocities are expected to reproduce lower shear rates. As the wellbore geometry is “telescopic” being the bigger annulus towards the surface (Figure 43), the implications of not having the rheological properties at lower shear rates than 3 rpm (5.11 s^{-1}) may impact the overall calculation for the entire well.

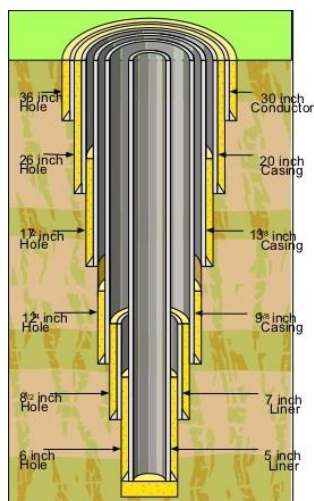


Figure 43 - Typical Casing Program and Annulus

7

Validating the Shear Rate Map: CFD Numerical Verification

The awkward results of shear rates obtained by the direct formulas of API RP 13 D required the implementation of a verification method rather than analytical. Due to the nature of a non-Newtonian flow problem, the course of the study decided to rely on numerical methods as secondary form of verification.

The numerical solution of the non-Newtonian flow obtained with the aid of the Computational Fluid Dynamics (CFD) using the Fluent Software by ANSYS - version 15.07 (released 2014) and version 16.0 (released 2015) - allowed to proof the application of standards early tested.

Equally, the cases formulated and solve by the API 13 D methods were solved using the CFD Technique in an assessment of the analytical solution method against a numerical method. The utilization of the CFD also permitted the direct evaluation of curve fitting and equipment implemented to obtain the fluid data.

In this chapter, a briefly discussion of the method is presented along with the relevant modeling of the problem and the setup performed to ensure the physics, boundaries. At the end, the results comparison of shear rates are presented and preliminary conclusions stated in regards to the API 13 B and API 13 D standards.

7.1. About ANSYS Fluent

ANSYS Fluent provides comprehensive modeling capabilities for a wide range of applications; among them is the analysis of incompressible laminar non-Newtonian fluid flow, which is the main interest for the current study

ANSYS Fluent uses a control-volume-based technique to convert a general scalar transport equation to an algebraic equation that can be solved numerically. This control volume technique consists of integrating the transport equation about each control volume, yielding a discrete equation that expresses the conservation law on a control-volume basis.

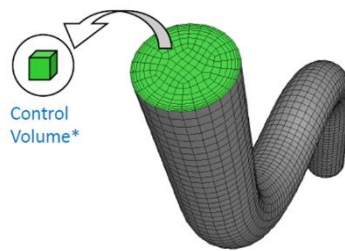


Figure 44 - Control Volume Example

In summary, the control-volume-based technique consists of three (3) steps:

1. Division of the domain into discrete control volumes using a computational grid.
2. Integration of the governing equations on the individual control volumes to construct algebraic equations for the discrete dependent variables (“unknowns”) such as velocities, pressure, temperature, and conserved scalars.
3. Linearization of the discretized equations and solution of the resultant linear equation system to yield updated values of the dependent variables.

7.2. Computational Fluid Dynamics Setup

7.2.1. Solver and Solution Methods

7.2.1.1. Pressure Based Solver

In this type of solver, the velocity field is obtained from the momentum equations. The pressure field is extracted by solving a pressure or pressure correction equation that is obtained by manipulating continuity and momentum equations. ANSYS Fluent will solve the governing integral equations for the conservation of mass and momentum.

$$\underbrace{\frac{\partial}{\partial t} \int_V \rho \phi dV}_{\text{Unsteady}} + \underbrace{\oint_A \rho \phi \mathbf{V} \cdot d\mathbf{A}}_{\text{Convection}} = \underbrace{\oint_A \Gamma_\phi \nabla \phi \cdot d\mathbf{A}}_{\text{Diffusion}} + \underbrace{\int_V S_\phi dV}_{\text{Generation}}$$

Equation	ϕ
Continuity	1
X momentum	u
Y momentum	v
Z momentum	w
Energy	h

Figure 45 - Transport Equations

The pressure-based solver employs the algorithm that belongs to a general class of methods called the projection method. The constraint of mass conservation (continuity) of the velocity field is achieved by solving a pressure (or pressure correction) equation.

The pressure equation is derived from the continuity and the momentum equations in such way that the velocity field, corrected by the pressure, satisfies the continuity. Since the governing equations are nonlinear and coupled to one another, the solution process involves iterations wherein the entire set of governing equations is solved repeatedly until the solution converges.

Yet, the pressure-based solver approach is applicable for low-speed incompressible flows.

7.2.1.2.

General Scalar Transport Equation Setup – Solution Methods

Under the pressure-based solver, the solution method selected was the Pressure-Velocity Coupling in the Coupled scheme.

The Coupled scheme provides a robust and efficient single phase implementation for steady-state flows, with superior performance compared to the segregated solution schemes [28].

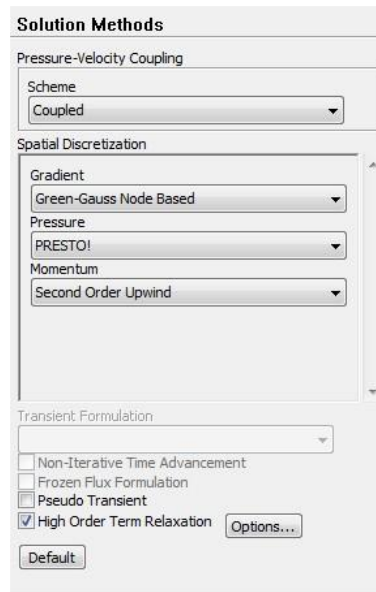


Figure 46 - Fluent Solution Methods

Spatial Discretization (Solution Methods) were set as “Green Gauss Node Based” for gradient, PRESTO! for pressure and “Second Order Upwind” for Momentum (Figure 46). Regarding the Solution Controls, the explicit relaxation factors were 0.5 for pressure and 0.5 for momentum while the under-relaxation factors were set to 1 for density and body forces (Figure 47).

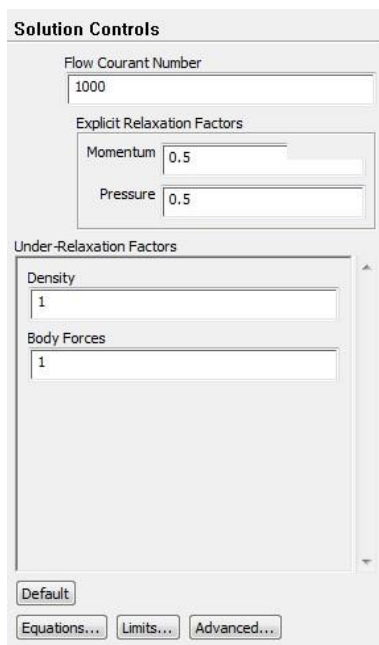


Figure 47 - Fluent Solution Controls

Justifications of the selected methods are further explained on the following sections.

7.2.1.2.1. Discretization (Interpolation Method)

As the ANSYS Fluent uses a control-volume-based technique to convert a general scalar transport equation to an algebraic equation that can be solved numerically, it requires the field variables (stored at cell centers) must be interpolated to the faces of the control volumes.

$$\frac{\partial(\rho\phi)}{\partial t} V + \sum_f \rho_f \mathbf{V}_f \phi_f \cdot \mathbf{A}_f = \sum_f \Gamma_\phi \nabla \phi_f \cdot \mathbf{A}_f + S_\phi V$$

Figure 48 - Discretization - Interpolation Methods

Among the interpolation schemes available for the convection term (Momentum), the Second-Order Upwind has been chosen. The Second Order Upwind quantities at cell faces are computed using a multidimensional linear reconstruction approach and uses larger stencils for 2nd order accuracy. It is remarkably to note that convergence may be slower when this scheme is selected.

7.2.1.2.2. Interpolation Method - Gradients

Gradients of solution variables are required in order to evaluate diffusive fluxes, velocity derivatives, and for higher-order discretization schemes.

$$\frac{\partial(\rho\phi)}{\partial t} V + \sum_f \rho_f \mathbf{V}_f \phi_f \cdot \mathbf{A}_f = \sum_f \Gamma_\phi \nabla \phi_f \cdot \mathbf{A}_f + S_\phi V$$

Figure 49 - Gradients - Interpolation Methods

The gradients of solution variables at cell centers can be determined using three approaches:

- Green-Gauss Cell-Based – The default method; solution may have false diffusion (smearing of the solution fields).
- Green-Gauss Node-Based – More accurate; minimizes false diffusion; recommended for tri/tet meshes.

- Least-Squares Cell-Based – Recommended for polyhedral meshes; has the same accuracy and properties as Node-based Gradients.

The interpolation method for gradient on all simulated cases was chosen as Green Gauss Node Based. To note, the method computes the gradient of the scalar at the cell center by the arithmetic average of the nodal values on the face of the element.

7.2.1.2.3. Interpolation Methods for Face Pressure

Interpolation scheme for calculating cell-face pressures were selected as PRESTO! (PREssure STaggering Option). The scheme uses the discrete continuity balance for a “staggered” control volume about the face to compute the “staggered” (that is, face) pressure. This procedure is similar to the staggered-grid schemes used with structured meshes. The PRESTO! scheme applies when large surface-normal pressure gradients near boundaries with steep pressure changes are present in the flow.

7.3. Critical Shear Rate Selection for Non-Newtonian Fluids

ANSYS Fluent defines a normalized version of Herschel-Bulkley (H-B) model to be able to numerically solves the equation.

While the Herschel-Bulkley (HB) model is usually defined as previously defined on equation (2), the normalization is achieved by replacing equation (20),

$$\eta = \frac{\tau_0}{\dot{\gamma}} + k \left(\frac{\dot{\gamma}}{\dot{\gamma}_c} \right)^{n-1} \quad (20)$$

into equation (21)

$$\tau = \eta \dot{\gamma} \quad (21)$$

Resulting in equation (22).

$$\tau = \tau_0 + \frac{k}{\dot{\gamma}_c^{n-1}} \dot{\gamma}^n \quad (22)$$

Where

$\dot{\gamma}_c$ is the critical shear rate[1/s].

The normalized viscosity equation for H-B model calculated by Fluent can then be expressed as equation (23) below:

$$\text{For } \dot{\gamma} > \dot{\gamma}_c \quad \eta = \frac{\tau_0}{\dot{\gamma}} + k \left(\frac{\dot{\gamma}}{\dot{\gamma}_c} \right)^{n-1} \quad (23)$$

$$\text{For } \dot{\gamma} < \dot{\gamma}_c \quad \eta = \tau_0 \frac{(2 - \dot{\gamma}/\dot{\gamma}_c)}{\dot{\gamma}_c} + k \left[(2 - n) + (n - 1) \frac{\dot{\gamma}}{\dot{\gamma}_c} \right]$$

Granting a value of critical shear rate must be input on ANSYS Fluent as one of the requirements for the H-B property as indicated on Figure 50.

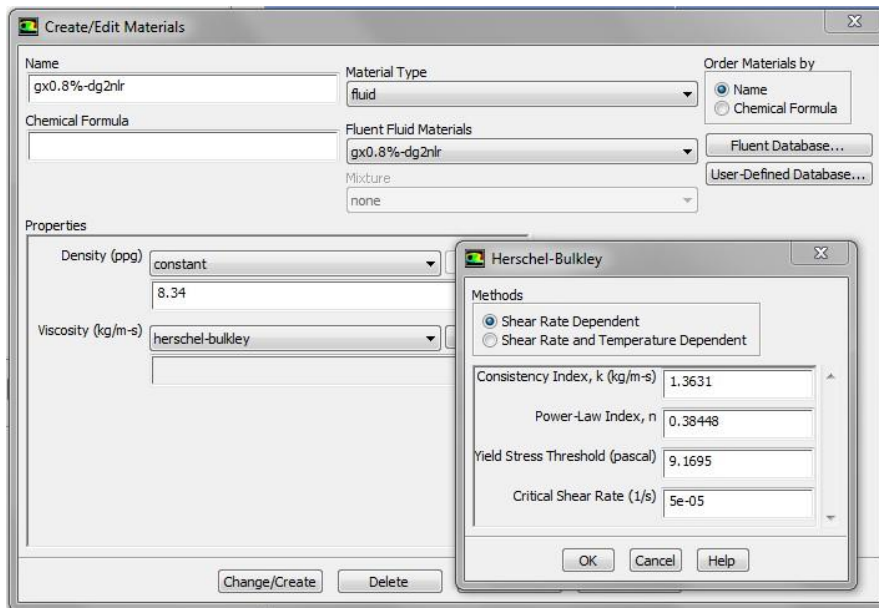


Figure 50 - ANSYS Fluent - Fluid Properties Input Screen (H-B Model)

The impact of chosen Critical Shear Rate value versus the shear rate of the flow are exemplified on the sensitivity analysis by application of the equation (23) for various shear rates. As observed, high critical shear rates leads to the numerical solution to be solved as the fluid as Newtonian or near solid (constant viscosity).

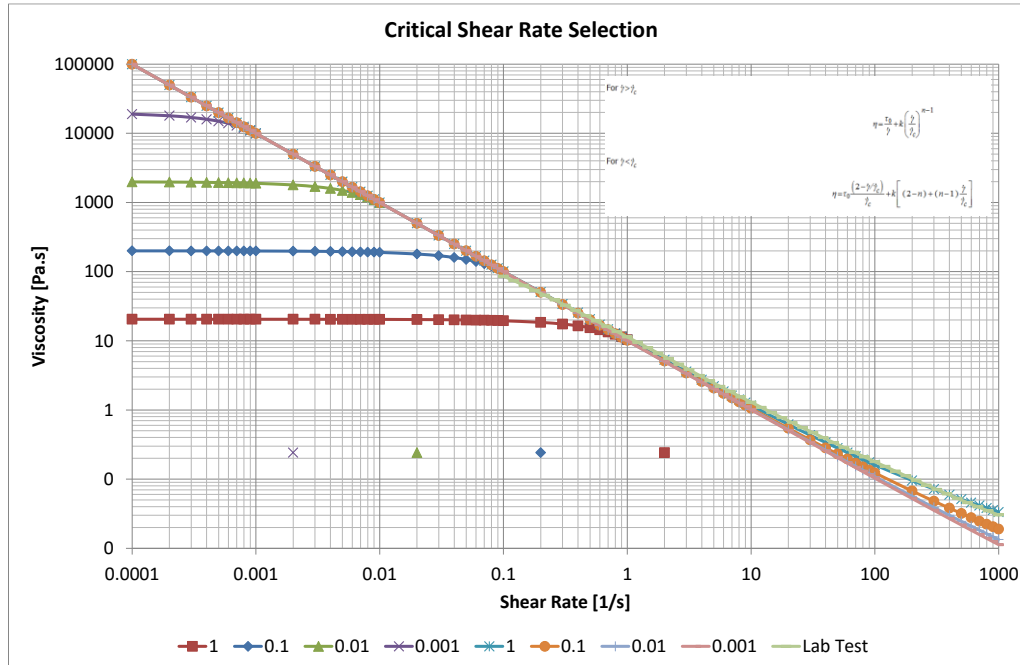


Figure 51 - Critical Shear Rate Selection and Behavior

M. Soares et al [29] suggested that critical shear rate value should be in the order of thousands of the shear rate observed in the flow. After several tests

performed, a critical shear rate value was established as $5e10^{-5}$ [1/s] for all cases ran on Fluent. The selection allowed satisfactory results and convergence.

7.4. Geometry and Meshing Considerations

The numerical solution was modeled for half of the annular space, in a bi-dimensional (2D) axisymmetric plane for both annulus geometries (Case (a) and Case (b)).

Figure 52 illustrates the 2D numerical mesh, with 8,500 axial and 60 radial divisions, which lead to 510000 cells (maximum allowed by ANSYS Fluent Version 15.07– Student License capped in 512000 cells). Mesh Control through Inflation of the cells at the inner and outer wall in a proportion of 1.1 has been applied.

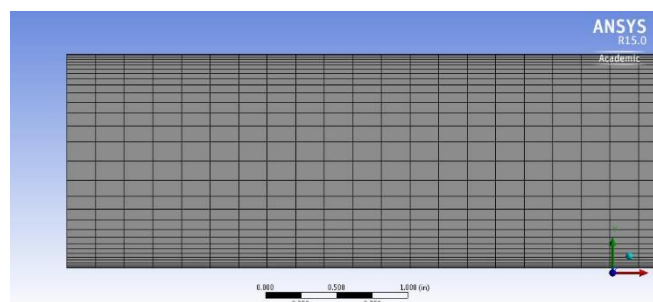


Figure 52 – 2D Mesh Transversal View

To achieve satisfactory mesh quality in terms of skewness and orthogonality controls, the total length of the annulus was defined as 500 inches (12.7 m) and 1000 inches (25.4 m) respectively for the Case (a) and Case (b).

The quality have been checked and considered satisfactory for orthogonality and skewness. The experimental simulation of a Newtonian fluid (pure water - Figure 53) of developed fluid velocity profile (compared against the non-Newtonian fluid (Xanthan Gum 0.8% - Figure 54) had also tested the mesh quality.

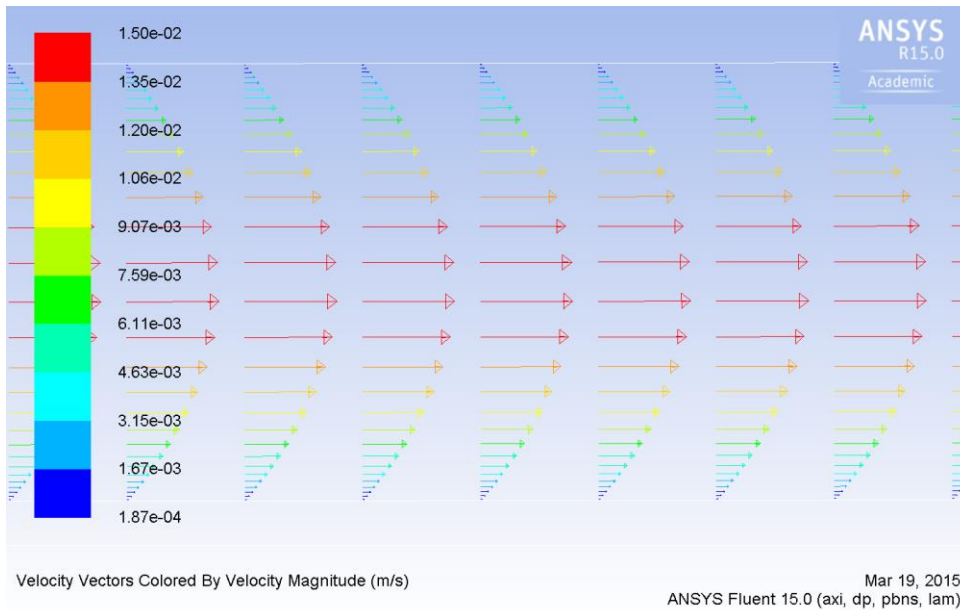


Figure 53 - Velocity Profile of Newtonian Fluid at 1000 gpm in the 12.25 Section

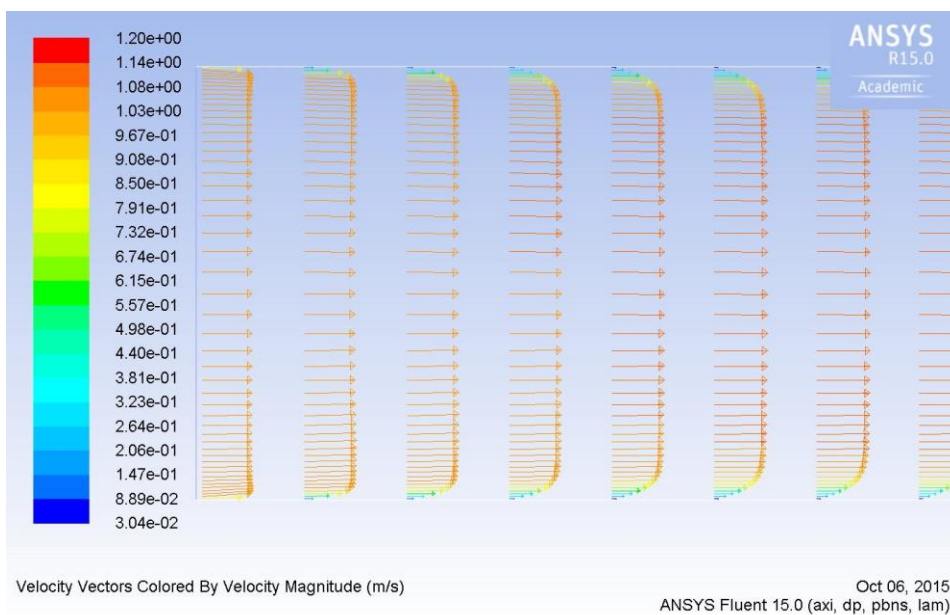


Figure 54 - Velocity Profile of Non-Newtonian Fluid at 1000 gpm in the 12.25 Section

7.5. Physics and Boundaries

The flow was modeled as laminar steady-state with double digit precision. The flow is isothermal, so the energy equation was not solved.

The boundary conditions were defined as below, being \mathbf{u} the vector velocity component in x-axis and \mathbf{v} in the y-axis:

1. uniform velocity prescribed at the inlet (Figure 55) according to the Table 23 - Annulus Fluid Velocity for 8.5 Section – Case (a) and Table 24 – Annulus Fluid Velocity for 12.25 Section – Case (b);
 - $u=C, v=0$
2. fully-developed condition at the outlet;
 - $d/dx=0$
3. impermeability and no slip wall condition at cylinder walls;
 - $u=v=0$
4. symmetry conditions at the symmetry plane.

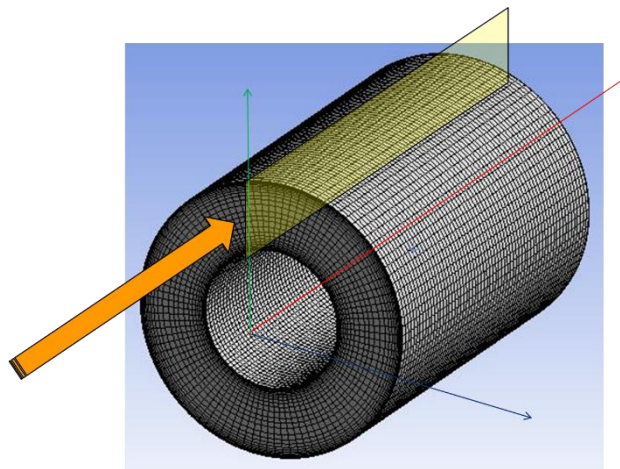


Figure 55 – Representation of the Annulus Flow: 3D Mesh – Perspective View

7.6. Convergence Criteria & Monitoring

At convergence, all discrete conservation equations (momentum, energy, etc.) are obeyed in all cells to a specified tolerance, or the solution no longer changes with subsequent iterations. The convergence criteria ensured that overall mass, momentum, and scalar balances were achieved.

The Residual History has been utilized as control parameter for all cases. Generally, a decrease in residuals by three orders of magnitude indicates at least qualitative convergence. At this point, the major flow features should be established. In this evaluation, the convergence criteria for the residuals were set as $10e^{-10}$ for Continuity, X-Velocity and Y-Velocity and demonstrated to be satisfactory for all cases.

A secondary quantitative convergence used was the standard deviation of the velocity at the centerline of the annular flow. This monitoring technique ensured

the appropriate selection of the values observed in the fully developed region of the flow (no variation of velocity along the X-axis), as illustrate on Figure 56 and Figure 57 for cases (a) and (b). In the case, Observation Points (OP) for the shear rate and shear stress were then set at half of the length for each case (i.e.: 250 and 500 inches respectively on X-axis position) to ensure an undisturbed flow distant from the inlet and outlet.

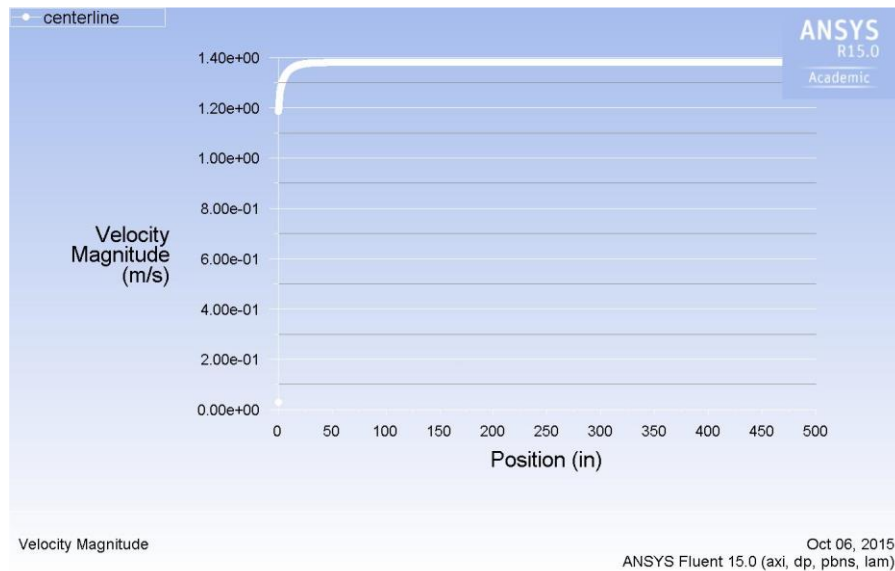


Figure 56 - Annulus Flow Development - Case (a) - 400 gpm

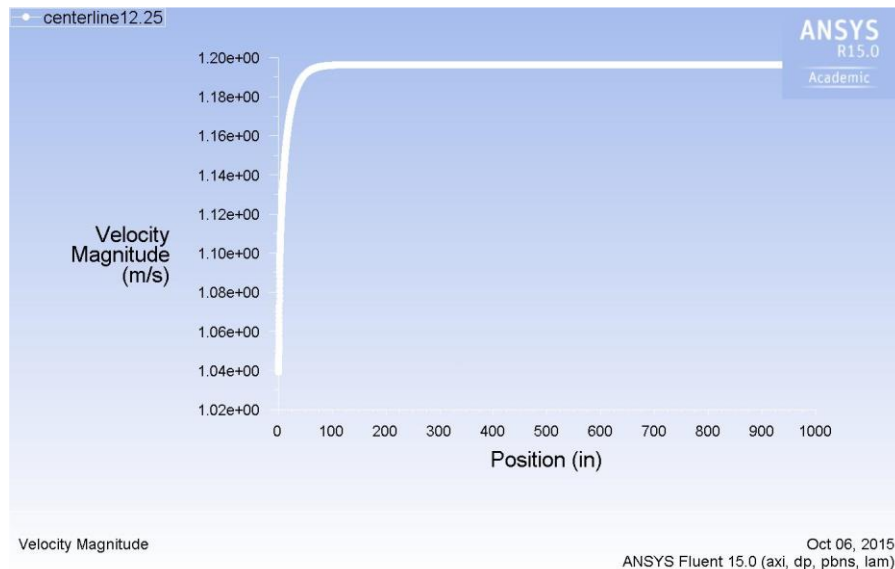


Figure 57 - Annulus Flow Development - Case (b) - 1000 gpm

This technique allows obtaining the velocity profile (Figure 58), shear rate (or strain rate) distribution along the annulus - YZ plane at 500 inches located on X axis - (Figure 59), and shear stress at the wall measurements (Figure 60) for all simulated cases.

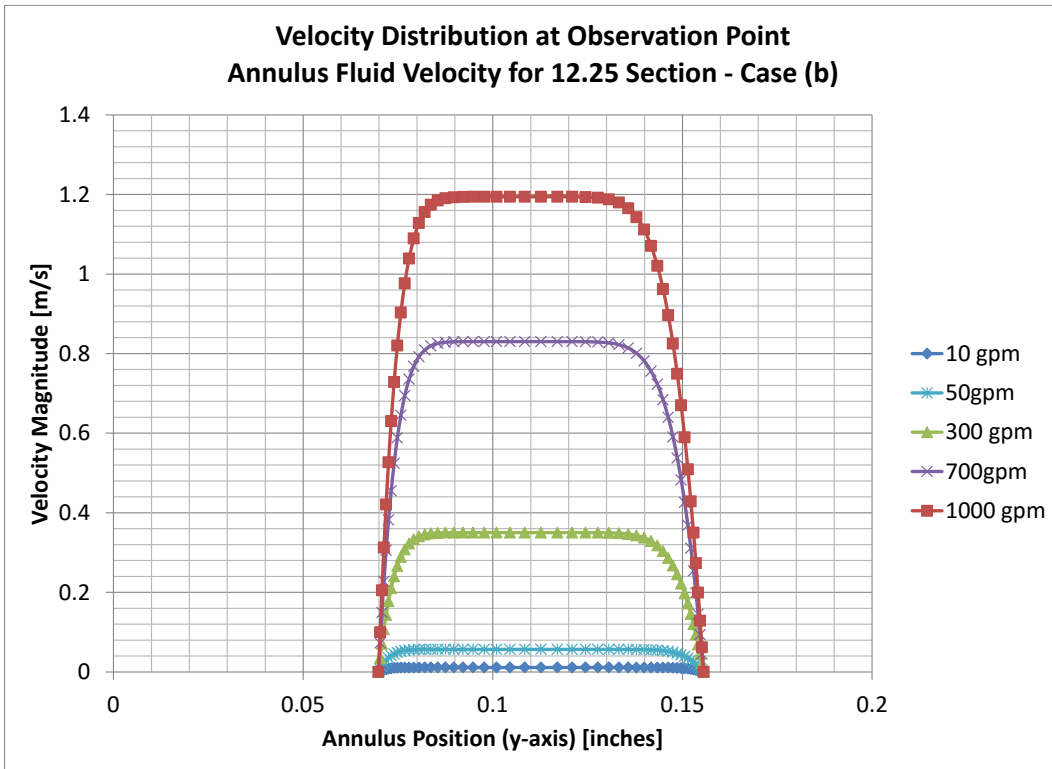


Figure 58 - Velocity Distribution at Observation Point (12.25 Section - GX0.8% - Physica NLR)

PUC-Rio - Certificação Digital Nº 1412759/CA

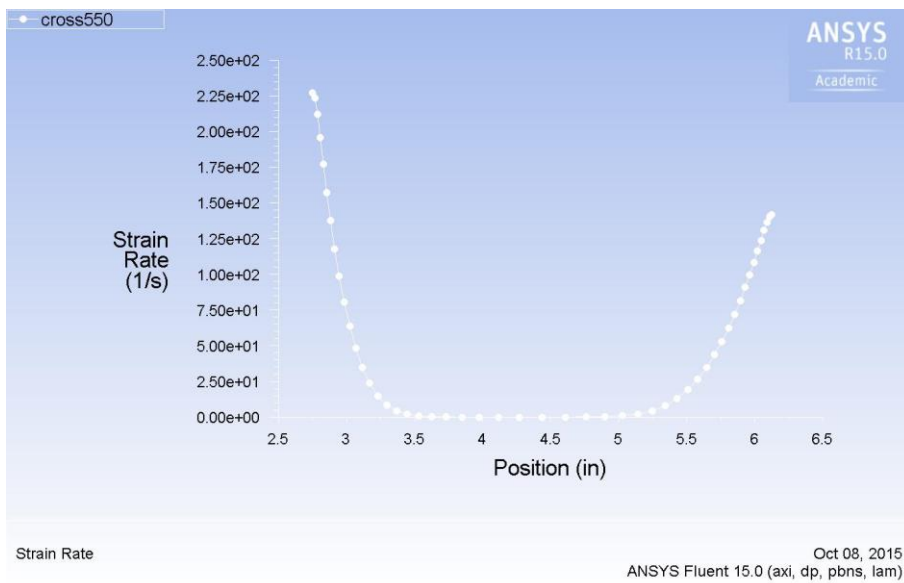


Figure 59 -Strain Rate distribution at Observation Point (12.25 Section - GX0.8% - Physica NLR - 1000 gpm)

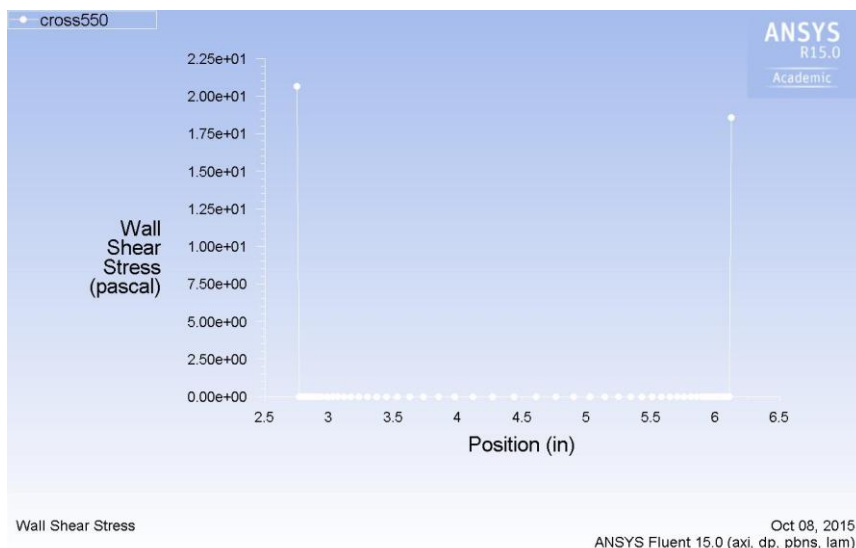


Figure 60 – Wall Shear Stress at Observation Point
(12.25 section - GX0.8% - Physica NLR – 1000 gpm)

7.7. CFD ANSYS Fluent: Shear Rates Mapping Cases

The usage of CFD Method had the objectives achieved. It allowed the comparison of two different scenarios relevant for MPD Applications:

The first comparison attempted to compare the influence of calculation method. In specific the API RP 13D Direct Formula Calculation versus the numerical results obtained by software Fluent ANSYS CFD.

In this scenario (Figure 61), the same H-B fluid properties model parameters (n and K) was used as input for the application of formulas while in API and description of the fluid on the software. The model index properties used are found on Table 20 - Rheological Parameters: H-B Model - API RP 13 D Method- Xanthan Gum 0.8% - Fann 35 PUC.

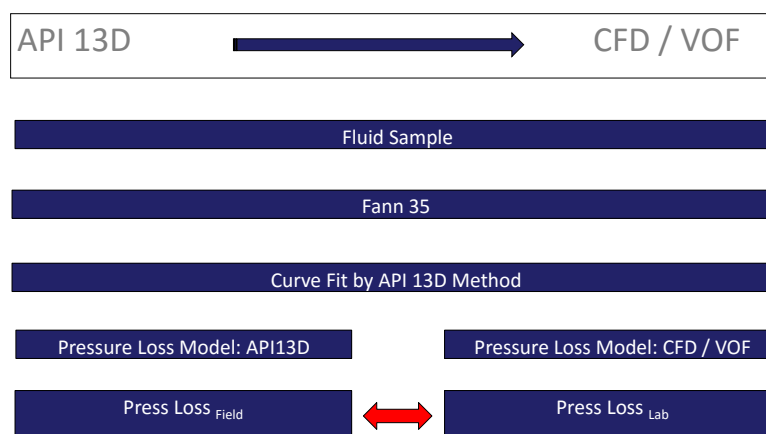


Figure 61 - Influence of Hydraulic Modeling: Analytical vs Numerical

The second analysis attempted to evaluate the curve fitting methodology and equipment accuracy. Subsequently, the discrepancy in results between the field⁶ and the laboratory environment⁷ has been examined in terms of fluid characterization. Figure 62 illustrates the comparison thought process herein proposed. Such comparison allowed to understand in a better way how the measurement process and curve fitting technique can influence the results for pressure loss estimation in a given annulus.

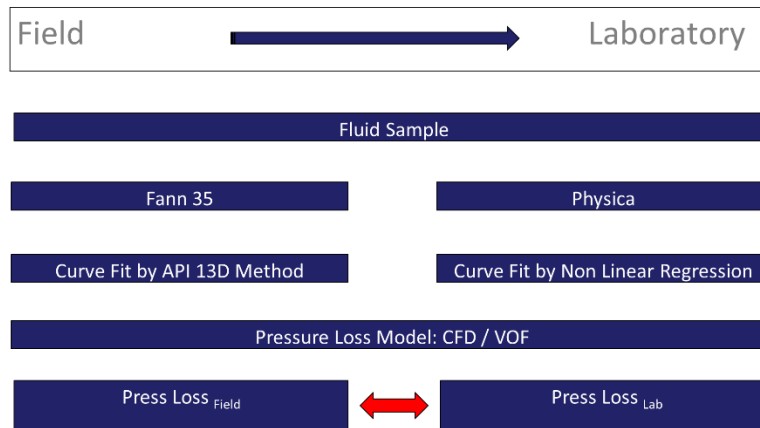


Figure 62 – Influence of Environment: Field versus Laboratory

The numerical solutions of shear rates according to the Table 23 - Annulus Fluid Velocity for 8.5 Section – Case (a) and Table 24 – Annulus Fluid Velocity for 12.25 Section – Case (b) have been successfully obtained from the simulations considering the fluid properties obtained from “Table 20 - Rheological Parameters: H-B Model - API RP 13 D Method- Xanthan Gum 0.8% - Fann 35 PUC” and “Table 8 - Rheological Parameters: H-B Model - NLR Method - Xanthan Gum 0.8% Test#2”.

In total, 26 CFD simulations were performed for case (a) and 32 CFD simulations for case (b). After all, on each proposed case - (a) and (b) – 3 sets of data were available for comparison purposes as previously outlined:

1. Rheological Properties measured by FANN35 following the API RP 13B guidelines, curve fitted and HB rheological parameter described by API

⁶ Defined as the fluid properties measured at FANN35 and Curve Fitted by API RP 13D Method

⁷ Defined as the fluid properties measured at Physica and Curve Fitted by Non Linear Regression

RP 13D Method and Pressure Loss calculated by API RP 13D direct formula Method.

2. Rheological Properties measured by FANN35 following the API RP 13B guidelines, curve fitted and HB rheological parameter described by API RP 13D Method and Pressure Loss calculated by Fluent Ansys CFD.
3. Rheological Properties measured by HPR, curve fitted and HB rheological parameter described by NLR Method and Pressure Loss calculated by Fluent Ansys CFD.

7.7.1. Influence of Hydraulics and Environment: Results

The direct comparison results indicate that there were minor variations of shear rates when considered the four sets of results (APPENDIX B CFD by ANSYS Fluent – Results) from the numeric solution obtained by ANSYS Fluent hydraulic simulator. The proposed comparison of the Field and Laboratory scheme indicates that that curve fitting method and equipment has minimal impact when regarding shear rates values.

Controversially of the shear rate obtained from API RP 13D analytical calculations, as shows on Figure 63 and Figure 64, the numerical results suggest that the shear rate ranges for 8.5” section are confirmed within the 3-100 rpm (5.11 s⁻¹ - 170.23 s⁻¹) of FANN35 readings. The same conclusions of the numerical results for the 12.25” section are observed.

PUC-Rio - Certificação Digital Nº 1412759/CA



Figure 63 - Numerical Solution for Shear Rate vs. Flow Rate in 8.5” Section and API13D Comparison

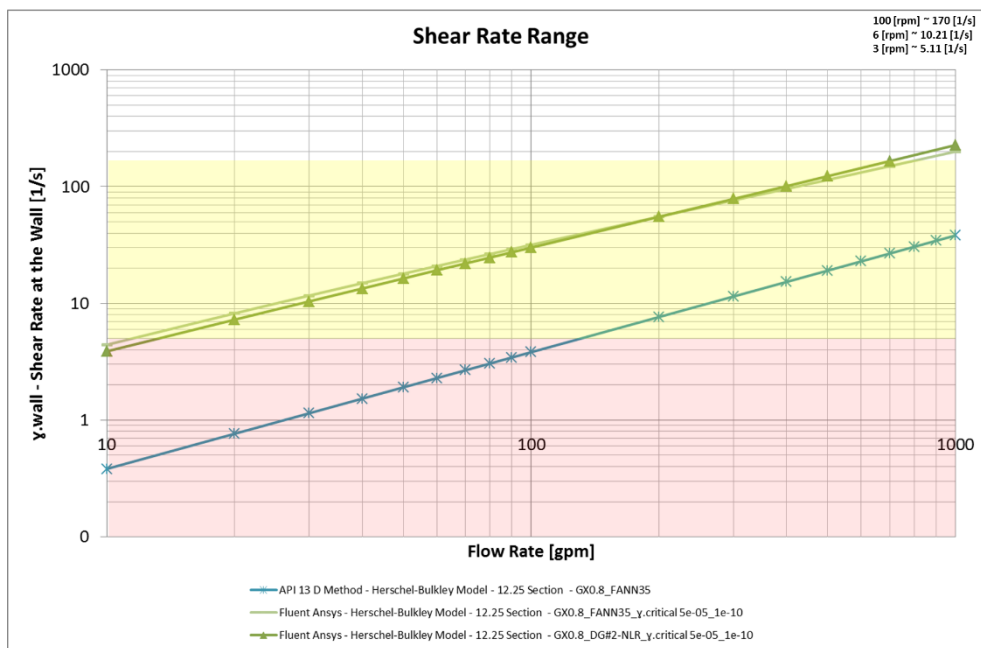


Figure 64 - Numerical Solution for Shear Rate vs. Flow Rate in 12.25" Section and API13D Comparison.

Such results, leads to suggest that API RP 13B does encompass the shear rate range interval (yellow zone highlighted) usually seen on 8.5" and 12.25" annulus for flow rates low as 10 gpm.

Nonetheless, the numerical results demonstrated a wide difference from the analytical formulas for shear rate calculations obtained by API RP 13D (Chapter 0), indicating that equations (10), (11) and (12) may not be appropriated for shear rate predictions. Further analyses of those equations have not been performed on this study and they are suggested for future work as an initial process to understand the API 13 D limitations and later errors on pressure losses predictions.

8 Pressure Losses Estimations

The utmost objective of a pump step-down schedule used in MPD is the accurately predict the pressure loss estimation at various flow rates.

The aid of numerical results allowed the representation of the field conditions versus laboratory conditions in a first instance and the validation of analytical methods suggested by API.

Although previously observed that shear rates estimation are not major impacted by the measurement device and curve fitting technique, the same conclusions could not be observed for shear stress and consequently pressure loss estimations.

The pressure loss estimation was mapped for the flow rate interval suggested by the two annulus geometries and a qualitative analysis conducted. Applications of formulas found on API RP 13 D and from numerical simulations allowed estimating the pressure loss per unit of length.

8.1. Case (a): “8.5 Section”

The numerical outcomes for case (a) – 8.5” section – in respect of field and laboratory circumstances for fluid characterization points out that laboratory pattern (green line) delivers the approximately same “slope” of the pressure loss by flow rate curves obtained by field patterns (light blue line).

The results from a fluid sample characterized in a laboratory environment present a higher value by average of 7% in comparison with the same fluid characterized in a field environment. The minimum and maximum differences observed at low and high end of the flow rates are 9% and 2% respectively (Figure 65). The difference is attributed to the process in obtaining the fluid properties as extensively discussed earlier and suggests that an enhanced method should be evaluated for MPD Applications.

Still, if considered the pressure loss per 1,000 ft (304.8m) of 8.5” by 5.5” annulus – case (a) - only 3 psi (0.0206843 MPa) in difference is perceived. The

difference may not be representative enough to justify different methods for MPD fluid characterization; however, an enhanced method would be justified by the assurance of correct rheology model selection or when a more challenging and complex well with minimal operation window is ought to be drilled.

While comparing the API 13 D analytical method for pressure loss estimation (dark blue line), indicates that the slope of the curves is not analogous. Differences between the analytical method and the numerical results using the same FANN 35 properties values (green line) produces a variation of -7% at low flow rates (e.g.: 10 gpm) up to 22% at 450 gpm (Figure 65).

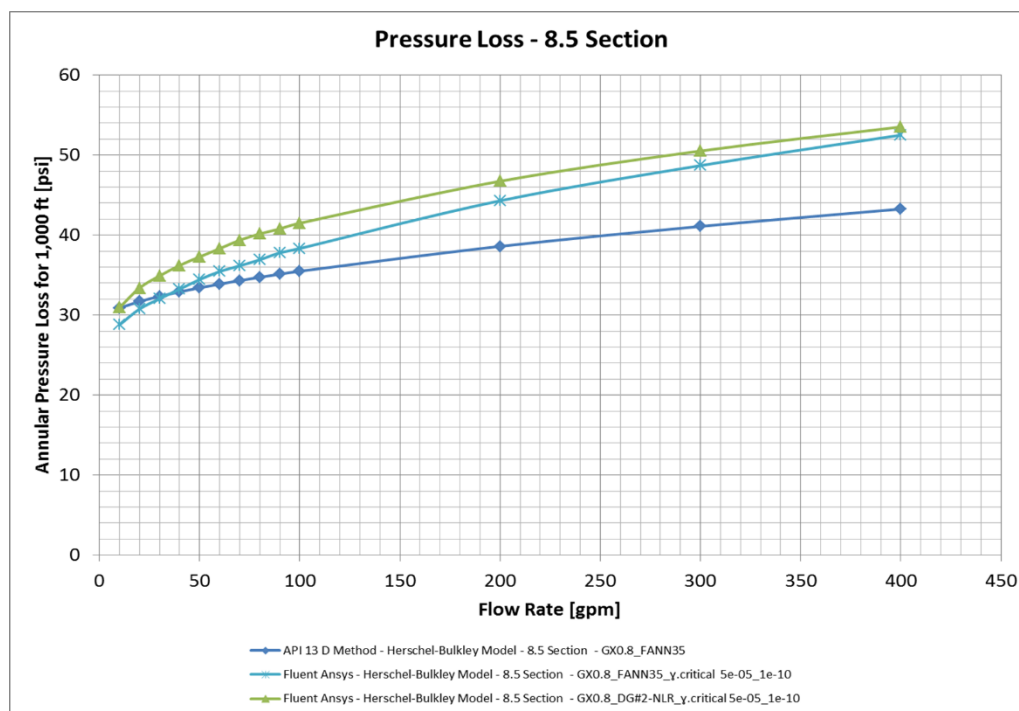


Figure 65 - Pressure Loss Estimation: 8.5" Section (case (a))

In this case, the analytical formulas suggested by API 13D should be avoided whenever possible. Pressure loss prediction for critical operations such MPD, which has significant impact and consequences due to wrong estimations, must rely on more complex and precise forms of hydraulic calculations.

8.2. Case (b): "12.25 Section"

The case (b) – 12.25" section - which encompass the lower end range of shear rate values due to the lower flow velocities (larger annulus) indicates a slighter higher difference in relative values of 9% between the two numerical

environments.. The minimum and maximum differences observed are 3.5% and 9.5% respectively, as illustrated on Figure 66. Although, the absolute values for those differences are no bigger than 2 psi for 1,000 ft (304.8m) of 12.25" by 5.5" annulus.

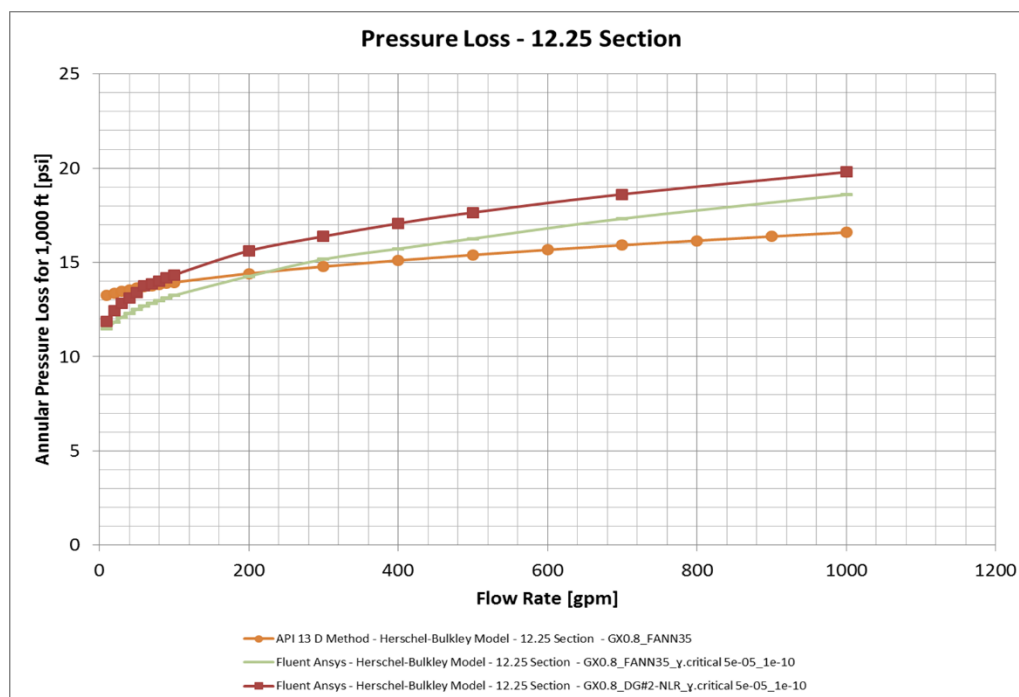


Figure 66 - Pressure Loss Estimation: 12.25" Section (case (b))

The slope of the curves, used as baseline for a smooth transition of flow rates against the surface back pressure to be added, likewise reveals dissimilarities between the two approaches at flow rates lower than 100 gpm. To satisfy the objective of this study and the suggestions herein proposed, such trend is further discussed in attempt to enlighten the proposed enhanced method for drilling fluid characterization on MPD application.

Likely attributed to the fact that the set of data obtained from FANN35 readings (represented by the green line) accounts on the curve fitting process with only 2 points, being the lowest reading 3 rpm (5.11 s^{-1}) and 6 rpm (10.21 s^{-1}). In this case the pressure loss model is probable extrapolated from the curve fitting parameters of a mathematical H-B model.

On other side, as the laboratory environment (represented by the red line) allowed to capture a larger amount of shear stress values in a wider shear rate interval, being the lower limit measured at the shear rate of 0.1 s^{-1} . This resulted in a more accurate representation of the fluid properties and more precise

mathematical representation obtained from the curve fitting parameters for the shear rates interval observed on the flow rates of 12.25" section.

As it can be inferred from the study, attribution to the variance is due to the equipment used to obtain the viscosity properties of the fluid (FANN 35 vs. Physica) and the technique used to manipulate the properties, since all calculations, software engine and set up process was the same for all the samples.

Reasonably assuming that the numerical results are accurate, the pressure loss results obtained by numerical simulation indicates that although shear rate ranges are very similar, they do not reproduce the same results on shear stress (and consequently on pressure loss estimation). From these results, it is valid to state that MPD application, in terms of drilling fluid characterization, would benefit from the use of an enhanced method, which could improve the accuracy of API 13B (six points and FANN35).

As a last observation, in regards to the comparison with API 13 D hydraulic equations (**orange** line), the numerical simulation provided a difference up to 13% on 12.25" Section over the API RP 13D and the same conclusions ought to be found as stated for 8.5" Section.

9 Recommendations and Conclusions

Hydraulics play an important role in many oil field operations including drilling, completion, fracturing, acidizing, workover and production. The standard API methods for drilling fluid hydraulics assume either Power Law, Bingham plastic or Herschel-Bulkley rheological model. These models and corresponding hydraulic calculations do provide a simple way for fair estimates of hydraulics for conventional vertical wells using simple drilling fluids.

In Managed pressure drilling (MPD) technique, pressure losses become critical to accurate estimate and control the well within the operational window. Therefore, it is necessary to use appropriate rheological model for mathematical modelling of fluid behavior. The fluid characterization is still the utmost importance on the process of proper model selection, and it can only be achieved through a reasonable amount of rheology readings that allows infer about the fluid property, later generating a mathematical model and curve fit.

MPD technique is quite often used to drill the more challenging wells, and as a result, greater understanding of fluid hydraulics for the different phases of this technique is required. The impact on the well through use of inadequate dynamic modelling is increasing as wells with narrower operational windows are drilled. This study highlighted several areas where improvements in fluid characterization can improve the overall understanding of fluid behavior as it transitions from static to fully dynamic, and thus further enable MPD as a solution to drilling challenging wells.

Shear rates in the 12.25" and 8.5" hole sections were found to be within the 3-100 rpm range when numerical simulation methods are used. The interval of shear rate for the given flow rates (0-400 gpm and 0-1000 gpm) contains only three measurement points when following API RP 13B, which is insufficient for correct fluid characterization.

The method proposed by API RP 13D infers a shear rate range below 3rpm when modeling a 12.25" hole section with a flow rate of below 100gpm. The result of pressure loss estimation is only based on the extrapolation of selected rheological model. These aspects may lead to potential risks such as a loss of well control.

In terms of fluid characterization equipment, the Couette geometry associated with the FANN35 Viscometer appears inadequate for low viscous fluids. Instead, the available geometry in high precision rheometers such as "double gap" or "cross-hatch" plate proved more efficient, although not available on FANN35 devices. A further drawback of FANN35 is its limited shear rate range (minimum and maximum) and limited speed settings. Both pose problems when using it for MPD operations.

Rheology measurements must be more vigilant regarding the time taken for dial deflection readings or shear stress values to stabilize. Whenever possible, Non Linear Regression methods and larger amounts of data points should be obtained to better characterize a drilling fluid. This will produce a more accurate understanding of the rheology property and aid in improved model selection, which in turn, improves pressure loss estimation accuracy.

It appears to be appropriate when selecting a rheological model, that it should be valid for the range of shear rates that will constitute the process. If the selected rheological model does not satisfy the entire range, the problem can be solved by sub-dividing the shear rate range and selecting a rheological model for each sub-range. Alternatively, investigation into a rheological model - other than H-B or PL - that is continuous across the entire shear rate range should be made.

Finally, the results demonstrate that utilizing an appropriate geometry while conducting a rheogram test, 50 point readings, and NLR method for curve fitting, will result in about a 9% difference when compared to traditional methods.

Ultimately, to improve the accuracy when modeling fluid dynamics during a typical MPD connection procedure, several areas of improvement exist. These include:

- Increasing the number of data points sampled.
- Focusing on the shear rate range applicable to that anticipated while transitioning from drilling rate to a connection,
- Selection of the more appropriate rheological model
- Curve fitting method that will deliver the most representative index parameters for the selected rheological model.
- Increased used of more tailored and accurate measuring equipment.

The MPD industry would be prudent to focus on developing enhanced modeling methods beyond the existing ones in order to improve accuracy and operational safety.

10

Bibliographic References

- [1] Blade Energy Partners. *Managed Pressure Drilling - Well Design and Operations*, Frisco, Dallas, 2013.
- [2] IADC, "INTERNATIONAL ASSOCIATION OF DRILLING CONTRACTORS" [Online]. Available: <http://www.iadc.org/>.
- [3] A. T. Bourgoyne. *Applied drilling engineering*, Richardson, Texas: SPE, 1991.
- [4] A. Pilehvari, R. Serth and V. Lagad. *Generalized Hydraulic Calculation Method Using Rational Polynomial Model*, New Orleans, Louisiana, 2001.
- [5] E. C. Bingham. *An investigation of the laws of plastic flow*, vol. 13, Bulletin of the Bureau of Standards, 1917, pp. 308-352.
- [6] W. Ostwald. "The velocity function of viscosity of disperse systems", *Kolloid Zeitschrift*, vol. 47, no. 2, pp. 176-187, 1929.
- [7] W. H. Herschel and R. Bulkley. "Konsistenzmessungen von Gummi-Benzollösungen", *Kolloid-Zeitschrift*, vol. 39, no. 4, pp. 291-300, 1926.
- [8] M. Zamora and D. Power. "Making a case for AADE hydraulics and the unified rheological model - AADE-02-DFWH-HO-13", *AADE 2002 Technology Conf*, Houston, TX, 2002.
- [9] A. Pilehvari and T. Reed. *A New Model for Laminar, Transitional, and Turbulent Flow of Drilling Muds*. Oklahoma City, Oklahoma: SPE Production Operations Symposium, 1993.
- [10] A. Merlo, R. Maglione and C. Piatti. *An Innovative Model For Drilling Fluid Hydraulics*. Kuala Lumpur: SPE Asia Pacific Oil and Gas Conference, 1995.
- [11] W. Bailey and J. Peden. "A Generalized and Consistent Pressure Drop and Flow Regime Transition Model for Drilling Hydraulics," *SPE Drilling & Completion*, vol. 15, no. 01, pp. 44 - 56, March 2000.
- [12] R. Maglione, G. Robotti and R. Romagnoli. "In-Situ Rheological Characterization of Drilling Mud", *SPE Journal*, vol. 5, no. 04, pp. 377 - 386, December 2000.
- [13] M. Okafor and J. Evers. *Experimental Comparison of Rheology for Drilling Fluids*. Bakersfield, California: SPE Western Regional Meeting, 1992.

- [14] J. Savins and W. Roper. *A Direct-indicating Viscometer for Drilling Fluids*. D. a. P. Practice, Ed., New York, New York : American Petroleum Institute, 1954.
- [15] Q. D. Nguyen and D. V. Boger. *Characterization of Yield Stress Fluids with Concentric Cylinder Viscometers*. vol. 26, Rheologica Acta, 1987, pp. 508-515.
- [16] J. A. Klotz and W. E. Brigham. "To Determine Herschel-Bulkley Coefficients", *Journal of Petroleum Technology*, vol. 50, no. 11, pp. 80-81, November 1998.
- [17] American Petroleum Institute API. *API Recommended Practice 13D*. 6th ed., 2010.
- [18] O. Erge, E. M. Ozbayoglu, S. Z. Miska, Y. Mengjiao, N. Takach, A. Saasen and R. May. *CFD Analysis and Model Comparison of Annular Frictional Pressure Losses While Circulating Yield Power Law Fluids*. Bergen: Society of Petroleum Engineers, 2015.
- [19] Company, Fann Instrument. *Fann 35 - Instruction Manual*. Houston, Texas, USA, 2013.
- [20] American Petroleum Institute API. *API Recommended Practice 13B-1*. 4th ed., 2009.
- [21] P. R. Souza Mendes. "Diretrizes para o programa de comparação interlaboratorial de caracterização reológica de um fluido de perfuração", PUC-Rio, Rio de Janeiro, 2013.
- [22] Schlumberger. "Drillbench Dynamic Drilling Simulation Software", Schlumberger Software, [Online]. Available: <http://www.software.slb.com/products/foundation/Pages/drillbench.aspx>.
- [23] M. Zamora and D. Lord. "SPE 4976 - Practical analysis of drilling mud flow in pipes and annuli", in *SPE 1974 Annual Technical Conference*, Houston, Texas.
- [24] A. Metzner and J. Reed. "Flow of non-Newtonian fluids – correlation of laminar, transition and turbulent flow regions", *American Institute of Chemical Engineers*, vol. 1, no. 4, pp. pp. 434-440, December 1955.
- [25] Spears & Assoc. Inc. "Oilfield Market Report", Tulsa, Oklahoma, 2014.
- [26] M. F. Naccache. "Introdução aos reômetros e reometria rotacional", Rio de Janeiro-RJ, 2012.
- [27] K. Simon. *The Role of Different Rheological Models in Accuracy of Pressure of Pressure Loss Prediction*. vol. 16, Zagreb, Zagreb: Faculty of Mining, Geology and Petroleum Engineering, University of Zagreb, Croatia, 2004, pp. 85-89.

- [28] ANSYS, Inc. *ANSYS Fluent Theory Guide*. Release 15.0 ed., ANSYS, Inc., 2013.
- [29] M. Soares, M. F. Naccache and P. R. Souza Mendes. "Heat transfer to viscoplastic materials flowing laminarly in the entrance region of tubes", *International Journal of Heat and Fluid Flow*, pp. 60-67, 1999.
- [30] Wikipedia. "Wikipedia", 17 December 2015. [Online]. Available: https://en.wikipedia.org/wiki/Curve_fitting. [Accessed 04 January 2016].

APPENDIX A

API 13 D Method – Results

PUC-Rio - Certificação Digital Nº 1412759/CA

Table 27 - API 13 D Method - Herschel-Bulkley Model - 8.5 Section - GX0.8_FANN35

Q - Flow Rate [gpm]	Va - Annulus Fluid Velocity [ft/min]	$\dot{\gamma}_{wall}$ - (see 7.4.7) Shear Rate at the Wall [1/s]	τ_f - Shear Stress at the Wall [lbf / 100 ft ²]	τ_f - Shear Stress at the Wall [Pa]	Annulus Pressure Loss (Laminar Flow - see 7.4.12.2) [psi]	Reynolds Number (generalized) (see 7.4.9.1)	Laminar Flow Friction Factor f-lam (see 7.4.11.1)	Frictional Pressure Loss/Annulus (see 7.4.12) [psi]
10	5.836	2.4528	27.8047	13.3130	31	0.528	30.32418572	30.891
20	11.671	4.9057	28.5328	13.6616	32	2.057	7.779563881	31.700
30	17.507	7.3585	29.1173	13.9415	32	4.535	3.528421099	32.350
40	23.343	9.8114	29.6247	14.1844	33	7.923	2.019317497	32.913
50	29.179	12.2642	30.0813	14.4030	33	12.192	1.312285041	33.421
60	35.014	14.7171	30.5013	14.6041	34	17.315	0.924032124	33.887
70	40.850	17.1699	30.8930	14.7917	34	23.269	0.68759965	34.322
80	46.686	19.6228	31.2621	14.9684	35	30.034	0.532732754	34.732
90	52.521	22.0756	31.6124	15.1361	35	37.590	0.425641738	35.122
100	58.357	24.5285	31.9469	15.2963	35	45.922	0.348417896	35.493
200	116.714	49.0569	34.7447	16.6359	39	168.896	0.094732667	38.602
300	175.071	73.5854	36.9909	17.7114	41	356.941	0.044825382	41.097
400	233.429	98.1139	38.9403	18.6447	43	602.794	0.026543066	43.263

Table 28 - API 13 D Method - Herschel-Bulkley Model - 12.25 Section - GX0.8_FANN35

Q - Flow Rate [gpm]	Va - Annulus Fluid Velocity [ft/min]	$\dot{\gamma}_{wall}$ - (see 7.4.7) Shear Rate at the Wall [1/s]	τ_f - Shear Stress at the Wall [lbf / 100 ft ²]	τ_f - Shear Stress at the Wall [Pa]	Annulus Pressure Loss (Laminar Flow - see 7.4.12.2) [psi]	Reynolds Number (generalized) (see 7.4.9.1)	Laminar Flow Friction Factor f-lam (see 7.4.11.1)	Frictional Pressure Loss/Annulus (see 7.4.12) [psi]
10	2.046	0.3822	26.8389	12.8505	13	0.067	238.2000487	13.253
20	4.091	0.7643	27.0845	12.9681	13	0.266	60.09483977	13.374
30	6.137	1.1465	27.2816	13.0625	13	0.595	26.90322898	13.471
40	8.183	1.5286	27.4527	13.1444	14	1.051	15.22797222	13.556
50	10.228	1.9108	27.6067	13.2182	14	1.633	9.800577362	13.632
60	12.274	2.2929	27.7484	13.2860	14	2.339	6.840874735	13.702
70	14.320	2.6751	27.8805	13.3492	14	3.168	5.049877667	13.767
80	16.366	3.0572	28.0049	13.4088	14	4.120	3.883573383	13.828
90	18.411	3.4394	28.1231	13.4654	14	5.192	3.081448403	13.887
100	20.457	3.8215	28.2359	13.5194	14	6.385	2.505985319	13.942
200	40.914	7.6430	29.1794	13.9712	14	24.713	0.647431769	14.408
300	61.371	11.4645	29.9370	14.3339	15	54.197	0.295217864	14.782
400	81.828	15.2860	30.5944	14.6487	15	94.280	0.169706885	15.107
500	102.285	19.1076	31.1862	14.9321	15	144.517	0.110713343	15.399
600	122.742	22.9291	31.7305	15.1926	16	204.536	0.078226027	15.668
700	143.199	26.7506	32.2381	15.4357	16	274.012	0.05839167	15.919
800	163.656	30.5721	32.7164	15.6647	16	352.661	0.045369382	16.155
900	184.113	34.3936	33.1704	15.8821	16	440.227	0.036344873	16.379
1000	204.570	38.2151	33.6039	16.0896	17	536.479	0.02982407	16.593

APPENDIX B CFD by ANSYS Fluent – Results

PUC-Rio - Certificação Digital Nº 1412759/CA

Table 29 - Fluent Ansys - Herschel-Bulkley Model - 8.5 Section - GX0.8_FANN35_y.critical 5e-05_1e-10

Fluent Ansys - Herschel-Bulkley Model - 8.5 Section - GX0.8_FANN35_y.critical 5e-05_1e-10									
Q - Flow Rate [gpm]	Va - Annulus Fluid Velocity [m/s]	$\dot{\gamma}_{wall}$ Max Shear Rate at the Wall [1/s]	τ_{w} Max Shear Stress at the Wall [Pa]	μ Apparent Viscosity [Pa.s]	Reynolds Number	L (developed flow) - [m]	L (developed flow) - [in]	ΔP [Pa/100 in]	ΔP [psi /1000 ft]
10	0.029645	19.6651	12.6392	0.9253	2.4398	0.0093	0.3660	1653.8	28.8
20	0.059291	34.3749	13.5377	0.6219	7.2606	0.0277	1.0891	1767.4	30.8
30	0.088936	47.3281	14.2052	0.5012	13.5113	0.0515	2.0267	1841.2	32.0
40	0.118582	59.4097	14.7650	0.4323	20.8907	0.0796	3.1336	1910.1	33.2
50	0.148227	70.9527	15.2589	0.3862	29.2297	0.1114	4.3845	1979.3	34.4
60	0.177873	82.0162	15.7023	0.3529	38.3848	0.1462	5.7577	2036.9	35.5
70	0.207518	92.5844	16.1029	0.3277	48.2298	0.1838	7.2345	2078.4	36.2
80	0.237163	102.8755	16.4756	0.3075	58.7388	0.2238	8.8108	2121.4	36.9
90	0.266809	113.1276	16.8330	0.2905	69.9302	0.2664	10.4895	2171.8	37.8
100	0.296454	122.8501	17.1585	0.2768	81.5703	0.3108	12.2355	2202.9	38.3
200	0.592909	215.3201	19.8573	0.2013	224.3426	0.8547	33.6514	2545.4	44.3
300	0.889363	300.4378	21.9949	0.1681	402.8330	1.5348	60.4249	2797.9	48.7
400	1.185817	382.0287	23.7073	0.1482	609.2173	2.3211	91.3826	3017.3	52.5

Table 30 - Fluent Ansys - Herschel-Bulkley Model - 8.5 Section - GX0.8_DG#2-NLR_y.critical 5e-05_1e-10

Fluent Ansys - Herschel-Bulkley Model - 8.5 Section - GX0.8_DG#2-NLR_y.critical 5e-05_1e-10									
Q - Flow Rate [gpm]	Va - Annulus Fluid Velocity [m/s]	$\dot{\gamma}_{wall}$ Max Shear Rate at the Wall [1/s]	τ_{w} Max Shear Stress at the Wall [Pa]	μ Apparent Viscosity [Pa.s]	Reynolds Number	L (developed flow) - [m]	L (developed flow) - [in]	ΔP [Pa/100 in]	ΔP [psi /1000 ft]
10	0.029645	17.8414	13.6299	0.6542	3.4508	0.0131	0.5176	1777.2	30.9316
20	0.059291	32.6659	14.7145	0.3774	11.9646	0.0456	1.7947	1918.6	33.3926
30	0.088936	46.4070	15.4708	0.2755	24.5862	0.0937	3.6879	2005.6	34.9066
40	0.118582	59.6300	16.0785	0.2205	40.9508	0.1560	6.1426	2080.8	36.2154
50	0.148227	72.3933	16.5905	0.1859	60.7221	0.2314	9.1083	2142.4	37.2877
60	0.177873	84.9630	17.0440	0.1616	83.8228	0.3194	12.5734	2201.7	38.3198
70	0.207518	97.3989	17.4544	0.1435	110.1348	0.4196	16.5202	2262.0	39.3685
80	0.237163	109.5154	17.8236	0.1296	139.3173	0.5308	20.8976	2307.6	40.1624
90	0.266809	121.3109	18.1590	0.1187	171.1816	0.6522	25.6772	2343.4	40.7849
100	0.296454	133.0835	18.4750	0.1096	205.9484	0.7847	30.8923	2384.3	41.4978
200	0.592909	245.7881	20.8800	0.0652	692.3140	2.6377	103.8471	2685.8	46.7450
300	0.889363	353.1490	22.5931	0.0483	1402.3452	5.3429	210.3518	2903.0	50.5260
400	1.185817	457.3163	23.9697	0.0391	2309.7348	8.8001	346.4602	3075.9	53.5348

Table 31 - Fluent Ansys - Herschel-Bulkley Model - 12.25 Section - GX0.8_FANN35_y.critical 5e-05_1e-10

Fluent Ansys - Herschel-Bulkley Model - 12.25 Section - GX0.8_FANN35_y.critical 5e-05_1e-10									
Q - Flow Rate [gpm]	Va - Annulus Fluid Velocity [m/s]	$\dot{\gamma}_{wall}$ Max Shear Rate at the Wall [1/s]	τ_{w} Max Shear Stress at the Wall [Pa]	μ Apparent Viscosity [Pa.s]	Reynolds Number	L (developed flow) - [m]	L (developed flow) - [in]	ΔP [Pa/100 in]	ΔP [psi /1000 ft]
10	0.010392	4.42363	11.39683	3.0296	0.5877	0.0050	0.1984	659.3076	11.4749
20	0.020784	8.21124	11.80487	1.8148	1.9623	0.0168	0.6623	679.5617	11.8275
30	0.031176	11.66858	12.11472	1.3737	3.8885	0.0333	1.3124	694.7546	12.0519
40	0.041569	14.90195	12.37308	1.1383	6.2571	0.0536	2.1118	707.3401	12.3109
50	0.051961	17.96953	12.59861	0.9890	9.0015	0.0772	3.0380	718.5564	12.5061
60	0.062353	20.90450	12.80063	0.8847	12.0751	0.1035	4.0754	728.3662	12.6769
70	0.072745	23.73370	12.98516	0.8070	15.4451	0.1324	5.2127	737.5119	12.8361
80	0.083137	26.46803	13.15532	0.7465	19.0822	0.1636	6.4402	745.2026	12.9699
90	0.093529	29.13529	13.31506	0.6976	22.9729	0.1969	7.7534	753.6860	13.1176
100	0.103921	31.73192	13.46503	0.6572	27.0932	0.2323	9.1439	761.0823	13.2463
200	0.207843	55.28186	14.65422	0.4528	78.6467	0.6742	26.5433	819.6636	14.2659
300	0.311764	76.45019	15.55790	0.3686	144.9302	1.2424	48.9139	871.2535	15.1638
400	0.415686	95.89343	16.29951	0.3208	222.0489	1.9035	74.9415	903.4477	15.7241
500	0.519607	114.46925	16.95356	0.2885	308.5698	2.6452	104.1423	934.3999	16.2628
700	0.727450	149.96634	18.09486	0.2465	505.5561	4.3339	170.6252	995.1919	17.3209
1000	1.039214	199.89505	19.52607	0.2097	849.1643	7.2795	286.5930	1068.4214	18.5954

Table 32 - Fluent Ansys - Herschel-Bulkley Model - 12.25 Section - GX0.8_DG#2-NLR_y.critical 5e-05_1e-10

Fluent Ansys - Herschel-Bulkley Model - 12.25 Section - GX0.8_DG#2-NLR_y.critical 5e-05_1e-10									
Q - Flow Rate [gpm]	Va - Annulus Fluid Velocity [m/s]	$\dot{\gamma}_{wall}$ Max Shear Rate at the Wall [1/s]	τ_{w} Max Shear Stress at the Wall [Pa]	μ Apparent Viscosity [Pa.s]	Reynolds Number	L (developed flow) - [m]	L (developed flow) - [in]	ΔP [Pa/100 in]	ΔP [psi /1000 ft]
10	0.010392	3.885308	11.886744	3.3846	0.5261	0.0045	0.1776	682.0867	11.8714
20	0.020784	7.253065	12.504663	2.0069	1.7745	0.0152	0.5989	714.8172	12.4411
30	0.031176	10.408469	12.937932	1.5023	3.5556	0.0305	1.2000	737.3899	12.8339
40	0.041569	13.422803	13.281775	1.2328	5.7774	0.0495	1.9499	754.1941	13.1264
50	0.051961	16.346148	13.573206	1.0615	8.3869	0.0719	2.8306	769.6565	13.3955
60	0.062353	19.245377	13.834332	0.9401	11.3643	0.0974	3.8355	789.4768	13.7405
70	0.072745	21.989248	14.056895	0.8528	14.6161	0.1253	4.9329	796.0520	13.8549
80	0.083137	24.701265	14.261642	0.7842	18.1650	0.1557	6.1307	804.5142	14.0022
90	0.093529	27.392117	14.452369	0.7286	21.9958	0.1886	7.4236	814.7265	14.1799
100	0.103921	30.039276	14.629037	0.6828	26.0777	0.2236	8.8012	823.7763	14.3374
200	0.207843	55.175179	15.968564	0.4534	78.5483	0.6734	26.5101	897.0004	15.6119
300	0.311764	78.576889	16.904856	0.3623	147.4205	1.2638	49.7544	941.3067	16.3830
400	0.415686	101.142320	17.657604	0.3106	229.2962	1.9556	77.3875	980.6494	17.0677
500	0.519607	123.069900	18.295843	0.2765	322.0231	2.7605	108.6828	1013.9707	17.6477
700	0.727450	165.591810	19.358303	0.2330	534.9154	4.5856	180.5339	1069.5942	18.6158
1000	1.039214	227.163710	20.632990	0.1954	911.0818	7.8102	307.4901	1137.2876	19.7940